

**Modelling urban pluvial flooding using  
BASEMENT (v2.8) to assess a potential hazard  
reduction by implementing nature-based  
solutions on today's parking spots**

**A case study in the city of Bern as proof of concept**

Master's thesis in the Science Faculty  
of the University of Bern

Written by  
**Eva Ammann**

**February 2022**

Supervisor  
Prof. Dr. Andreas Zischg



## **Abstract**

**Background.** Urban pluvial flooding is a special type of flooding that occurs in urban areas due to intense rainfall and a capacity overload of the sewer system. Urban pluvial flooding, while not a major risk to human life, can cause severe damage to infrastructure. The associated risk is expected to increase over the century as more intense rainfall events occur due to climate change. Nature-based solutions (NBS) are implementation measures that consist of or mimic natural landscapes to take advantage of the resilience of natural landscapes. Their definition states that, in addition to their specific purpose, they must provide additional benefits, so-called co-benefits. In research, the approach of NBS is currently very much pursued for various purposes, including mitigation effects on urban pluvial flooding. This paper investigates this mitigation effect using a simulated case study in the city of Bern in which all current parking spaces are replaced with NBS. Then, a potential damage reduction is calculated to show some of the currently externalized costs of parking lots in urban areas.

**Methods.** In this paper, the established river simulation tool BASEMENT (v2.8) is used to model urban pluvial flooding. Since there is no record of a preceding attempt, a completely new workflow must be developed. The simulation results are then post-processed and various hazard parameters calculated to grasp the extent to which the implementation of NBS can mitigate the urban pluvial flood hazard.

**Results.** This work is evidence that it is possible to simulate urban pluvial flooding with BASEMENT (v2.8), even though this is not its intended purpose. While the simulation provides plausible results for the maximum flow depth, the simulated flow velocities are overly influenced by steep elevation transitions in urban topography (e.g., houses to streets). The simulation results show that it is possible to reduce certain hazard parameters such as the maximum flow depth or the sum of predicted building damage by implementing NBS on today's parking areas. However, this reduction only occurs to a very small extent and decreases inversely proportional to the rainfall intensity. In addition, it is shown that the hazard parameters will increase toward the end of the century due to higher intensity storms caused by climate change. This increase is a multiple of the potential reduction through the implementation of NBS on today's parking areas.

**Conclusions.** While it is possible to model urban pluvial flooding with BASEMENT (v2.8), it is not recommended to do so. The workflow developed to model urban pluvial flooding is tedious, user-unfriendly and error-prone, requiring many manual correction steps. And due to the very limited predicted hazard mitigation, NBS cannot be recommended as a mitigation strategy for urban pluvial flooding. However, the small hazard reduction can still be credited as co-benefit when NBS are implemented to mitigate other risks in urban areas. The projected annual damage reduction of just over 14'000 CHF should be included in further cost-benefit analyses.

**Keywords.** Urban pluvial flooding · nature-based solutions · BASEMENT (v2.8) · flood simulation

## Table of content

1	Introduction and state of research .....	6
1.1	Different types of flooding .....	7
1.2	Definition of (flood) risk .....	9
1.3	The risk of urban pluvial flooding .....	10
1.4	Increased risk of urban pluvial flooding in the future .....	12
1.5	Modelling urban pluvial flooding.....	13
1.6	Urban water management.....	17
1.7	Nature-based solutions in the context of hydrology .....	18
1.8	Pluvial flooding and nature-based solutions.....	20
1.9	Measurable effects of nature-based solutions .....	22
1.10	Limitations of nature-based solutions .....	23
1.11	Co-benefits of nature-based solutions .....	24
1.12	Implementing NBS on today's parking spaces .....	25
1.13	Motivation for this paper .....	26
1.14	Study Area: Länggasse-Felsenau neighborhood in the city of Bern, Switzerland .....	27
1.15	Hypotheses and Research questions .....	28
2	Data and Methods.....	29
2.1	The different scenarios .....	29
2.2	The general workflow .....	30
2.3	Data procurement and the adapted workflow for the Bern simulation.....	31
3	Results .....	49
3.1	Proportion of parking area relative to the urban area .....	49
3.2	Modelling urban pluvial flooding with BASEMENT (v2.8).....	49
3.3	Hazard reduction through the implementation of NBS on today's parking spots .....	52
3.4	Hazard increase due to climate change .....	59
3.5	Co-benefits of replacing today's parking spots with nature-based solutions.....	63
4	Discussion .....	64
4.1	Proportion of parking area relative to the urban area .....	64
4.2	Modelling urban pluvial flooding with BASEMENT (v2.8).....	64
4.3	Hazard reduction through the implementation of NBS on today's parking spots .....	69
4.4	Hazard increase due to climate change .....	73
4.6	Co-benefits of replacing today's parking spots with nature-based solutions.....	75
4.7	Limitations of this work .....	75

5	Conclusion.....	77
5.1	Hypotheses.....	77
5.2	Wrap-up.....	77
5.3	Outlook .....	78

**Table of Figures**

Figure 1:	The Risk Triangle and the associated formula (own illustration after Crichton 1999) .....	9
Figure 2:	Flood Hazard Categories (own illustration after Rentschler and Salhab 2020) .....	10
Figure 3:	The Total Cost Matrix. Copied from Giupponi et al. 2015: 174. ....	12
Figure 4:	Overview Map of the Bern Simulation Perimeter.....	27
Figure 5:	3-step simulation process for BASEMENT (v2.8). The icons represent the most used software programs per process step. From left to right: QGis, BASEmesh, Python – BASEMENT (v2.8) – QGis, Python and Microsoft Excel (Own illustration, icons see Image Sources).....	30
Figure 6:	Map of StringDefs used in the Bern simulation .....	35
Figure 7:	Manual Correction Workflow (own illustration, icons see Image Sources).....	36
Figure 8:	Two screenshots of a "nest" in quality mesh in different zoom levels .....	36
Figure 9:	Manipulation steps applied to original DTM to obtain the manipulated DTM .....	37
Figure 10:	Map of Bern simulation perimeter displaying the different MatIDs .....	38
Figure 11:	Map of Bern simulation perimeter displaying the elevation in meters above sea level .....	38
Figure 12:	Conversion from rainfall intensity [mm/h] to the format required for the simulation.....	41
Figure 13:	Map of Bern simulation perimeter with applied outflow boundary conditions .....	43
Figure 14:	Adapted Flood Hazard Categories for Bern simulation (own illustration), original Flood Risk Categories from Rentschler and Salhab (2020).....	44
Figure 15:	Workflow for instability function hazard analysis (own illustration) .....	45
Figure 16:	Degree of loss and predicted damage in CHF hazard analysis process .....	45
Figure 17:	Process to extract the highest maximum flow depth for an individual building (future_noNBS scenario) .....	46
Figure 18:	Calculation of degree of loss as a function of maximum flow depth .....	47
Figure 19:	Degree of loss as a function of the maximum flow depth. In addition, the maximum flow depth in the future_noNBS scenario and the resulting degree of loss of the building from the example above are plotted.....	47
Figure 20:	Map of Bern simulation perimeter displaying the maximum flow depth per mesh element in the baseline scenario .....	50
Figure 21:	Map of Bern simulation perimeter displaying the boolean instability factor per mesh element in the baseline scenario .....	50
Figure 22:	Map of Bern simulation perimeter displaying the degree of loss per building in the baseline scenario .....	51
Figure 23:	Map of Bern simulation perimeter displaying the predicted damage in CHF per building in the baseline scenario.....	51
Figure 24:	Map of Bern simulation perimeter displaying the reduction in maximum flow depth through the implementation of NBS measures in the current scenario .....	53
Figure 25:	Stacked bar charts representing the area percentage of the simulation perimeter according to the different Hazard Categories.....	53

Figure 26: Map of Bern simulation perimeter displaying the change in the boolean stability indicator through the implementation of NBS measures in the current scenario .....	54
Figure 27: Map of Bern simulation perimeter displaying the change in degree of loss through the implementation of NBS measures in the current scenario .....	55
Figure 28: Map of Bern simulation perimeter displaying the simulated damage reduction in CHF through the implementation of NBS measures in the current scenario .....	55
Figure 29: Map of Bern simulation perimeter displaying the reduction in maximum flow depth through the implementation of NBS measures in the future scenario .....	56
Figure 30: Stacked bar charts representing the area percentage of the simulation perimeter according to the different Hazard Categories.....	57
Figure 31: Map of Bern simulation perimeter displaying the change in the boolean stability indicator through the implementation of NBS measures in the future scenario .....	57
Figure 32: Map of Bern simulation perimeter displaying the change in degree of loss through the implementation of NBS measures in the future scenario .....	58
Figure 33: Map of Bern simulation perimeter displaying the simulated damage reduction in CHF through the implementation of NBS measures in the future scenario .....	58
Figure 34: Map of Bern simulation perimeter displaying the increase in maximum flow depth through climate change .....	60
Figure 35: Stacked bar charts representing the area percentage of the simulation perimeter according to the different Hazard Categories.....	60
Figure 36: Map of Bern simulation perimeter displaying the change in the boolean stability indicator through climate change .....	61
Figure 37: Map of Bern simulation perimeter displaying the change in degree of loss through climate change .....	62
Figure 38: Map of Bern simulation perimeter displaying the simulated damage increase in CHF through climate change .....	62
Figure 39: Map of Bern simulation perimeter displaying the surface runoff risk map published by the FOEN (2018) .....	65
Figure 40: Map of Bern simulation perimeter displaying the maximum flow depth for the future_noNBS scenario using the same legend as the surface runoff risk map published by the FOEN .....	65
Figure 41: Closeup of Bern simulation perimeter locating the two areas with the highest predicted hazard in the current_noNBS scenario .....	66
Figure 42: two pictures showing hazard area #1 (own images taken on 13.01.2022) .....	66
Figure 43: Three pictures showing hazard area #2 (own images taken on 13.01.2022) .....	67
Figure 44: Closeup of Bern simulation perimeter displaying the reduction in max flow depth in the future scenario and the computational mesh MatID.....	70
Figure 45: Map of Bern simulation perimeter displaying the boolean instability factor per mesh element in the future_noNBS scenario with a selection of steep streets shown as blue arrows .	71
Figure 46: Map of Bern simulation perimeter displaying the boolean instability factor per mesh element in the future_withNBS scenario .....	71
Figure 47: Simulated damage reduction in CHF per building for the current and the future scenario. The chemistry building of the university of Bern is highlighted in a red circle .....	72
Figure 48: Visual representation of possible predicted damage reduction through the implementation of NBS on today's parking spots in the current scenario.....	75

## Table of Tables

Table 1: The four simulation setups for the Bern simulation perimeter .....	29
Table 2: Layers used from swissTLM3D model.....	31
Table 3: QGis Action performed on feature layers to harmonize the data .....	32
Table 4: Examples of manual correction on feature layers.....	33
Table 5: Urban features used in the Bern simulation and the attributed MatIDs.....	33
Table 6: StringDefs used in the Bern simulation .....	34
Table 7: QGis actions performed on urban feature polygon layers to compute quality mesh.....	35
Table 8: Computational efficiency gain through manual correction process .....	37
Table 9: Strickler coefficient assigned to the different MatIDs (Data from Ma, Ngoc Vo and Gourbesville 2018) .....	39
Table 10: The calculation of the excessive rainfall for an hourly 1-in-100 years rainfall event in the simulation perimeter.....	40
Table 11: Rainfall amount per MatID in m <sup>3</sup> /s calculated for the different simulation setups (rounded to two decimal places).....	41
Table 12: Rainfall amount per MatID in m <sup>3</sup> /s used in the four simulation setups (rounded to two decimal places).....	42
Table 13: Summary of dol and damage reduction through the implementation of NBS measures in the current scenario .....	56
Table 14: Summary of dol and damage reduction through the implementation of NBS measures in the future scenario.....	59
Table 15: Summary of dol and damage increase through climate change .....	63
Table 16: List of shortcomings and obstacles to model UPF with BASEMENT (v2.8) .....	68

## List of abbreviations

CHFSwiss Francs

DEMDigital Elevation Model

DTMDigital Terrain Model

GISGeographic Information System

NBSNature-based solutions

UPFUrban pluvial flood/floods/flooding

# 1 Introduction and state of research

This work aims to assess the applicability of the simulation software BASEMENT (v2.8) for simulating pluvial floods. In addition, a potential hazard reduction through the implementation of nature-based solutions (NBS) on today's parking spots is evaluated. As a proof of concept, this work runs through the entire process once for a neighborhood in the city of Bern. This includes the model setup, the simulation, the post-processing as well as the assessment of the results including a predicted damage reduction potential in Swiss Francs.

The objective of this work originally consisted of only the second part of the current objective formulation. This explains the extensive literature review presented later in this chapter. The simulation in BASEMENT (v2.8) seemed to be only a manageable part of the work and it was assumed that it would not cause too much trouble. However, this turned out to be wrong.

The Swiss Federal Institute of Technology Zurich (ETHZ 2021) developed the freely available simulation software BASEMENT (v2.8) to model river simulations and fluvial flood events. Since precipitation can play a significant role in catchment-wide river analyses, BASEMENT (v2.8) allows adding precipitation as an external water source. However, implementing precipitation as the only water source is not a defined use case for BASEMENT (v2.8). It turned out that there is no indication in the scientific literature or on the software's website, that BASEMENT (v2.8) has ever been used to model urban pluvial flooding (ETHZ 2021). Therefore, an entire simulation workflow had to be developed to accomplish just that.

As the research focus shifted from implementing NBS as a UPF mitigation measure to the simulation process in BASEMENT (v2.8), the research objective was updated. In summary, this paper provides a workflow for modeling UPF using BASEMENT (v2.8) and uses the simulated implementation of NBS as an UPF mitigation measure as proof of concept. The latter is evidence that although it is not an intended application of this software, it is still possible to model UPF. Further motivations for this paper can be found in the corresponding subchapter on page 26.

This chapter summarizes the current research on urban pluvial flooding, the risk it poses and will pose in the future as well as two possible modelling approaches. For a better understanding of the ongoing processes, some basics on urban water management are explained. Then, the concept of NBS is introduced and the connection between UPF and NBS is made. After explaining the measurable effects, the limitations and the co-benefits of NBS, the original idea of implementing NBS on today's parking spots is presented. The chapter concludes with the motivation for this paper, an overview of the case study area and the research questions. The chapter *Data and Methods* presents the complete adapted workflow to model urban pluvial flooding with BASEMENT (v2.8). This includes pre-processing, simulation and post-processing. In addition, all data used is explained and their sources provided. The



chapter *Results* presents the simulation outcomes processed as different hazard parameters. The results are shown per scenario setup, before and after the virtual implementation of NBS and how they are expected to change due to climate change. For better overview, the chapter is divided according to the research questions. The chapter *Discussion* puts the previously presented results into context. It analyzes and critically questions them. The results are, where possible, also set into context with the current state of research. Then, the advantages and disadvantages of the adapted workflow as well as the limitations of this work are presented. As the name suggests, the chapter *Conclusion* concludes this thesis by elaborating on the acceptance or rejection of the hypotheses and providing a research outlook.

### **1.1 Different types of flooding**

Flooding is one of the most prevailing natural hazards worldwide. Nearly 20% of the global population faces direct risks from a 1-in-100-year flooding event (Rentschler and Salhab 2020). However, not all types of flooding are the same. Different types of flooding can be distinguished according to different criteria.

For example, they can be distinguished according to the source of the water and the physical processes that lead to the flooding. In this case, a distinction is made between fluvial flooding, coastal flooding, groundwater flooding and pluvial flooding (Houston et al. 2011). Fluvial floods arise from rivers overtopping their banks. Coastal flooding occurs when sea water enters coastal areas. Groundwater flooding occurs when the ground water level rises after prolonged rainfall. And pluvial flooding is flooding caused by rainfall without the need of an overtopping water body close by.

Alternatively, the types of flooding can be distinguished by the location of the flooding. Depending on the flood site, it is then referred to as urban or rural flooding. A combination of these distinction attributes, e.g. urban pluvial flooding, leads to an even more precise flood definition.

This paper will focus on urban pluvial flooding (UPF), meaning flooding that happens in urban areas due to intense rainfall and a capacity overload of the local sewage system. As is discussed in Houston et al. (2011) and Zölch et al. (2017), it makes sense to specifically focus on UPF since pluvial flooding is more likely to occur in urban than in rural areas. First, urban areas have more impermeable surfaces and are characterized through a removal of vegetation. Both factors lead to the ground being less able to intercept, store and infiltrate water. Second, once a pluvial flood is occurring, the associated risk is much higher in urban than in rural areas due to the density of buildings and people.

To get a better understanding, a look shall be taken at different definitions for urban pluvial flooding. It is important to note that the given overview is not exhaustive. Hammond et al. (2013), who have published a state-of-the-art review on urban flood impact assessment, define urban pluvial flooding as a water overflow resulting from inadequate urban drainage with respect to rainfall in urban areas.

Similarly, Houston et al. (2011:7), who published an extensive report about pluvial flooding in urban areas, define “pluvial (rain-related) floods [as floods] which occur following short intense downpours that cannot be quickly enough evacuated by the drainage system or infiltrated to the ground.” They also emphasize that this type of flooding is less well understood scientifically and less well known to the public. Because pluvial flooding can occur in areas that are not normally susceptible to flooding, there is less awareness (Houston et al. 2011). Therefore, the researchers introduce the term *invisible hazard*.

Falconer et al. (2009:199), who published their research on the technical feasibility of a warning service for pluvial flooding, broadly defined pluvial flooding “(...) as flooding that results from rainfall-generated overland flow and ponding before the runoff enters any watercourse, drainage system or sewer, or cannot enter it because the network is full to capacity.” They further differentiate the term ‘pluvial flooding’ from the term ‘surface water runoff’. Surface water runoff is a more general term. It describes different types of flooding that can occur simultaneously in urban areas during intense rainfall. It includes pluvial flooding, sewer flooding, fluvial flooding (also from small watercourses) and groundwater flooding, e.g. from springs (Falconer et al. 2009).

The term urban pluvial flooding further needs to be distinguished from the term flash flood. Flash flooding is also associated with high-intensity rainfall and is defined by its short time scale, especially with a sudden onset (Kron 2002). Flash floods can occur in any area. The soil doesn’t have to be saturated. The rainwater intensity is simply exceeding the infiltration capacity. However, cited definitions in research literature are discordant whether flash floods need to emerge from an existing water course or not. While some definitions simply require heavy rainfall and a fast onset (Kron 2002), others imply a watercourse from which the flash flood can emerge from (Falconer et al 2009). Therefore, dependent on the applied definition, UPF can be a flash flood, but it doesn’t have to be one. Conclusively, urban pluvial flooding is a specific type of flooding that happens in urban areas, is triggered by intense rainfall, does not need a water body close by and is a result of sewer capacity exceedance.

Houston et al. (2011) explain that pluvial flooding is usually associated with short but high-intensity rainfalls. However, there is no uniform definition of *heavy precipitation* (Axelsson et al. 2021). The phenomenon of very intense but short rainfall events are also known under different names such as cloudburst, torrential rain and downpour (Rosenzweig et al. 2019). Houston et al. (2011) specify such short-duration storms as lasting up to three hours and exhibiting rainfalls of more than 20-25 mm/hour. However, pluvial flooding can also result from low-intensity rainfalls that last for a while. Houston et al. (2011:15) specifically mention rainfalls of 10mm/hour over longer periods. The latter pose an elevated risk if the surface is impermeable. This can be due to urbanization processes or because the ground is saturated or frozen.

## 1.2 Definition of (flood) risk

Since this paper follows a modeling approach, a quantitative risk analysis approach is chosen. Risk itself is a very complex and multifaceted concept and there is no globally accepted definition of risk. Schneiderbauer and Ehrlich (2004) published an extensive review of definitions and concepts of risk, hazard and people's vulnerability to natural hazards. After listing half a dozen different scientific definitions of natural hazard risk, their definition of risk is the following: "The probability of harmful consequences or expected losses resulting from a given hazard to a given element at danger or peril, over a specified time period. (Schneiderbauer and Ehrlich 2004:9)"

Regardless of what specific definition is used, risk is always a combination of several factors. Also, the risk of a natural hazard is time and place specific. A widely accepted concept of risk in natural hazard research is the risk triangle introduced by Crichton (1999). It can also be described as a formula.



$$\text{Risk} = \text{Hazard} \times \text{Exposure} \times \text{Vulnerability}$$

Figure 1: The Risk Triangle and the associated formula (own illustration after Crichton 1999)

The idea behind the risk triangle is that increasing one side of the triangle automatically increases the size of the entire triangle, also known as the risk. The same is true for increasing one of the factors in the associated formula.

The elements at risk can be freely determined. For example, it can imply loss of life, damage to infrastructure or economical loss. This formula is specifically used for flood risk by Kron (2002):

$$\text{Flood Risk} = \text{Hazard} \times \text{Exposure} \times \text{Vulnerability}.$$

The formula adapted by Kron (2002) is complemented with definitions for the variables. The hazard variable comprises the natural event itself and the probability of its occurrence. The exposure variable contains all values and humans that are present at the involved location. The vulnerability variable describes the lack of resistance to the incoming damaging forces. Kron (2002) also illustrates how the risk formula can be shortened to two factors. Thereto the exposure variable and the vulnerability variable are combined into a single consequences variable. This consequences variable is then multiplied with the probability of the hazard occurring.

$$\text{Flood Risk} = \text{Consequences} \times \text{Probability of occurrence}$$

### 1.3 The risk of urban pluvial flooding

In order to avoid confusion, the distinction between *hazard* and *risk* in the context of urban pluvial flooding is explained. The *hazard* of flooding only involves measurable characteristics of the flood event such as flow depth, flow velocity, flood duration and water quality. The *risk* of UPF, on the other hand, comprises the hazard, its likelihood to occur, the exposure and the vulnerability to the hazard. It can be assessed on individual, household or community level (Houston et al. 2011).

UPF poses some very distinct risks for society. First, the extent and resulting effects of UPF are difficult to assess. Unlike other types of flooding, there is no designated floodplain. Urban flooding can occur in any local depression (Houston et al. 2011). Second, UPF is often a result of intense precipitation. However, extreme weather events such as short-term heavy rainfall are difficult to predict (Moon et al. 2019). Third, UPF can occur very quickly, meaning there is not enough warning time (Houston et al. 2011).

Once UPF occurs, the associated risks are numerous. Like any type of flooding, it can pose a risk to life and result in property damage, power outages and obstruction of transport infrastructure (Hammond et al. 2013, van Dijk et al. 2014). The damage risk depends on flood characteristics such as flow depth and flow velocity (Hammond et al. 2013). In particular, the relative elevation of the doorway threshold to street level is critical in assessing potential damage (Falconer et al. 2009).

Focusing on flow depth, Rentschler and Salhab (2020) identify 0.15 m as the threshold between low and high flood risk. However, to obtain risk as result of the inundation depth, a vulnerability function must be considered in the calculation. In the absence of such a vulnerability function, it is advised to refer to the different inundation depth categories as flood *hazard* classifications. The flood hazard classification gradations used for this work can be found in Figure 2.

Flood Hazard Classification		Inundation Depth [m]
Low Hazard	No Hazard	0
	Low Hazard	0 – 0.15
High Hazard	Moderate Hazard	0.15 – 0.5
	High Hazard	0.5 – 1.5
	Very high Hazard	> 1.5

Figure 2: Flood Hazard Categories (own illustration after Rentschler and Salhab 2020)

While potential flow depth is considered to be the critical factor for damage to buildings and infrastructure, flow velocity must also be considered when assessing risk to pedestrians (Falconer et al. 2009). A study conducted by Martínez-Gomariz, Gómez and Russo (2016) illustrates the relationship between flow depth and flow velocity posing a danger to pedestrians. Their conclusion is a hazard function that is the product of the flow velocity  $v$  and the flow depth  $y$ . The researchers establish an instability threshold for this hazard function at  $(v \times y) = 0.22 \text{ m}^2/\text{s}$ .

Exceeding this threshold is associated with a loss of stability for pedestrians. In addition to this formula, all flow velocities near or above 2 m/s are considered limits, as they pose a significant hazard to adults, regardless of flow depth. In addition, flow depths above 0.5 m and 1.2 m are the limiting depths for children and adults, respectively. However, because many factors such as physical condition, type of footwear, freedom of hands, and visibility affect a person's ability to stand, the hazard formula and the resulting values should be treated with caution (Martínez-Gomariz, Gómez and Russo 2016).

Another major factor in the risk assessment of UPF is the urban stormwater drainage system. While it is specifically designed to transport away heavy rainfall, its capacity can be exceeded during extreme weather events. Additionally, the condition of the urban stormwater management system can add to the risks specifically associated with UPF. First, insufficient maintenance of the sewer system can lead to a capacity reduction. Second, old stormwater drainage system might be undersized. Third, the entrances of the sewer system can be blocked during heavy rainfall. This can lead to water not being able to enter the stormwater system at all, or at least only at a reduced capacity (Houston et al. 2011). Fourth, if the pressure on the sewer system is too big or the conveyance capacity is surpassed, water can spill out of manholes and gullies (Bulti and Abebe 2020, Jamali et al. 2018). A very unfortunate circumstance is presented when the storm water and the foul water sewers are a combined system. In that case, an exceedance of the sewer capacity leads to a mix of untreated sewage and rainwater spilling out to flood the urban area. This poses serious health risks (Houston et al. 2011).

The risks associated with UPF are multifaceted and difficult to quantify. A popular approach to capture the different costs, which are a consequence of the risk, is a 2x2 matrix called the total cost matrix. This matrix forms an inherent part of the integrated disaster risk assessment. The total cost matrix differentiates between direct and indirect as well as between tangible and intangible costs (Giupponi et al. 2015). Direct costs are costs monocausally attributed to the hazard. Indirect costs cover all costs resulting downstream in the process chain of the hazard. Tangible costs are costs that can be quantified in monetary units. Intangible costs are costs that cannot be transferred into a monetary equivalent. For a better understanding, the total cost matrix with examples is shown in Figure 3 on page 12.

Traditionally, risk assessments have only taken direct tangible costs into account (Giupponi et al. 2015). However, especially when indirect and intangible costs are taken into consideration, it becomes clear that UPF can lead to great financial, environmental and social damages (Axelsson et al. 2021). Financial damages cover the direct tangible costs but also potential additional costs that can arise from business disruption and supply chain shocks (Jongman 2018). This can also include blocked transport infrastructure or power lines. Such public infrastructure networks are often built along streets, which are known to be prone to flooding (Hobbie and Grimm 2019). Social damages can result from several sources such as an interruption of transport networks (Rosenzweig et al. 2019), the loss of a sense of

security and impacts on mental as well as physical health through experiencing climate-change-related hazards (Hobbie and Grimm 2019).

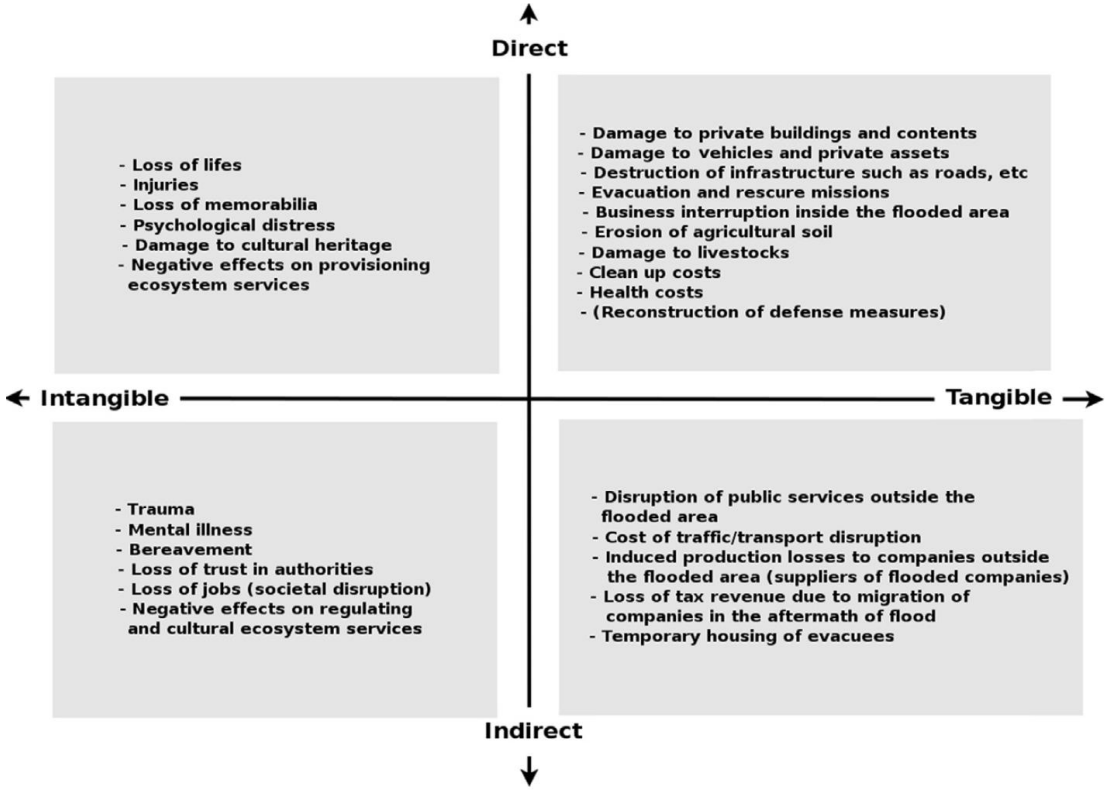


Figure 3: The Total Cost Matrix. Copied from Giupponi et al. 2015: 174.

**1.4 Increased risk of urban pluvial flooding in the future**

Two current processes are thought to further increase the risk of urban pluvial flooding in the future. The first process is the ongoing urbanization all around the world and the second one is climate change (Hammond et al. 2013). Both processes are largely irreversible transformations (Jiang et al. 2018).

In 2018, 55% of the global population lived in urban areas. This share is projected to increase to 68% by 2050 (United Nations 2019). Angel et al. (2011a) show that cities currently expand twice as much in area than in population. More people in urban areas will lead to further development within cities. Structural development is likely to replace green spaces with impermeable surfaces. Additionally, Houston et al. (2011) point out how urban development processes can add to the danger. They use the term ‘urban creep’ to summarize in-city developments that turn green and absorbent surfaces into impermeable surfaces. Urban creep includes paving over gardens, property extensions and urban ‘in-fill’ development. An increase in the share of impermeable surfaces inevitably heightens the risk for UPF.

Van Dijk et al. (2014), with reference to a paper written in Dutch by Kluck (2011), add that there are two more factors of current urban development that let the urban drainage systems overflow more frequently during heavy rainfall. First, space for water storage on streets is decreasing. Second, there

is a continuous reduction in the surface level differences between buildings and the street. All of the factors listed above increase the risk of blocked roads and flooded properties.

The other ongoing process that can increase the risk of UPF is climate change. Falconer et al. (2009) state that the phenomenon of pluvial flooding appears to be increasing. The cause seems to be climate change and therefore a further increase in the future is likely (van Dijk et al. 2014). Huang et al. (2020) convey that UPF events have increased compared to past decades. They accredit this phenomenon to the more frequently occurring extreme precipitation events resulting from climate change. It has to be considered that hydrological impacts of climate change will differ in magnitude and be spatially and temporally variable (Hobbie and Grimm 2019). However, the Intergovernmental Panel on Climate Change (IPCC 2013: 23) states that “[e]xtreme precipitation events over most of the mid-latitude land masses [...] will *very likely* become more intense and more frequent by the end of this century, as global mean surface temperature increases”. As extreme precipitation increases, the risk of pluvial flooding increases as well. Houston et al. (2017:7) single out pluvial flooding as the type of flooding “[...] most likely to increase in severity as a result of climate change”. While the course of climate change certainly has an impact on the future UPF risk, the exact increase in temperature seems to be of little importance. In a study that compared future flood risk in Europe under different climate scenarios (+1.5°C, +2°C and +3°C until the end of the century) it was shown that “[i]n most countries in Western and Central Europe, all models consistently predict a relevant increase in future flood impacts. (Alfieri et al. 2018: 12)” This is accompanied by a predicted 80% increase in damages (Alfieri et al. 2018).

It is foreseen that minor events leading to UPF will become more frequent and extreme events more severe (Rosenzweig et al. 2019). Altogether, an increase in UPF events is commonly accepted in scientific literature (e.g. Falconer et al. 2009, Zellner et al. 2016, Jiang et al. 2018). Research must be carried out in order to better understand the emerging risk from UPF. The assessment of damages caused by UPF events can either consist of ex-ante or ex-post techniques (Hammond et al. 2013). Ex-ante assessment techniques produce a forecast and estimate expected damages. In contrast, ex-post assessment techniques quantify the observed damages after an event has struck.

As UPF is likely to occur more frequently and in stronger intensities in the future, this paper will only focus on ex-ante assessment techniques. Since a clearly defined floodplain is missing in pluvial flood events, the location of interest has to be flooded virtually in order to identify the associated risk (Houston et al. 2011, van Dijk et al. 2014). This can be achieved through modelling.

### **1.5 Modelling urban pluvial flooding**

In order to model urban pluvial flooding, a closer look shall be taken at the process leading to the flood event. Bulti and Abebe (2020) nicely describe the rainfall-runoff-relation in urban areas in their review of flood modeling methods.

The initial process is rainfall, a specific form of precipitation. It falls from the sky onto the surface and is disclosed in mm/h. It is important to note that not all precipitation is converted to runoff. Initial and continuing losses reduce the rainwater amount that will turn into runoff. Initial loss consists of all the rainwater that is held back on buildings, on vegetation and in surface micro-depressions. Initial loss happens in vegetated areas, on permeable and impermeable surfaces. Overland runoff is only created if the amount of rainfall exceeds the initial loss (Loucks and van Beek 2017). Continuing loss is the amount of rainfall that is subtracted from the runoff because of infiltration and evapotranspiration (Bulti and Abebe 2020). Surface flow is only generated if the total rainfall exceeds initial and continuing loss. The surface flow then enters the drainage system. The runoff is steered by urban micro topography such as streets and natural depressions and flows in so called flow paths. In that state it is called gutter flow. After entering the sewer system through gullies or manholes, the runoff is called pipe flow (Bulti and Abebe 2020).

Only once the conveyance capacity of the pipe network is exceeded, the event is classified as a pluvial flood. A pluvial flood can either occur because not all the surface flow water can enter the drainage system or because the pipe drainage system is overloaded and spills out onto the street. Also, a combination of these two processes is possible (Bulti and Abebe 2020).

The drainage system comprises of two parts. The minor drainage system is the underground sewer pipe network. It is designed to transport away storm water efficiently. It is designed for rather frequent events. The major drainage system is the sum of the features that determine flow routes on the surface. It is made up of objects not initially designed to steer water, for example roads and walking paths. It does not only steer the water but also store it temporarily, e.g. on playing fields. The connection points of these two systems, namely the inlets such as manholes and gullies, are vital parts of the UPF analysis (Bulti and Abebe 2020).

Modelling urban pluvial flooding is not easy. Due to the many influencing factors and the general uncertainty, it is difficult to map the extent of UPF (Houston et al. 2011). There are several different methods to attempt to model such flood events. Regardless of the chosen modelling technique, some uncertainty and weaknesses are always incorporated (van Dijk et al. 2014). There is a lot of research literature about flood modelling, even specifically about UPF events. Some common major concerns, limitations or possible stumbling blocks can be identified. First, Mark et al. (2004) found that modelled urban areas need to have a high spatial resolution in order to produce good results. They recommend using a digital elevation model (DEM) with a spatial resolution of 1mx1m for urban flood analysis. Additionally, in order to correctly model the storm water flow path, critical height differences in urban water management infrastructure should be incorporated into the DEM. Among others, this includes street and curb levels (Houston et al. 2011). Second, the drainage capacity of the sewer system strongly affects the amount of surface water flow. However, this drainage capacity is difficult to model



(Houston et al. 2011). Additionally, the gullies or manholes could be blocked during an extreme rainfall event (Zellner et al. 2016). This increases the complexity to model the sewer system capacity. Third, the discharge behavior of unpaved areas is difficult to model. It depends on several factors such as “[...] soil conditions, slope, vegetation and precipitation characteristics (van Dijk et al. 2014: 4)”. Fourth, models using a DEM tend to miss tunnels and underground passages which, however, play a vital role in urban water management (van Dijk et al. 2014). Fifth, UPF models are predictive and most of them have not been validated yet (van Dijk et al. 2014). Since extreme precipitation events are likely to increase in magnitude, it is impossible to have such events validated at this point in time. Finally, the urban area is exposed to permanent change. Thus, in order to stay relevant and meaningful, UPF predictions need to be repeated periodically (van Dijk et al. 2014). Houston et al. (2011) further point out that different methods and data used produce different estimates of the pluvial flood risk extent. Such inconsistent flood risk maps hinder effective urban water management.

Regardless of the methods and variables used, it needs to be determined what combination of flow velocity and flow depth of a flood event is considered dangerous and what hazard return period is considered during the modelling phase. While attempts to determine critical values have been made, there is no clearly defined value for either of them (Rentschler and Salhab 2020 and Martínez-Gomariz, Gómez and Russo 2016). However, potential flood depth and velocity are important in quantifying the risk posed by urban pluvial floods. They affect the risk to human life and the extent of damage to buildings (Falconer et al. 2009).

Van Dijk et al. (2014) published a comparison of two model techniques for modelling UPF. They make a distinction between GIS-analysis (GIS: Geographic Information System) and coupled 1D-2D modelling. The GIS-analysis calculates flow paths based on a DEM and highlights local depressions in which pluvial flooding can occur. Generally, it does not consider the sewer system. However, the simulation operator can choose the value of the simulated rainfall as the actual rainfall less the sewer system capacity (see also: *excessive rainfall* on page 16). The advantages of a GIS analysis are the little modelling expertise required, the moderate effort and the short computation time. However, these advantages come at a cost. The disadvantages of simple GIS-analyses are numerous. First, they do not represent the interaction between the pluvial flooding in the urban area and the sewer system. Second, GIS analyses usually determine the preferred flow path only, ignoring uncertainty over several flow path options. Third, a GIS analysis only determines flow paths and flow depth but not flood duration.

Van Dijk et al. (2014) also evaluate coupled 1D-2D simulation models. They are composed of a 1D-part, namely the sewer system, and a 2D-part, namely the urban surface. Unlike the GIS-analysis, the urban surface is not just represented as a DEM but often as a Triangulated Irregular Network (TIN) in which cells can interchange water. The 1D part of the model is coupled with the 2D part through manholes

and gullies. The advantage of this modelling technique is that they currently provide the best modelling results for UPF. However, the computational effort and required technical knowledge is a multiple of that of GIS-analyses. Furthermore, while this modelling technique gives seemingly very good and exact results, there is still a lot of uncertainty. The physical processes that need to be modelled are very complex and calibration values are often missing. Additionally, while it is an improvement that the sewer system is taken into consideration, possible blockages of gullies are ignored. However, as discussed before, gully blockages can be one of the main drivers of UPF. The last mentioned disadvantage is that the sewer system is represented one-dimensionally, meaning that the influence of sewer capacity exceedance leading to urban pluvial flooding is ignored.

Bulti and Abebe (2020) published an even more extensive review on flood models. They examined six different flood modeling approaches ranging from simple 1D-models to coupled 2D-models. They confirm the previously listed results. The more factors and dimensions considered, the higher the accuracy for flood risk analysis. However, computational time and required modelling expertise go hand in hand with the higher accuracy.

As can be seen in both reviews the coupled and multidimensional models deliver the most accurate results (van Dijk et al. 2014, Bulti and Abebe 2020). A coupled model takes into account the interaction between the major and the minor system. It does this at the expense of computing time and accuracy. In order to identify the modelling approach best suited for the present needs, a closer look shall be taken at the role of the minor system.

It is widely acknowledged that an exceedance of the sewer capacity during an intense rainfall event leads to urban pluvial flooding (Huang et al. 2020). The mentioned capacity mainly depends on the structure of the sewer system (Coutts et al. 2012). Thus, thorough modelling practices seemingly require the incorporation of the subsurface pipeline network. In opposition to this assumption, Falconer et al. (2009) postulate that sewer capacity exceedance is a prerequisite for UPF. Therefore, the consideration of the storm water drainage system is of secondary importance. It is safe to assume that a rainfall leading to UPF exceeds the discharge capacity. Therefore, modelling intense rainfall events and their possible UPF risk can be based on the *excessive rainfall*. The *excessive rainfall* is the entire amount of precipitation less the sewer system capacity. So it seems that considering the minor system as a whole rather than in detail does not drastically degrade the results of an UPF model.

The BASEMENT (v2.8) simulation program used in this work has the potential to be used for a coupled 1D-2D modeling. However, in the simulation performed for this work, the coupling with the 1D part was replaced by using the *excessive rainfall* approach. The calculations are based on a TIN and flood-specific characteristics of the simulation area can be inserted into the model. The built-in complexity yields more accurate results than a simple DEM analysis. However, modeling expertise is required to

get the simulation working. More information about the software can be found in chapter 2 *Data and Methods* on page 29.

A general conclusion is that a modelling approach must be chosen that satisfies the criteria for accuracy but does not exceed run-time, computation capacity and modelling expertise. Before turning to the research questions of this paper, some more information about urban water management and nature-based solutions is provided.

## **1.6 Urban water management**

Generally, urban stormwater management is very complex. It has a long history and is constantly evolving (Jiang, Zevenbergen and Ma 2018). An important role in the management of urban pluvial flooding is held by the urban drainage system. Once a heavy rainfall event is taking place, it is the purpose of the drainage system to safely steer the water out of the urban area.

Houston et al. (2011) postulate that pluvial flooding, compared to coastal and fluvial flooding, is more likely to be manageable by appropriate infrastructure measures. Nevertheless, the researchers point out that it is impossible to have all the stormwater transported away by the sub-surface drainage network during an extreme rainfall event. Therefore, a certain amount of surface flow must be accepted. However, at least in theory, it would be possible to design the microtopography of an urban area so that no stormwater would accumulate in areas where it poses a danger. It would be possible to create safe flow-routes for stormwater to drain out of the urban area without posing a threat or being too disruptive. Suggested measures to channel the water to a safe outlet are microtopography alterations such as raised curb heights along specific roads (Houston et al. 2011).

A non-negligible aspect of present-day stormwater management is that current infrastructure is outdated. It was dimensioned for old assumptions and built using old techniques (Hobbie and Grimm 2019). Climate change is foreseen to bring intense extreme events more often and at an increased scale (Hobbie and Grimm 2019). As surface flow must be accepted already now, the predicted increase in heavy precipitation events as a result of climate change is merely adding to the challenge (Houston et al. 2011).

While urban stormwater management used to be primarily an engineering problem, it has progressed to a much more holistic challenge. As Jiang, Zevenbergen and Ma (2018) explain, urban stormwater management is nowadays required to cover multiple dimensions including nature protection, residential recreation, sustainable water use and aquatic ecology. Such a paradigm shift is accompanied by expanded requirements for the management of urban stormwater. They include in-depth knowledge about urban hydrology, landscape imperviousness and its hydrological impact, stormwater runoff dynamics, available technical measures and their performance, spatial

heterogeneity and adaptability, catchment and basin effect, management strategy, and reliable hydrological modeling assessment.

As part of the evolving development of urban stormwater management, a shift from traditional grey infrastructure to blue-green infrastructure is promoted (Axelsson et al. 2021). The grey infrastructure refers to concrete infrastructure aiming to remove rainfall water out of urban areas. In contrast, the blue-green infrastructure refers to infrastructure that mimics the rainwater reaction behavior of natural landscapes.

### **1.7 Nature-based solutions in the context of hydrology**

The previously mentioned transformation in stormwater management towards the more holistic approach and blue-green infrastructure is part of the concept of nature-based solutions (NBS). The concept itself is very broad, and multiple different definitions are used. A very general definition is presented by Cohen-Shacham et al. (2016:xii):

*“Nature-based Solutions (Nbs) are defined by IUCN [International Union for Conservation of Nature and Natural Resources] as actions to protect, sustainably manage and restore natural or modified ecosystems, which address societal challenges (e.g. climate change, food and water security or natural disasters) effectively and adaptively, while simultaneously providing human well-being and biodiversity benefits.”*

The European Commission (2015) dedicates an entire half page to the definition and limitation of the concept of nature-based solutions. It defines NBS as solutions that help society to address several simultaneously occurring challenges at once. They should sustainably help to solve environmental, social and economic challenges. The mentioned solutions are “[...] inspired by, supported by or copied from nature [...] (European Commission 2015: 24)”. The actions are defined such that they are mimicking, applying or manipulating the complex behavior of nature. Two of many desirable attributes of natural landscapes are carbon storage and water flow regulation. NBS are means to incorporate these advantages into urban areas by urban planners and engineers. Among benefits such as an environment that improves human well-being and socially inclusive green growth, NBS aim to reduce disaster risk. Additionally, NBS is said to be change-resilient, cost-efficient and conservative on resource consumption (European Commission 2015, Huang et al. 2020). However, NBS are not a one-size-fits-all. For NBS to unfold their full potential, they must be adapted to local conditions (European Commission 2015).

Hobbie and Grimm (2019) set a slightly different focus in their definition of NBS. Instead of mimicking or learning from nature, they define NBS as strategies “[...] which use living organisms, soils and sediments, and/or landscape features to reduce climate change hazards [...] (Hobbie and Grimm 2019: 1)”. In Hobbie and Grimm’s (2019) definition, unlike the European Commission’s (2015) definition, NBS do not only pick out single favorable traits of natural ecosystems that should benefit

urban areas, but the goal is to restore holistic aspects of natural ecosystems. According to the researchers, NBS are supposed to be more flexible, multi-functional and adaptable compared to traditional urban engineering measures. These advantages are even more important in the face of an uncertain and non-stationary climate future (Hobbie and Grimm 2019).

NBS can also be very broadly defined as “[...] solutions to societal challenges that are inspired and supported by nature (Raymond et al. 2017: 15)”. As such, NBS bring nature back into urban areas. And nature comes with many positive attributes. Whether the positive attributes of natural landscapes are implemented directly or come as a secondary benefit is of lesser importance. It is important to note, however, that NBS can incorporate or be designed to mimic several different aspects of nature, not only from the hydrological sphere. However, this paper will only focus on hydrology-based NBS. From this point on, the term *NBS* refers to hydrology-related NBS.

NBS, their approaches and implementation technologies have evolved in different parts of the world and under different conditions. Therefore, they are known under different names. Cohen-Shacham et al. (2016: xii) refer to NBS as “[...] an umbrella concept that covers a range of different approaches.” The technologies and frameworks have names such as *Low Impact Development*, *Best Management Practices*, *Water Sensitive Urban Design*, *Sustainable Urban Drainage System*, *Green (Stormwater) Infrastructure* and *Sponge City*. While each of these concepts has its own origin, history, definitions and limits, their differences are marginal and thus negligible in the context discussed at hand. In this paper, they are all treated as one. For interested readers, the paper by Huang et al. (2020) is recommended. It offers a very extensive and understandable overview of the different terminologies.

NBS represent a whole set of new features and possibilities in urban stormwater management. They incorporate features from natural landscapes into urban areas to reduce disaster risk. Furthermore, NBS are thought to have the potential to provide the same effect against flooding as grey infrastructure, while also providing additional ecosystem services at no additional cost (Huang et al. 2020). They are further attributed with self-regulating properties that could be especially useful as storm characteristics are changing (Green et al. 2021). It is foreseen that NBS can enhance urban development in general and strengthen the resilience of urban areas. The importance of NBS is also represented by the big role they are attributed to in achieving the Sustainable Development Goals (Huang et al. 2020).

Blue-green Infrastructure can be understood as an implementation instrument for NBS and the antagonist to grey infrastructure (Krauze and Wagner 2018). It is seen as an economically more viable management method than traditional stormwater infrastructure (Jayasooriya and Ng 2014). According to Krauze and Wagner (2018), blue-green infrastructure is resilient whereas grey infrastructure isn't. This is supported by Green et al. (2021) and Huang et al. (2020) who proclaim the transition from *flood defense* to *flood resilience* as a paradigm shift in stormwater management.

However, this transition is not easy to implement. While knowledge about sewer systems is continually growing, old sewer pipes, designed with outdated techniques, are still in use. It is impractical to retrofit an entire city's subsurface drainage pipe network as scientific understanding is evolving. It would lead to exorbitant costs and the disruptions for the urban area would outweigh the benefits (Houston et al. 2011).

Therefore, grey and blue-green infrastructure co-exist. The goal of urban engineers must therefore be to find ways in which grey and blue-green infrastructures can optimally complement each other and how a smooth transition to modern urban stormwater management can be achieved (Cohen-Shacham et al. 2016, Houston et al. 2011). It is suggested that opportunities such as introducing new technologies and retrofitting critical points in the sewer system should be used when roads are dug up for other work or when urban areas are being resurfaced (Houston et al. 2011).

In order to stay within the scope of this paper, only NBS approaches specifically concerning urban pluvial flooding will quickly be presented. It is important to note that replacing or supplementing grey infrastructure with blue-green infrastructure can fundamentally change the stormwater management (Huang et al. 2020).

### **1.8 Pluvial flooding and nature-based solutions**

When it comes to urban pluvial flooding, NBS have two main goals. To control runoff volumes and to reduce peak flows (Huang et al. 2020). Additional benefits can be an improvement of the water quality and the maintaining of natural waterways in cities. These goals are thought to be achieved through natural retention, detention, infiltration and drainage (Huang et al. 2020).

Different infrastructure elements aiming to achieve these processes can be attributed to NBS. Green roofs, infiltration trenches, permeable/porous pavement and vegetable swales are some of them (Huang et al. 2020). According to Jayasooria and Ng (2014), some of the most used NBS for urban stormwater management are trees, green roofs, rain gardens, permeable pavements, native vegetation and swale systems. These elements, once implemented, become part of the urban ecosystem and the urban hydrological cycle (Huang et al. 2020). The positive effects of urban trees, for example, result from several characteristics. They include canopy interception as well as an increase in evapotranspiration and infiltration (Zölch et al. 2017). The positive effects of rain gardens and permeable pavements result from a reduced share of sealed surfaces and, as a consequence, higher infiltration of rainwater into the ground (Zölch et al. 2017).

For an understandable overview of the mode of operation of different NBS measures, the reader is again directed to the overview study of Huang et al. (2020). There, the mechanisms of some selected NBS measures are described. Another very informative source of mechanisms of NBS approaches is the paper published by Coutts et al. (2012).

With the current state of research, it is not clear which NBS measures have the biggest effect on effectively mitigating urban pluvial flood risk (Zölch et al. 2017). In general, a certain diversity in flood risk management approaches is considered to be positive (Priest et al. 2016). What can be said with certainty is that regardless of how much water exactly can be retained or evapotranspired by implemented NBS, a reduction in available water for surface flow inevitably reduces the pressure on the sewer system. With reduced surface flow, the sewer system has less water to handle and hence the risk for UPF is decreased (Zölch et al. 2017).

NBS approaches, such as the introduction of permeable surfaces or gravel filtration beds, can lower the risk of UPF (Houston et al. 2011). However, once an UPF event is taking place, i.e. the sewer system capacity is exceeded, overflow water has to be managed at the surface. Therefore, a sensible combination of grey and blue-green infrastructure is advocated to manage urban pluvial flooding (Houston et al. 2011).

In terms of grey infrastructure, this may mean alterations to the micro-topography to create safe flow routes for the stormwater (Houston et al. 2011). In terms of blue-green infrastructure, the concept of Sustainable Urban Drainage Systems (SUDS) is suggested (Houston et al. 2011). SUDS are also an implementation strategy for NBS. A main component of SUDS is the decrease of impermeable surfaces and an increase in porous surfaces in urban areas (Lashford et al. 2019). This would allow for water to infiltrate and attenuate run-off during a rainfall event.

A rather new but attention-grabbing approach is the concept of *Sponge Cities*. It was introduced in 2014 by the Chinese government (Jiang et al. 2018). *Sponge Cities* are seen as a holistic approach concretely focusing on lowering the risk for UPF while improving ecosystems, ecosystem services and the environment (Jiang et al. 2018). The *Sponge City* water management approach aims at reducing stormwater runoff compared to conventional urban water management through increased infiltration and evaporation (Lashford et al. 2019). The *Sponge City* approach relies on both blue-green infrastructure as well as traditional water management technologies and can be described by six words: infiltrate, detain, store, cleanse, use and drain (Jiang et al. 2018, Lashford et al. 2019).

Generally speaking, the *Sponge City* approach aims at rebuilding sponge-like attributes of natural landscapes. The goal is to manage rainwater efficiently, carefully and sustainably. Rainfall shall be retained during rainfall events, thereby alleviating the risk for UPF (Jiang et al. 2018). And like a sponge, the stored rainwater shall be redistributed during dry times. The overall goals for this approach are an increased water resilience and sustainable urban development (Jiang et al. 2018).

When it comes to UPF, water is often solely seen as a hazard. And thus, the attention lies in steering the stormwater out of the urban area as fast as possible. This paradigm is also followed by traditional water management. However, water is also a valuable resource (Houston et al. 2011). Especially

rainwater can be used for many non-potable uses (Houston et al. 2011). Therefore, NBS in general and Sponge Cities in particular extend their stormwater management to releasing the water at a given opportune time. The stormwater release adds a new dimension to urban water management. This function will gain importance as climate change will make heat waves and drought periods more likely (IPCC 2013). However, this paper will only focus on reducing peak flows during UPF. The newly added dimension of water release shall be mentioned but not investigated any further.

### **1.9 Measurable effects of nature-based solutions**

Measuring the exact results of specific NBS-measures poses two major challenges. First, the concrete benefit of NBS that have already been implemented in cities is difficult to measure during extreme rainfall events. It might be possible to quantify the overall risk reduction, but it is not possible to split the shares according to the individual NBS measure. Second, while many approaches are well researched in scientific literature, and their positive effects can be demonstrated using modelling, it is not clear to what extent the results can be reproduced in real life. In addition, the effectiveness of NBS heavily depends on the magnitude of the event as well as the spatial scale of implemented NBS (Green et al. 2021). The lack of robust results makes it difficult to assess the sustainability of NBS as urban flood mitigation infrastructure (Green et al. 2021). Keeping these limitations in mind, a look shall be taken at some published results that try to quantify the tangible effects of NBS in stormwater management to reduce urban pluvial flooding.

It was shown that rainwater can be held back on site by NBS measures. In a study conducted by Dietz (2007), for example, green roofs and pervious pavements showed successful retention of stormwater. Green roofs have shown to retain between 60% and 70% of the rainfall water amount in different climates. The same study found that pervious pavements still keep some retention capacity with frost. This allows NBS to mimic pre-development hydrologic function (Dietz 2007).

In a different study, published by Armson, Stringer and Ennos (2013), it was found that on a 9 m<sup>2</sup> plot, grass could eliminate surface runoff completely. Also, trees with their associated tree pits were able to reduce runoff by 62% compared to asphalt.

In the study conducted by Zölch et al. (2017), the decrease in urban runoff was measured against a baseline scenario. The baseline scenario is a traditional apartment block equipped with a few trees in Munich, Germany. The study reveals that the runoff reduction increases proportionally with the number of trees, the share of green cover and permeable surfaces. The biggest effect was achieved when all the roofs were turned into green roofs. In that case, the overall surface runoff was reduced by approximately 15%. This study provides empirical evidence that greening approaches with trees and green roofs have a positive but very limited effect.



The big difference in runoff reduction potential is not surprising in this field of research. Huang et al. (2020) published a detailed overview over various efficiency studies of NBS in the context of UPF. The studies show that NBS could reduce peak flow and runoff volumes, however, the reduction amount is not consistent among the different studies and study areas. The cited results range from less than 1% to 92% in runoff reduction and from just above 1% to 92% in peak flow reduction. A pattern, however, that is consistent among most cited studies is the decreased runoff and peak flow reduction potential with increased rainfall intensity (Huang et al. 2020). This hypothesis is also supported by Green et al. (2021). They argue that green infrastructure has the potential to reduce frequent low- to moderate-intensity flooding. And if the measures are applied at a very large scale, e.g. catchment-wide, a risk reduction can be expected even for extreme events. However, this is less likely in an urban setting.

### **1.10 Limitations of nature-based solutions**

One of the mentioned limitations concerns NBS as a concept. It is very broad, thus, it is not clear what is included and what is not. Krauze and Wagner (2019) even describe the concept as under-defined. As NBS are an umbrella concept of multiple approaches, it is difficult to compare results of specific studies. For example, it is not clear whether pervious pavement is part of NBS or not. While it is attributed to NBS in some studies (Huang et al. 2020, IUCN Water 2021), it is listed as grey infrastructure in other studies (Hobbie and Grimm 2019). This lack of operational clarity lowers the credibility of this rather young concept (Cohen-Shacham et al. 2016). It is further stressed that there is no consistent research-based design tool to model the effects of NBS (Dietz 2007) and that implementing several interacting NBS is very complex (Jiang et al. 2018). Apart from theoretical limitations, there are also some practical limitations to specific NBS implementations.

NBS need space. And space is a very scarce resource in urban areas. Hobbie and Grimm (2019), for example, point out that urban areas might be limited in the amount of space they can offer for vegetation roots. Also, soils are likely to be compacted in urban areas (Hobbie and Grimm 2019). Lashford et al. (2019) point out that implemented NBS also require maintenance, just like grey infrastructure. If not maintained properly, NBS implementations will decrease in their efficiency.

It has been shown that NBS need to be implemented at a large enough scale to serve its purpose. One study showed that NBS can only work effectively if NBS measures have been implemented in more than 10% of the urban area (Zellner et al. 2016). However, in order to be beneficial in larger storms, the required spatial share would need to be doubled or tripled (Zellner et al. 2016). Studies generally suggest that NBS have considerable effects on moderate rainstorms but fail to dampen the effects of extreme or even catastrophic events (Hobbie and Grimm 2019, Huang et al. 2020). As climate change is likely to increase the intensity of storms, NBS might have limited capacity to decrease the risk of urban pluvial flooding.

To implement the best urban stormwater management, it is proposed to carefully combine NBS and grey infrastructure. The complementary conjunction of these two approaches is also referred to as *hybrid water management* (Jongman 2018). However, Green et al. (2021), who also believe that an integrated approach is needed to mitigate the risk of pluvial flooding in cities, point out that too little research has been done on the interaction between gray and blue-green infrastructure. This is despite the fact that understanding them would be critical, especially in light of the uncertain climatic future.

### **1.11 Co-benefits of nature-based solutions**

It is not easy to determine to what extent NBS shall be used to modernize urban water management. Unlike traditional stormwater measures, a simple cost-benefit analysis will not suffice. The reason for this is that benefits of NBS are not one-dimensional. Rather, NBS can have benefits in multiple different dimensions. These are also called the co-benefits of NBS.

Co-benefits are already imprinted on some of the definitions used for NBS. In the NBS principles proposed by Cohen-Shacham et al. (2016: xii), NBS are described to “produce societal benefits in a fair and equitable way [...]” and to “maintain biological and cultural diversity [...]” at the same time. While the co-benefits are kept very general in this definition, there are also some very specific co-benefits of NBS in urban stormwater management.

A main concern for cities facing climate change is the Urban Heat Island (UHI) effect. UHI describes the phenomenon that temperatures are higher in cities than in surrounding areas (Zhao et al. 2014). The UHI leads to an overproportioned heat stress on the urban population (Hobbie and Grimm 2019). A combination of several factors such as lack of vegetation, heat storage in building materials, aerodynamic resistance and waste energy from heating as well as vehicles can cause this effect (Zhao et al. 2014). NBS approaches, such as urban green space, green roofs, permeable pavements and trees, have the potential to reduce the UHI effect. The temperature reduction is associated to evaporative cooling, reduced heating of the pavement, provision of shady areas and low heat storage (Hobbie and Grimm 2019, Huang et al. 2020, Bowler et al. 2010). The relief from heat waves in urban areas will increase in importance since climate change will increase the likelihood of heatwaves.

Further benefits are listed in the overview study of Huang et al. (2020). NBS that are designed to mitigate the risk of urban pluvial flooding have shown that they can also exhibit economic, ecological and social benefits. More precisely, NBS can benefit as climate mitigation measures, they can create more attractive outdoor spaces for recreation, improve air and water quality, enhance biodiversity and help to conserve ecosystems (Huang et al. 2020, Coutts et al. 2012, Lashford et al. 2019, Houston et al. 2011, Krauze and Wagner 2018). These co-benefits of NBS help cities to transition to a more eco-friendly and sustainable economy and help to unleash a city’s economic potential (Huang et al. 2020). NBS have also shown to provide amenities that promote human physical and mental wellbeing

(Houston et al. 2011, Huang et al. 2020) and to facilitate the creation of future-proof green jobs (Raymond et al. 2017). Since the UPF mitigation capacity of NBS has not yet been sufficiently clarified, Green et al. (2021) suggest prioritizing the co-benefits sought. They are thought to have cross-sectoral impacts and bridge societal and economic interests (Raymond et al. 2017). All things considered, NBS enhance an urban area's general resilience, not only against UPF (Zölch et al. 2017).

It has been criticized that these important potential benefits of NBS are relegated to co-benefits (Axelsson et al. 2021). Since a widely accepted framework for assessing their value is missing, the co-benefits of NBS are likely to be excluded from cost-benefit analysis (Raymond et al. 2017). It is assumed that taking the co-benefits into account makes NBS more efficient and cost-effective than traditional urban water management approaches (European Commission 2015).

### **1.12 Implementing NBS on today's parking spaces**

The implementation of NBS in urban water management is facing some challenges. For example, it is still unclear how to specifically implement NBS in cities for a risk reduction in urban pluvial flooding (Zellner et al. 2016). Since a clear best-practice approach is missing, it is crucial to share ideas and knowledge gained about NBS through different studies and modelling approaches (Lashford et al. 2019). In that light, the situation calls for experimentation with different ideas, for example using parking spaces as possible implementation areas for NBS approaches. This idea is supported by the following arguments.

1. It is not possible to retrofit entire urban drainage systems since this would be too expensive and too disruptive (Houston et al. 2011). Therefore, easy-to-retrofit areas such as parking spaces should be considered.
2. The idea of using permeable pavement on parking is not new and has been proposed by other researchers, too (Jayasooriya and Ng 2014).
3. One study showed that grass and planted trees could substantially (62-100%) reduce surface runoff on a 9 m<sup>2</sup> area compared to asphalt (Armson, Stringer and Ennos 2013). And a parking lot is currently nothing more than a few square meters of asphalt.
4. At the moment, parking spaces do not provide any co-benefits.
5. It has been shown that NBS improve in performance of reducing UPF when located adjacent to roads and close to sewer outlets (Zellner et al. 2016). These are two requirements perfectly matched by parking spaces.
6. While other asphalt area such as driveways were also suggested for retrofitting (Zellner et al. 2016), the land tenure is less complicated and dispersed with public parking spaces. Therefore, timely action could theoretically be initiated.

7. Implementing NBS is not an exclusive land use. Depending on the selected implementation measures, the area could continue to be used as a parking lot or in other ways providing even more co-benefits.
8. It has been shown that pervious pavements also work in colder climate with ground frost (Dietz 2007). This characteristic is an advantage in Bern.
9. In the light of the ever-more-popular approach of car-free cities, a lot of currently occupied urban space will be freed up (Nieuwenhuijsen and Khreis 2019).

Furthermore, cities provide optimal ground to give new ideas a try and offer the context for innovative interventions (European Commission 2015). And lastly, a study has already been conducted on the runoff reduction of permeable pavements (Dietz 2007). Therefore, usable and meaningful numbers of potential rainwater retention are published.

### **1.13 Motivation for this thesis**

In all of Switzerland, the summer of 2021 was accompanied with a lot of rain. Among overtopping rivers and lakes, heavy rainfalls lead to flooding of railway stations and underpasses (see also 20 Minuten 2021 and Tages-Anzeiger 2021). This happened for example in Lausanne and Zug where it led to transport interruptions. While the city of Bern did not experience any urban pluvial flooding, it did receive a lot of rainfall. Between the 12<sup>th</sup> and the 15<sup>th</sup> of July, the city of Bern received between 80 - 100mm of rainfall (Federal Office for the Environment [FOEN] 2021). Some of the surrounding districts even received between 100-130mm in the same time span (FOEN 2021). While Bern's urban drainage system was able to mitigate the risk of this specific event, it is not clear whether the system will also withstand even stronger torrential rainfalls as are predicted in the future.

The paper on hand shall push the research boundary of urban pluvial flood modelling. So far (as of November 2021), no paper or thesis has been published using the software BASEMENT (v2.8) to simulate urban pluvial flooding (ETHZ 2021). The goal is to produce evidence on whether the simulation program BASEMENT (v2.8) can be used to model UPF. Additionally, a proof of concept shall be provided that the hazard reduction through the implementation of NBS on today's parking spots can be modelled with this simulation software. The results should provide an estimate to which the implementation of NBS can mitigate the urban pluvial flood hazard. This insight is intended to make a small contribution to the understudied but nevertheless very important interaction between grey and blue-green stormwater infrastructure (Green et al. 2021).

### 1.14 Study Area: Länggasse-Felsenau neighborhood in the city of Bern, Switzerland

The proof of concept is simulated on a part of the Länggasse-Felsenau neighborhood in the city of Bern in Switzerland. Bern is the Swiss capital, approximately 52 km<sup>2</sup> in size and has a little over 143'000 inhabitants (Stadt Bern 2021a, Stadt Bern 2021b). Bern has a long history of flooding (Stadt Bern 2015). The danger came from the Aare River, which flows through the city of Bern. Therefore, only fluvial flooding was considered a risk. However, the rainy summer of 2021 has raised awareness of the risk of urban pluvial flooding. Bern has a combined stormwater and foul water drainage system (Flückiger 2021). Therefore, but only in extreme cases, contaminated water may leak onto the streets and pose a health risk. However, the experts consider the risk to be very small because the shafts are laid very deep (Flückiger 2021).

It is computationally very costly to model the entire city of Bern within the scope of a thesis. Therefore, the simulation area is limited. The delineation of the area studied in this paper can be seen in Figure 4. The area does not include any water bodies and is therefore not susceptible to other forms of flooding. In addition, the area is heavily built-up, meaning that most of the ground area is sealed. There are also many parking lots along the streets. These characteristics make the area interesting for investigation as a possible UPF area.

From now on, this paper refers to this restricted perimeter as the *Bern simulation perimeter*.

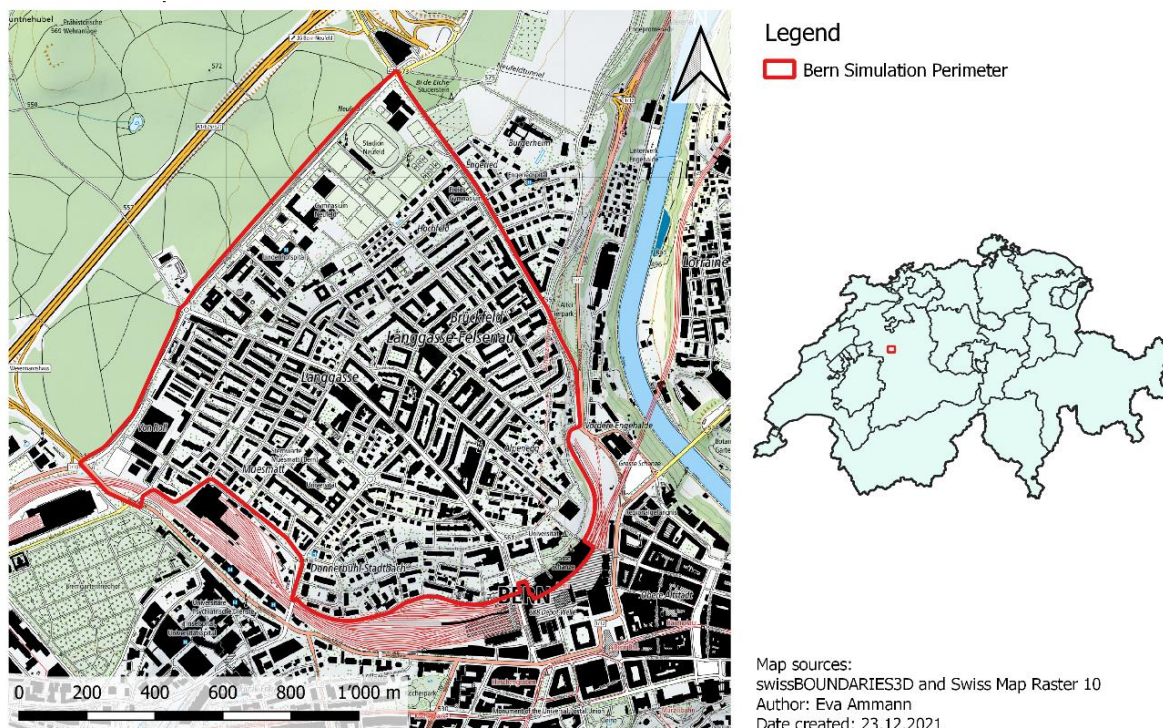


Figure 4: Overview Map of the Bern Simulation Perimeter

### **1.15 Hypotheses and Research questions**

This master thesis is based on the following research questions, always referring to the delimited research area:

1. What is the current proportion of public parking spots relative to the urban area?
2. Can the simulation program BASEMENT (v2.8) be used to model urban pluvial flooding?
3. What is the associated hazard reduction by replacing today's parking spots with nature-based solutions? How do the results with today's rainfall values differ from those with the assumed end-of-century values?
4. What is the simulated hazard increase due to higher precipitation intensities assumed due to climate change? Are the magnitudes of hazard increase due to climate change and hazard reduction through the implementation of NBS measures on today's parking spots comparable?
5. What are the co-benefits of replacing today's parking spots with nature-based solutions?

The research questions lead to the following two hypotheses:

1. The simulation program BASEMENT (v2.8) can be used to model possible urban pluvial flooding.
2. Replacing today's parking spots with nature-based solutions in the defined research area will reduce the present and future urban pluvial flood hazard modeled by the BASEMENT (v2.8) program.

It is important to point out that this work does not aim to create a hazard map for urban pluvial flooding. This has already been done by the FOEN (2018) and can be found online.

## 2 Data and Methods

In this paper, the simulation program BASEMENT (v2.8) is used to model urban pluvial flooding. Version 2.8 is used for the simulations performed. The simulation program BASEMENT (v2.8; basic-simulation-environment) provides “[...] a flexible and functional environment for numerical simulation of alpine rivers and sediment transport involved. (Vetsch et al. 2020:9)” The program is designed for large-scale river analysis. The software is freely available and a user forum is hosted to provide help (<http://people.ee.ethz.ch/~basement/forum/index.php>).

Urban pluvial flooding can be caused by both short but high-intensity rainfall as well as long-lasting low-intensity rainfall (Houston et al. 2011). However, since UPF is usually associated with the former and a shorter simulation time results in lower computational effort, a short-duration rainfall event is chosen for this work. While the rainfall duration is set to one hour, the simulation duration is set to two hours to allow the last fallen raindrop to find its way out of the system or into a local depression.

### 2.1 The different scenarios

In order to calculate a potential hazard reduction through the implementation of NBS on today’s parking areas, two different simulations need to be conducted. One simulation represents the status quo and the other one the current conditions with NBS implemented on the parking spot areas. In the simulation, the implementation of NBS is achieved by not letting any water enter the system through these mesh elements. This process is explained in more detail later in this chapter.

Since the risk of UPF is said to increase due to climate change, the two simulation setups *noNBS* and *withNBS* are carried out for a stronger rainfall event which could occur at the end of the century (*future*). In addition, the *future* scenario serves as sensitivity analysis for the simulation program. The four simulation setups are shown in Table 1.

Table 1: The four simulation setups for the Bern simulation perimeter

	Current hourly 1-in-100 years rainfall event	Future hourly 1-in-100 years rainfall event
<b>No NBS implemented</b>	<i>Current_noNBS</i>	<i>Future_noNBS</i>
<b>With NBS implemented</b>	<i>Current_withNBS</i>	<i>Future_withNBS</i>

The *current\_noNBS* simulation represents the baseline scenario. While the rainfall input varies across the different scenarios, they are all carried out using the same computational mesh. The generation of this computational mesh is explained in the subchapter 2.3.1 *Pre-Processing in the Bern simulation*.

## 2.2 The general workflow



Figure 5: 3-step simulation process for BASEMENT (v2.8). The icons represent the most used software programs per process step. From left to right: QGIS, BASEmesh, Python – BASEMENT (v2.8) – QGIS, Python and Microsoft Excel (Own illustration, icons see Image Sources)

The simulation workflow follows a 3-step-process and is presented in Figure 5. The pre-processing itself is also a 3-step-process and is performed in Quantum GIS (QGIS). A specially developed plugin called BASEmesh can be installed to create the computational mesh used for the simulation in BASEMENT (v2.8). First, all the topographical data must be collected, harmonized and put into the required form. This form consists of breaklines (all topographical data in a line layer), StringDefs (system boundaries as a single line layer) and region points (centroids of elements defining the Material ID). In a second step, a triangulated irregular network (TIN), called the quality mesh, can be created using the BASEmesh plugin. With a TIN's special property, it is possible to optimize computational efficiency. In areas where there are many breaklines (e.g., where roads, parking lots, and buildings meet), the triangles have a smaller area, and in areas where the breaklines are far apart (e.g., large buildings), the triangles have a larger area and therefore require less computational power. Thus, the TIN optimizes the tradeoff between spatial resolution and computational power. According to Houston et al. (2011), another advantage of this method is that it is the only way to properly represent flood-critical urban microtopography such as street and curb heights. In a third step, the obtained quality mesh is interpolated using a digital elevation model (DEM). The result is a so-called computational mesh in .2dm file format. This computational mesh can then be used for the simulation process.

The second step of the simulation process is the actual numerical simulation. In order to run the simulation, all necessary data needs to be stored in a single folder. This includes the computational mesh, the hydrological data and the simulation file. This simulation file can be edited either through the user interface of the BASEMENT (v2.8) software or through any editor program such as Notepad++. Within this simulation file, additional definitions for the simulation area, all hydrological parameters as well as the export parameters and formats are defined. Once everything is defined and valid, the simulation can be started. Throughout the simulation, warnings and certain intermediate results can be tracked in the output Log.

Once the simulation has finished, the created results file can be used for post-processing. Since different export formats are available, the post-processing is not a standardized process.



Since the simulation software BASEMENT (v2.8) is intended to conduct fluvial modelling, adaptations to the existing workflow must be made in order to model pluvial flooding. For traceability reasons, the exact workflow and the data origins are presented in the following subchapter.

## 2.3 Data procurement and the adapted workflow for the Bern simulation

### 2.3.1 Pre-Processing in the Bern simulation

#### 2.3.1.1 Data Procurement

In order to do the pre-processing in QGIS (Versions 3.16 and 3.18 were used), all the topographical data for the study area has to be collected. Most of this data is obtained from the Federal Office of Topography swisstopo. Since March 2021, this federal office follows an Open Government Data approach and most of their data is open to the public free of cost (Federal Office of Topography swisstopo 2021a).

The swissTLM3D (large-scale Topographic Landscape Model of Switzerland) is a vector-based model covering both natural and artificial landscape features of Switzerland. For well-defined objects such as buildings and streets, the accuracy is 0.2-1.5m and for objects not well-defined, such as forests, the accuracy is 1-3m (Federal Office of Topography swisstopo 2021b). Table 2 shows which layers from the swissTLM3D model are used.

Table 2: Layers used from swissTLM3D model

Original name of the layer swissTLM3D_TLM_ [...]	Features used from this layer	New feature name	Geometry
GEBAEUDE_FOOTPRINT	All	buildings	Polygon
STRASSE	All	streets	Line
VERKEHRSAREAL	Oeffentliches Parkplatzareal	parkingarea	Polygon
BODENBEDECKUNG_west	Wald	forest	Polygon
	Gehoelzflaeche	forest	Polygon
SPORTBAUTE_PLY	Sportplatz <sup>1</sup>	sports	Polygon

<sup>1</sup>: Only grass sports areas are considered. Concrete surfaces (including tartan tracks and sand tennis courts) do not let any water percolate (Illgen 2000, Sportplatzwelt 2021 and Tennis Uni 2020). The sports areas are distinguished according to their surface type with the help of satellite imagery (Google Maps Satellite Only layer, OpenStreetMap).

The swissTLM3D model contains many more layers than those used. Most other layers were not considered because either their features are not present in the simulation perimeter (e.g. walls, rivers and lakes) or because they are not of great importance for UPF (e.g. protected areas). However, some layers are left out for simplicity's sake. For example, the layer showing every individual tree in the urban area. As shown in the literature section of this paper, trees are an implementation approach for NBS. However, since the effect is not defined per tree and since inserting every single tree would fragment the simulation mesh, they are not considered. Hydraulic structures such as artificial ponds and private water basins are also ignored because their influence on the UPF is not clear, and their cumulative area is very small in relation to the simulation perimeter.

In addition to the data from the swissTLM3D model, the shape file containing all public parking spots in the city of Bern was used. This data is generously provided by the civil engineering office of the city of Bern (Stadt Bern 2021c). The polygons are added to the model and processed with the feature name *parkingspots*.

2.3.1.2 Polygon manipulation



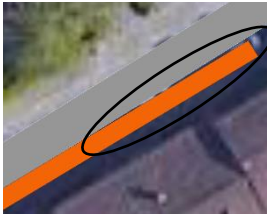
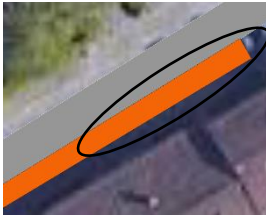
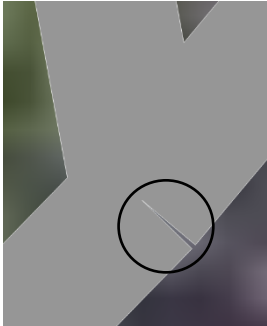
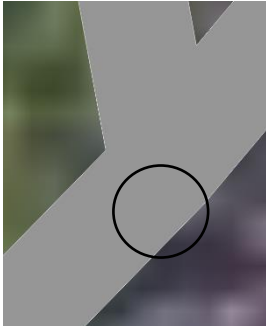
As a first step, the streets layer, which is only available as a line layer, is converted into a polygon layer. To achieve this, a buffer is calculated around the line layer. Since the width of the individual streets is available as attribute, half of the specified road width is used as buffer width. Table 3 shows the processes applied to the individual urban feature layers to harmonize the data.

Table 3: QGis Action performed on feature layers to harmonize the data

QGIS action on layer	Cut to perimeter	Merge layers	Dissolve	Simplify	Manual correction	Multi- to singleparts	
Buildings	✓	→	✓	→	✓	→	✓
Streets	✓	→	→	→	✓		
Parkingarea	✓	→	✓	→	✓	→	✓
Parkingspots	✓	→	✓	→	✓	→	✓
Forest	✓	→	→	→	✓	→	✓
Sports	✓	→	→	→	✓		

For a better understanding why every layer needs manual correction, a few examples are presented in Table 4 on page 33. The manual corrections are done to improve computational efficiency. They are based on satellite imagery, logic (e.g., parking area must touch the street) and, where the situation allows, the removal of small (<0.25 m) features.

Table 4: Examples of manual correction on feature layers

Feature Layer	Before	After	Explanation
Parking			These two adjacent parking areas can be treated as one
Parking			Parking areas must touch the street
Street			Such spikes appear during the buffering of the street line layer and must be corrected

After the manual correction and logic adjustments, the road layer is still overlapped by the parking and forest layers. The solution is to define a *new streets layer* consisting of the *old streets layer* without the overlaps.

### 2.3.1.3 Defining centroids

Once all the polygons are satisfactory, each polygon is assigned a point. All centroid points together are saved in the centroid layer. Its attribute table contains polygon-specific attributes such as the Material ID (MatID), the binary definition of whether the specified polygon is a hole or not, and the maximum area allowed for the individual triangles to be formed within this polygon. Table 5 shows the MatIDs assigned to the different urban features in the Bern simulation.

Table 5: Urban features used in the Bern simulation and the attributed MatIDs

Urban feature	MatID
Buildings	1
Street	2
Parking	3
Forest	4
Sports	5
Rest <sup>1</sup>	0

<sup>1</sup>: The MatID 0 is automatically assigned to all surfaces that are not previously assigned a specific urban feature MatID.

### 2.3.1.4 StringDefinitions

Since the BASEMENT (v2.8) simulation program is designed for river modeling, the simulation perimeter is treated as an empty riverbed. If there were no river outlet, the system would simply fill up with water. This would lead to a so-called bathtub situation. To prevent this, the system's boundary conditions must be defined through StringDefs. These StringDefs form a line layer and define where the water can enter or exit the system. For the simulation to work, an outflow direction must be defined. This direction is determined by virtually standing on the first point of a StringDef and mentally walking to the second point. In this virtual passage it must be determined whether the water comes or would come from the left or from the right.

While StringDefs can be defined within the entire simulation area, they are only defined along the system boundary for the Bern simulation. In a first attempt of the simulation, the StringDefs are defined all along the perimeter for the water to leave the system at any point. However, this setup leads to multiple error messages. Therefore, the StringDefs are logically adjusted. Downward-sloped streets are treated as channels and the StringDefs are then defined at the outlet of this channel. In general, the StringDef is only defined at the lowest points of the street. Since all boundary StringDefs are defined counterclockwise and rainwater can only flow out of the system, all StringDefs have the outflow direction left. An overview of the StringDefs implemented in the Bern simulation can be found as a list in

Table 6 and as a map in Figure 6 on page 35.

Table 6: StringDefs used in the Bern simulation

Name	Outflow direction	Length [m]	Name	Outflow direction	Length [m]
Murtenstrasse_northwest	left	32.25	Engestrasse	left	28.64
Murtenstrasse_southwest_v1	left	53.29	Bremgartenforest_north_v1	left	59.51
Murtenstrasse_southwest_v2	left	40.29	Bremgartenforest_north_v2	left	116.99
Murtenstrasse_southwest_v3	left	132.75	Bremgartenforest_north_v3	left	62.75
Murtenstrasse_southeast	left	35.00	Bremgartenforest_north_v4	left	128.19
Waldheimstrasse	left	34.79	Bremgartenforest_north_v5	left	143.89
Depotstrasse_v1	left	29.19	Bremgartenforest_north_v6	left	108.95
Depotstrasse_v2	left	20.95	Bremgartenforest_north_v7	left	113.44
Depotstrasse_v3	left	28.00	Bremgartenforest_north_v8	left	89.13
Buehlstrasse	left	20.06	Bremgartenforest_north_v9	left	50.41
Stadtbachstrasse_v1	left	104.09	Bremgartenforest_north_v10	left	38.90
Stadtbachstrasse_v2	left	116.29	Laenggasse_roundabout	left	20.96
Schanzenstrasse	left	20.48	Bremgartenforest_south_v1	left	164.02
Post_stairs	left	15.34	Bremgartenforest_south_v2	left	134.76
Schuetzenmattstrasse_v1	left	13.04	Bremgartenforest_south_v3	left	139.13
Schuetzenmattstrasse_v2	left	25.01	Bremgartenforest_south_v4	left	86.56
Neubrueckstrasse_v1	left	105.65			

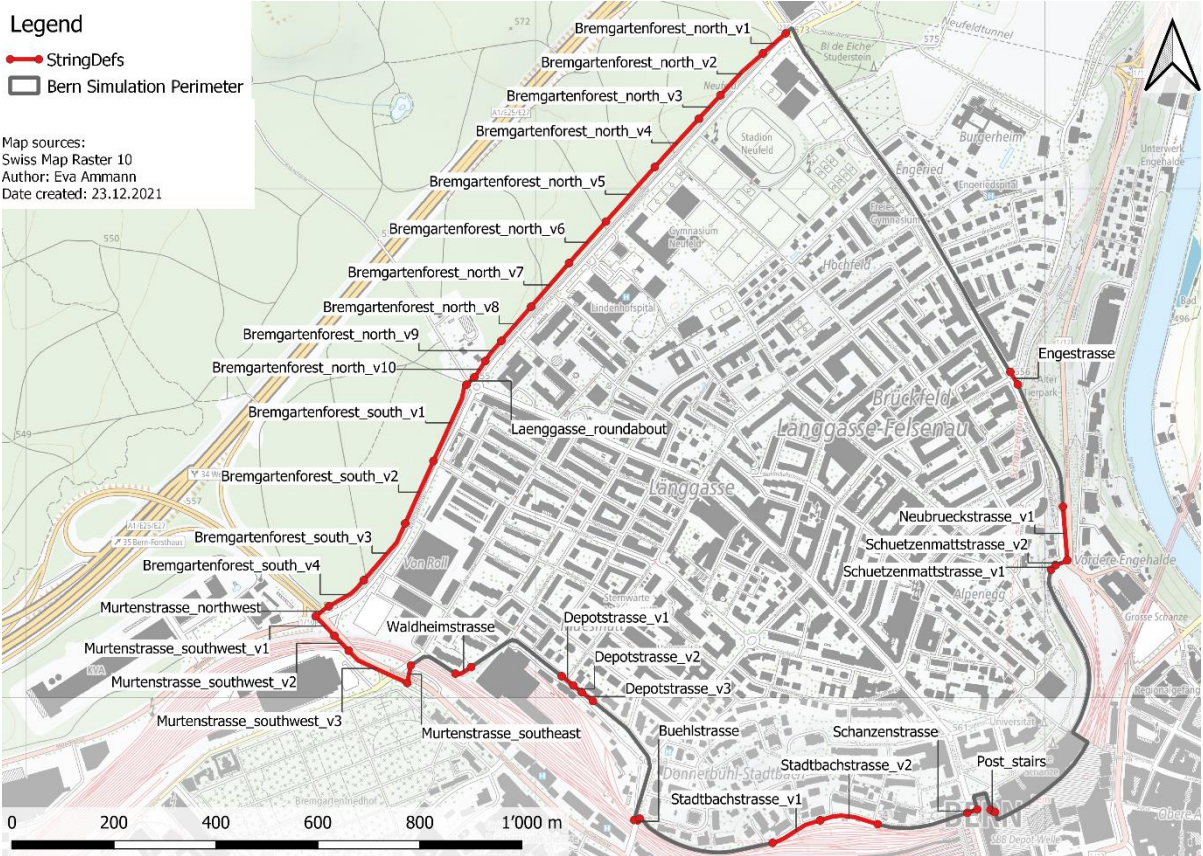


Figure 6: Map of StringDefs used in the Bern simulation

2.3.1.5 Creating the Quality Mesh

Once the centroid and the StringDef layers are finished, the polygon layers of the different features need to be merged and brought into the requested line form. The following table summarizes the subsequent working steps.

Table 7: QGIS actions performed on urban feature polygon layers to compute quality mesh

QGIS action on layer	Merge layers	Polygon to line	Delete double vertices	Explode lines	Delete double geometries	Manual correction	Quality mesh
Buildings		✓	✓	✓	✓		✓
Streets		✓	✓	✓	✓		
Parking		✓	✓	✓	✓		
Forest		✓	✓	✓	✓		
Sports		✓	✓	✓	✓		

The manual correction is made to simplify the quality mesh. A clean quality mesh without superfluous mesh elements requires less computational effort. The manual correction consists of a 3-step-process and is illustrated in Figure 7 on page 36. The process is repeated until the quality mesh satisfies the quality requirements.

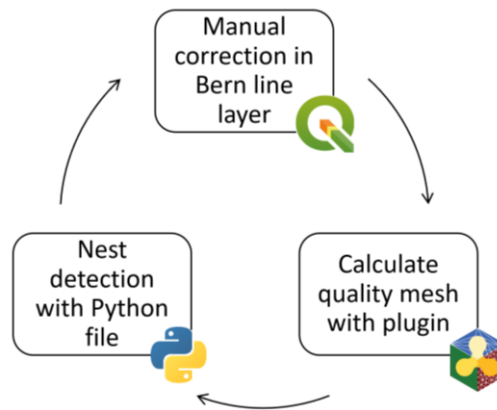


Figure 7: Manual Correction Workflow (own illustration, icons see Image Sources)

The first step is to use the BASEmesh plugin to create a quality mesh based on the Bern line, StringDef and centroid layer. The snapping tolerance is set to  $10^{-2}$  m to eliminate inaccuracies introduced by the manual processing of the input layers. It turns out that some nodes of the newly created mesh are extremely close to each other, resulting in very short connecting edges. This leads to so-called *visual nests* in the quality mesh. An example is shown in Figure 8.

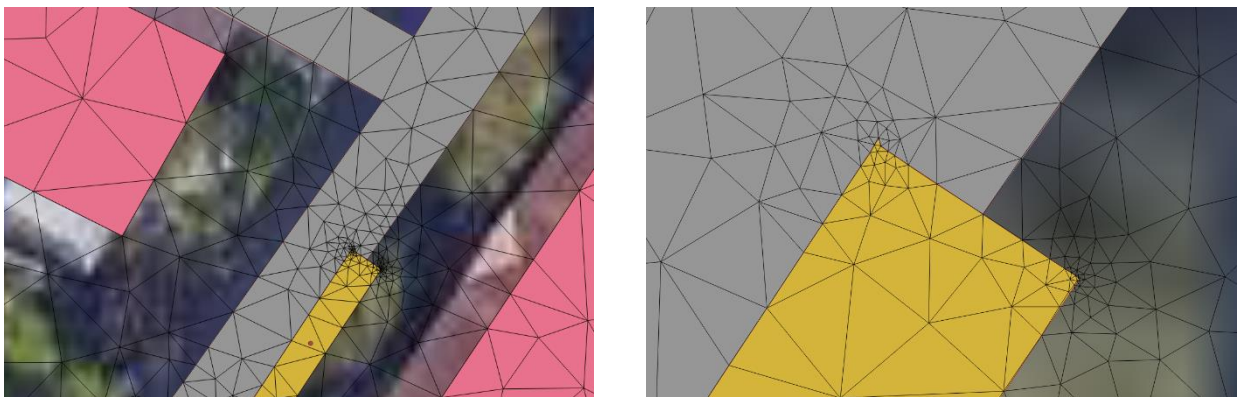


Figure 8: Two screenshots of a "nest" in quality mesh in different zoom levels

These *nests* are not easy to locate throughout the study area. Therefore, a Python script called "DoubleNodes.py" (see appendix) is developed. This Python script checks all node coordinates in the .2dm mesh file and returns a list of coordinates that are too close to each other. To be precise, the Python script returns a list of X and Y coordinate pairs that are equal to one decimal place. Since the map unit of the coordinate system used (CH1903+/LV95 – EPSG:2056) is meters, this results in a search radius of about 10 cm. Using the exported list of affected coordinate pairs, it is possible to zoom into each area where a nest is located. Once zoomed in, the nest is easily visible by eye. By zooming in further, it is usually possible to identify the troublesome and nest-causing artifact. Once the error is found, it can be manually corrected in the Bern line layer. In the example from the Bern simulation shown in Figure 8, a spike in the parking layer is causing the nest. The solution is to remove the spike and change it to a right angle. Once the entire list of double nodes is processed, a new quality mesh can be created, and the manual correction workflow is restarted.

Two additional processes are performed on a one-time basis to further simplify the quality mesh. First, all short (<1m) lines in the Bern line layer are inspected. If the surroundings allow it, the line is manually removed, and the surroundings adapted. Second, once a quality mesh has passed the manual correction process described in Figure 7, the mesh is dissected and all mesh edges shorter than 1 m are analyzed and, if necessary, the Bern line layer is manually corrected.

As can be seen from Table 8, all applied corrections together result in a reduction of the number of nodes and mesh elements by about 20%.

Table 8: Computational efficiency gain through manual correction process

	Count before corrections	Count after corrections	Reduction
Nodes	82'454	65'983	-20.0%
Mesh elements	164'908	130'903	-20.6%

2.3.1.6 From quality mesh to computational mesh

Once the quality mesh is ready, it only takes one more step to transform it into a computational mesh needed for the simulation. With the BASEmesh plugin, height values can be assigned to the nodes and mesh elements from a digital elevation model (DEM). Since BASEMENT (v2.8) is developed for river modeling, the DEM must not be too steep. Otherwise, numerical problems will arise during the simulation. However, the DEM of a city is generally very steep. In the Bern simulation perimeter, for example, there is a high-rise building and a church tower. Therefore, a creative approach must be taken in order to obtain a DEM that is suitable for the simulation. One solution is to take the Digital Terrain Model (DTM) and manipulate it by putting artificially small buildings on it afterwards. For the Bern simulation, the DTM provided by the Canton of Bern is used (KAWA Amt für Wald des Kantons Bern 2014 and 2015). Then, with the help of the previously used buildings polygon layer, each building is set at 2m height. The process steps of this DTM manipulation can be seen in Figure 9.

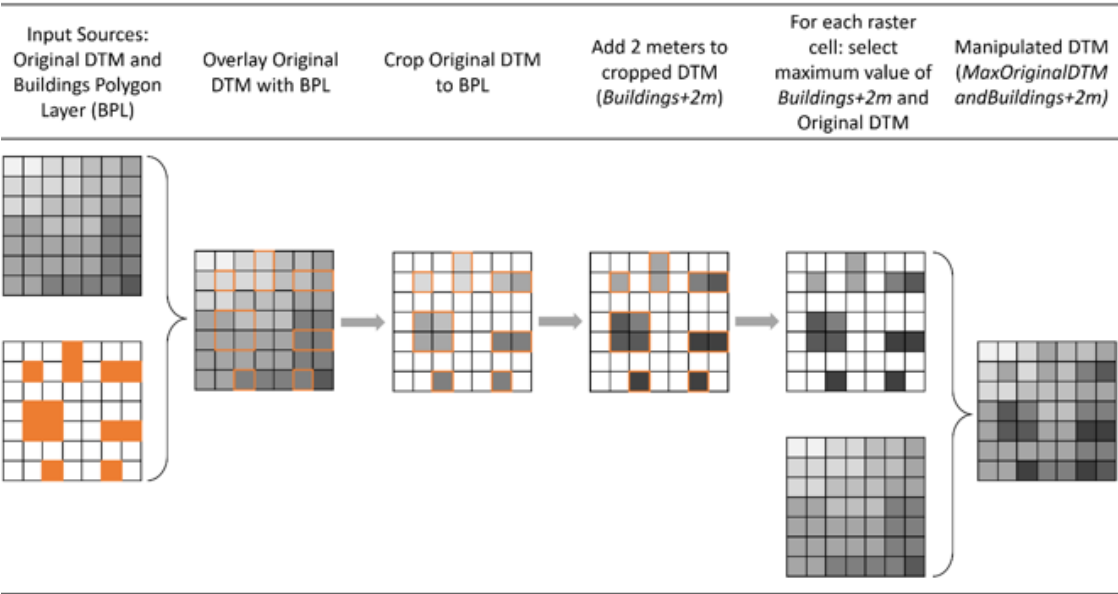


Figure 9: Manipulation steps applied to original DTM to obtain the manipulated DTM

With the help of the BASEmesh plugin, the quality mesh is interpolated with the manipulated DTM ( $MaxOriginalDTMandbuildings+2m$ ). This process results in the computational mesh and is the last step of the Pre-Processing. The computational mesh used for the Bern simulation is shown in Figure 10 and Figure 11 displaying the different MatIDs and the elevation, respectively.

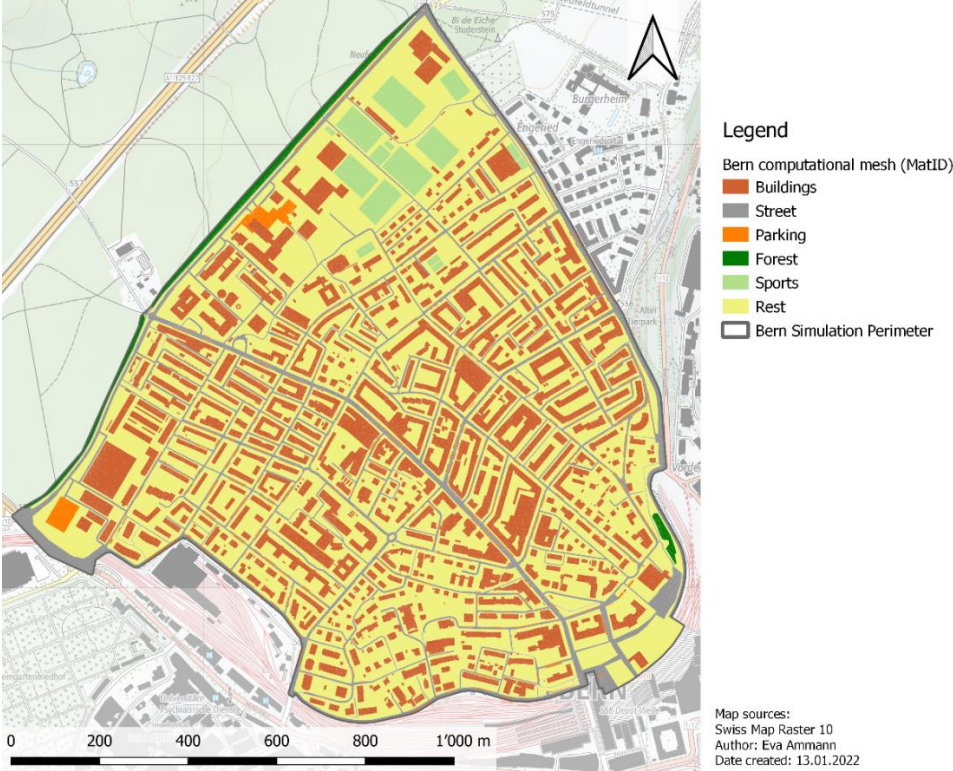


Figure 10: Map of Bern simulation perimeter displaying the different MatIDs

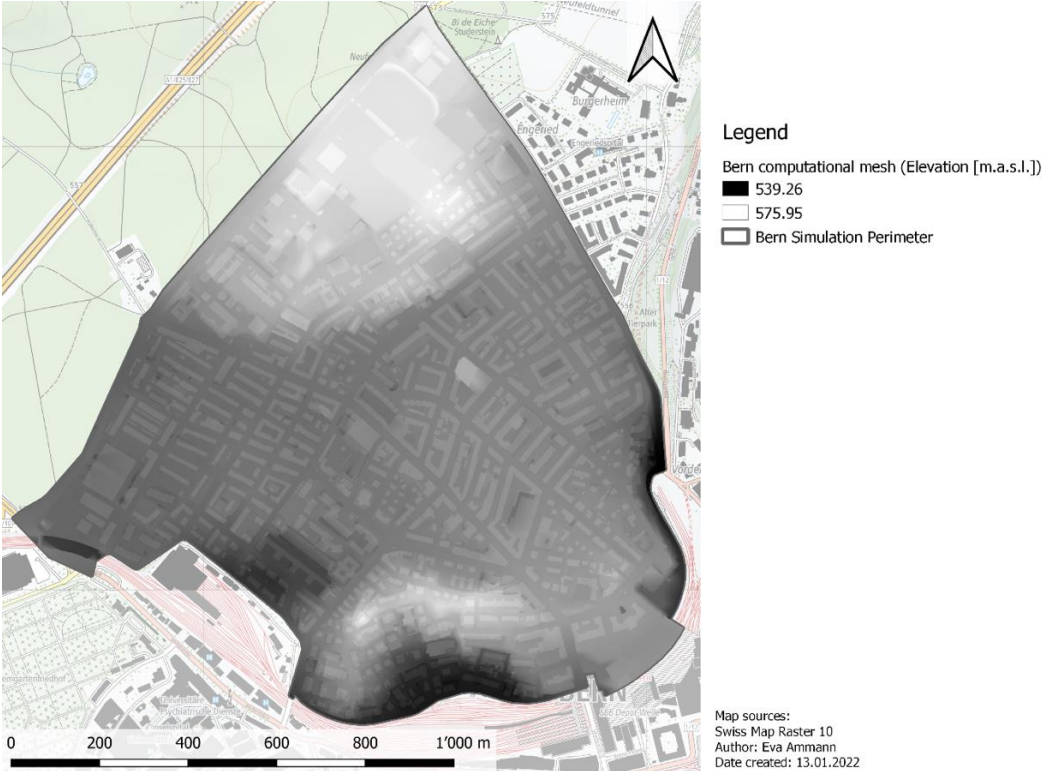


Figure 11: Map of Bern simulation perimeter displaying the elevation in meters above sea level



### 2.3.2 The simulation process of the Bern simulation

A lot of parameters can be defined in the BASEMENT (v2.8) program for the simulation. Most of them have a default value. Where possible, the Bern simulation is executed using these. Interested readers can find the command file with all the parameters at the end of the appendix.

Some data needed for the simulation, however, has to be collected and brought into the required form. This includes the amount of rainfall, the capacity of the stormwater system and the permeability of the different urban surfaces.

#### 2.3.2.1 Friction parameter

Friction is one of the hydrological parameters to be defined for the simulation. For the Bern simulation, the Strickler coefficient is used. An individual Strickler coefficient is assigned to each MatID. The applied values can be seen in Table 9.

Table 9: Strickler coefficient assigned to the different MatIDs (Data from Ma, Ngoc Vo and Gourbesville 2018)

MatID	Strickler Coefficient [ $\text{m}^{1/3}/\text{s}$ ]
0 - Rest	50
1 - Building	50
2 - Street	50
3 - Parking	50
4 - Forest	2
5 - Sports	2.5

#### 2.3.2.2 Rainfall

The simulation is based on a predicted hourly 1-in-100 years rainfall event. This value is published in the Extreme Value Analysis done by the Federal Office of Meteorology and Climatology MeteoSwiss (MeteoSwiss 2021). Unfortunately, no measurement station is located within the simulation perimeter. The closest measurement station is Bern/Zollikofen. It is located a little under 4 km away from the simulation perimeter. With a height of 553 meters above sea level it represents the conditions of the simulation perimeter which exhibits heights from 539 – 576 meters above sea level. Since this simulation is no more than a proof of concept and the hourly 1-in-100 years precipitation value is only a statistical value, an interpolation of different values from various surrounding measuring stations is omitted. The simulation is executed using the value assigned to the Bern/Zollikofen measurement station. To avoid superfluous words, the values assigned to the Bern/Zollikofen measurement station are from now on called *Bern values*. The predicted hourly 1-in-100 years rainfall event for Bern is 43.1 mm/h. This value is employed for the *current* simulations. For the *future* simulations, information on the predicted intensity increase is needed.

The Swiss National Centre for Climate Services (NCCS) publishes the Swiss Climate Change Scenarios such as the CH2018. The scenarios with their scientific background, the consequences for the Swiss population and more can be found online (<https://www.nccs.admin.ch/nccs/en/home/>)

climate-change-and-impacts/swiss-climate-change-scenarios.html). Within these scenarios, an increase in heavy rainfall event is predicted. The NCSS (2021) predicts an intensity increase of 20% for a 100-year single-day rainfall event in summer by the end of the century compared to 1980-2010. While no data is explicitly available for hourly rainfall events, the mentioned 20% increase at the end of the century is assumed for the hourly rainfall events for simplicity. For the *future* Bern simulations, this results in a designed hourly 1-in-100 years rainfall event amounting to 51.72 mm/h.

### 2.3.2.3 Capacity of the stormwater management system

Since introducing the sewer system into the simulation is beyond the scope of this paper, the *excessive rainfall* method is applied to the Bern simulations. The use of the *excessive rainfall* is explained at the end of chapter 1.5 *Modelling urban pluvial flooding*. The *excessive rainfall* can be calculated as follows.

$$\text{Excessive rainfall} \left[ \frac{\text{mm}}{\text{h}} \right] = \text{Actual rainfall} \left[ \frac{\text{mm}}{\text{h}} \right] - \text{Sewer capacity} \left[ \frac{\text{mm}}{\text{h}} \right]$$

In the city of Bern, the rainwater infrastructure is designed to mitigate an hourly 1-in-5 years rainfall event (Flückiger 2021). For every rainfall event that is below this threshold, the sewer system must be able to transport away the water and every piece of land must also retain the rainfall. Only if the 1-in-5 years rainfall amount is exceeded, there can be a backlog in the sewer system. And only in extreme cases, this leads to surface runoff which is needed for UPF (Flückiger 2021). For simplicity, it is assumed that the entire urban system can handle an hourly 1-in-5 years rainfall event and every raindrop that exceeds that amount leads to surface runoff and therefore poses a risk for UPF.

The hourly 1-in-5 years rainfall event assigned to the measurement station Bern/Zollikofen is 23.6 mm/h. For the simulation setup, this value is assumed to be Bern's stormwater infrastructure capacity. Subtracting this value from the predicted rainfall amount results in the *excessive rainfall* used for the simulation. Table 10 shows the considered rainfall amounts for the Bern simulation. It is assumed that the sewer capacity remains at its current level until the end of the century. For the remainder of the simulation explanation, the term rainfall references to the previously introduced *excessive rainfall*.

Table 10: The calculation of the excessive rainfall for an hourly 1-in-100 years rainfall event in the simulation perimeter

	Rainfall amount [mm/h]	Sewer capacity [mm/h]	Excessive rainfall [mm/h]
<i>Current</i>	43.1	23.6	19.5
<i>Future</i>	51.72	23.6	28.12

### 2.3.2.4 Implementing (excessive) rainfall in the simulation

There is no trivial way to implement precipitation in BASEMENT (v2.8). The simulation program expects water to flow into the system through a boundary condition, as is usual for a river. This method, however, is not appropriate for rainfall. Luckily, a work-around exists. By adding the amount of rainfall as *external\_source* it is possible to have water enter the system through mesh elements. This is how precipitation is simulated. The process is further facilitated by defining the amount of rain per MatID. Thus, only 6 (each MatID) instead of 130'903 (each mesh element) different rainfall amounts are

required. Since the standard unit for rivers is  $\text{m}^3/\text{s}$ , the precipitation amount must also be converted to  $\text{m}^3/\text{s}$ . The area-dependent conversion process is shown in Figure 12.

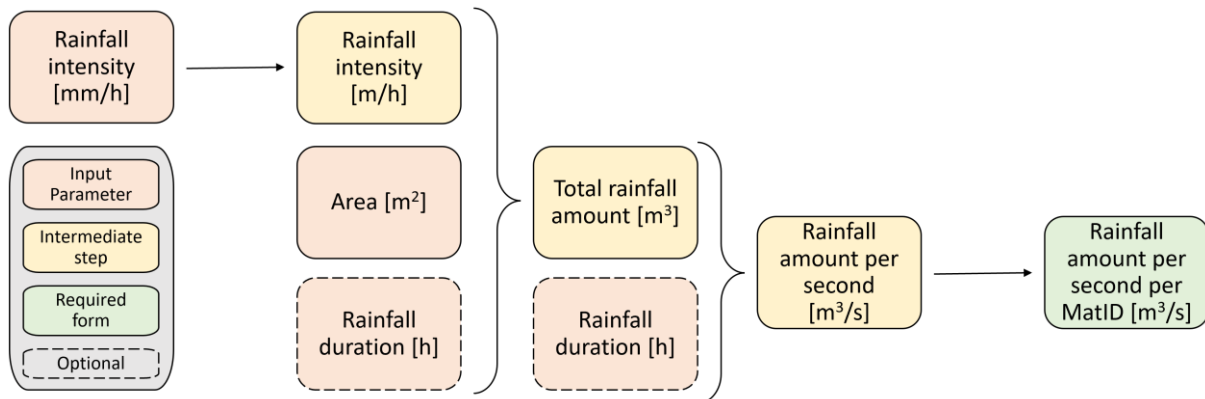


Figure 12: Conversion from rainfall intensity [mm/h] to the format required for the simulation

This process is executed with the *excessive rainfall* for the *current* as well as the *future* scenario. The precipitation amounts calculated for the Bern simulation are shown in Table 11.

Table 11: Rainfall amount per MatID in  $\text{m}^3/\text{s}$  calculated for the different simulation setups (rounded to two decimal places)

MatID	Area [%]	Current [ $\text{m}^3/\text{s}$ ]	Future [ $\text{m}^3/\text{s}$ ]
0 - Rest	55.44	4.16	6.00
1 - Building	27.08	2.03	2.93
2 - Street	11.71	0.88	1.27
3 - Parking	1.94	0.15	0.21
4 - Forest	0.88	0.07	0.10
5 - Sports	2.95	0.22	0.32

### 2.3.2.5 Permeability of urban surfaces and implementation of NBS on parking areas

The different permeability of the urban surfaces make some further adjustments for the Bern simulation necessary. Since it is not possible to implement different permeability values in the simulation setup, a work-around is applied. Instead of allowing the water to enter the system first and then defining some surfaces as permeable, the *excessive rainfall* approach explained above is used. For example, a fully permeable surface results in an *excessive rainfall* of 0, while an impermeable surface receives the original *excessive rainfall* value. As is described in the study conducted by Armson, Stringer and Ennos (2013: 282), “(...) grass almost totally eliminated surface runoff, (...)”. Assuming that all water can be retained, and no water is contributed to surface water runoff, the *excessive rainfall* for grass-covered areas (MatID 5 - Sports) is set to 0 for all simulation setups. Since forest soils are even more permeable and forests exhibit an additional interception storage capacity, the excessive rainfall for the MatID 4 – Forest is also set to 0 (Cheng, Lin and Lu 2002).

To observe the hazard reduction introduced by implementing NBS on parking areas, the MatID 3 – Parking exhibits a different permeability among the *noNBS* and *withNBS* scenarios. In the *noNBS* scenarios, the parking area is part of the major urban rainwater infrastructure system and is treated just like the street areas. It exhibits excessive rainfall which leads to surface runoff. In the *withNBS*

scenarios, however, the parking area is treated as a fully permeable surface. This means that there is simply no excessive rainfall on parking areas in the simulation setups with NBS. In other words, the implementation of NBS on the parking areas is simulated by not letting any water enter the system through mesh elements assigned to the MatID 3 - Parking. Table 12 displays the rainfall amount assigned to the different MatIDs per simulation scenario. The blue arrows highlight the change implemented in the *excessive rainfall* on MatID 3 - Parking.

Table 12: Rainfall amount per MatID in m<sup>3</sup>/s used in the four simulation setups (rounded to two decimal places)

MatID	current_noNBS	current_withNBS	future_noNBS	future_withNBS
0 - Rest	4.16	4.16	6.00	6.00
1 - Building	2.03	2.03	2.93	2.93
2 - Street	0.88	0.88	1.27	1.27
3 - Parking	0.15	0.00	0.21	0.00
4 - Forest	0.00	0.00	0.00	0.00
5 - Sports	0.00	0.00	0.00	0.00

2.3.2.6 Boundary conditions

For the water to be able to leave the system, the outflow boundary conditions need to be defined in the BASEMENT (v2.8) user interface. According to the block list reference manual of BASEMENT v2.8 (available online under <https://basement.ethz.ch/download/documentation/docu28.html>), the outflow boundary condition *zero\_gradient* would be the most suitable for this kind of simulation. *Zero\_gradient* allows for transient outflow of water from the system. However, because the microtopography of a city, even with the houses truncated at 2 meters, is so complicated, BASEMENT (v2.8) struggles to solve the simulation with the *zero\_gradient* outflow boundaries. Even though the computational mesh and the StringDefs are well defined, the simulation program produces negative outflows and flow velocities that exceed 200 m/s. With the help of other users in the BASEMENT (v2.8) user forum (<http://people.ee.ethz.ch/~basement/forum/viewtopic.php?id=5234>), the *zhydrograph* boundary condition can be implemented. With the *zhydrograph* boundary condition, it is possible to create a virtual lake behind the outflow boundary by defining this lake’s surface water elevation in a separate text file. The boundary condition then calculates the required outflow of water from the system depending on the lake’s water surface elevation. It is chosen to set the virtual lake water surface elevation 1-2 m below the lowest point of the respective StringDef to let the water flow out freely.

Ultimately, a functioning solution is to use *zero\_gradient* for as many StringDefs as possible and apply the *zhydrograph* workaround for the StringDefs where the *zero\_gradient* condition leads to numerical problems. This results in six StringDefs with the boundary condition *zero\_gradient* and 26 StringDefs with *zhydrograph*. Figure 13 shows the distribution of the different boundary conditions. A bigger version of this map can be found in the appendix.

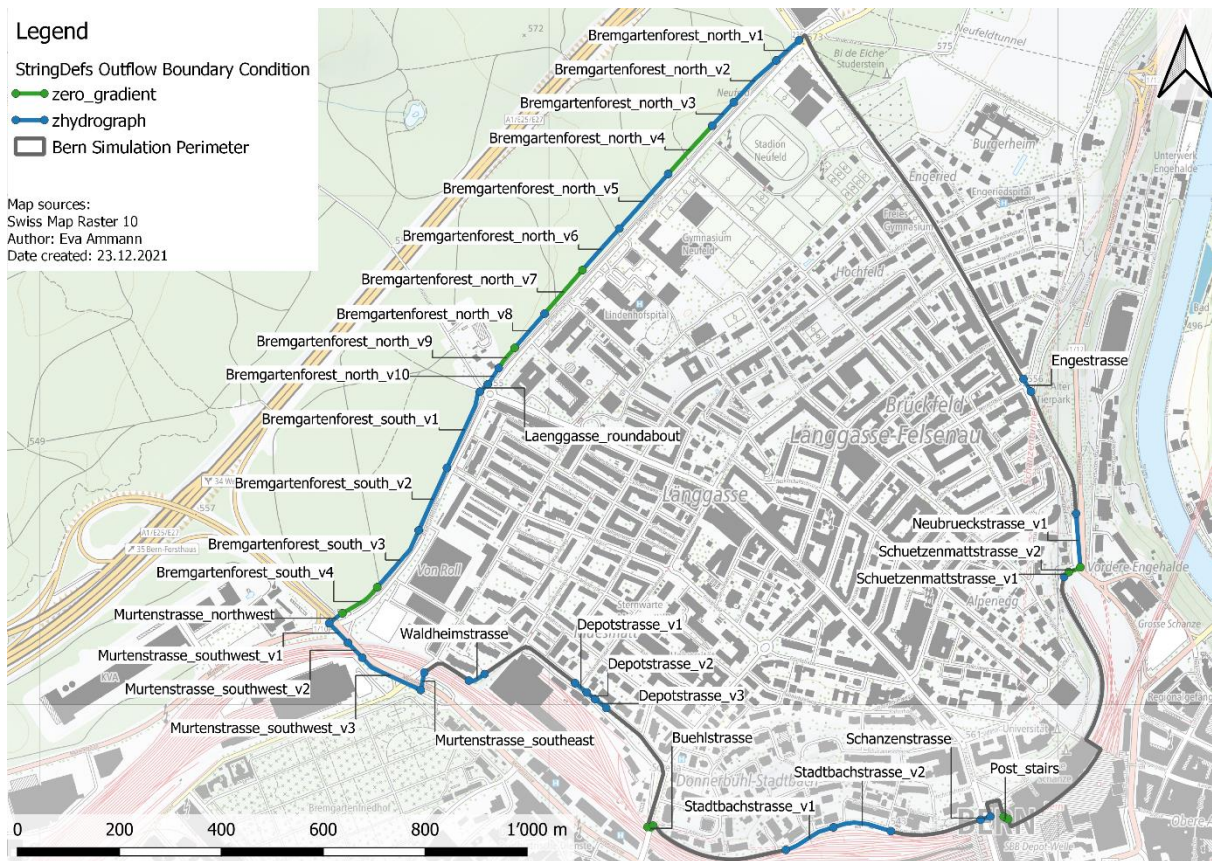


Figure 13: Map of Bern simulation perimeter with applied outflow boundary conditions

### 2.3.2.7 Output formats

Among the different possible output formats, shapefile (.shp) is chosen for the Bern simulation for easy post-processing. With the inserted SPECIAL OUTPUT blocks, the BASEMENT (v2.8) simulation program creates four shapefiles (track, depth, velocity x and velocity y) and a text file for the outflow values at the boundary conditions per simulation. Once all files are prepared and all parameters set, the simulation can be started.

### 2.3.3 The Post-Processing of the Bern simulation

The post-processing depends on the chosen output parameters and output file forms. Therefore, it is not a standardized process. In this chapter, only post-processing steps used for this paper are described. As a first step, the results of the flood simulations can be visualized. Since shapefile is chosen as output format, the results can be visualized in any GIS. Once the attribute tables are exported as comma separated values (CSV) files, they can be further processed using Python or any other data analysis program. Since some research questions focus on a possible hazard reduction through the implementation of NBS on today's parking areas, the assessed hazard parameters are shortly explained in the following subchapters.

At this point, the reader is made aware that the only risk component varying in magnitude among the different scenarios is hazard. There is no change in vulnerability and exposure. Under these conditions,

a change in hazard magnitude naturally leads to a change in flood risk. However, to stay concise, it is referred to hazard reduction and hazard increase rather than risk reduction and risk increase.

*2.3.3.1 Flow depth*

The most straight-forward hazard analysis is to analyze the maximum flow depth of each triangle. For this analysis, the flood hazard classification according to Rentschler and Salhab (2020) are used. They are shown in Figure 2 on page 10. However, a slight adaptation is made for the Bern simulation. The *Low Hazard* category is divided into two different hazard categories, namely the *Low Hazard* and the *Minor Hazard* category, covering the inundation depths of 0 - 0.06 m and 0.06 - 0.15 m, respectively. This hazard category division is introduced because the curb height in Bern is mostly set between 3 cm and 6 cm (Stadt Bern 2018). With these new hazard categories, it is possible to distinguish whether the surface runoff will overflow the pavements or remain in the streets. The revised flood hazard classifications can be seen in Figure 14.

Flood Hazard Classification		Inundation Depth [m]
Low Hazard	No Hazard	0
	Low Hazard	0 – 0.06
	Minor Hazard	0.06 – 0.15
High Hazard	Moderate Hazard	0.15 – 0.5
	High Hazard	0.5 – 1.5
	Very high Hazard	> 1.5

*Figure 14: Adapted Flood Hazard Categories for Bern simulation (own illustration), original Flood Risk Categories from Rentschler and Salhab (2020)*

### 2.3.3.2 Instability

The second hazard parameter is the instability analysis introduced by Martínez-Gomariz, Gómez and Russo (2016). To conduct this analysis, the process shown in Figure 15 is executed. This analysis is conducted using the python script “VelocityandStability.py”, which can be found in the appendix.

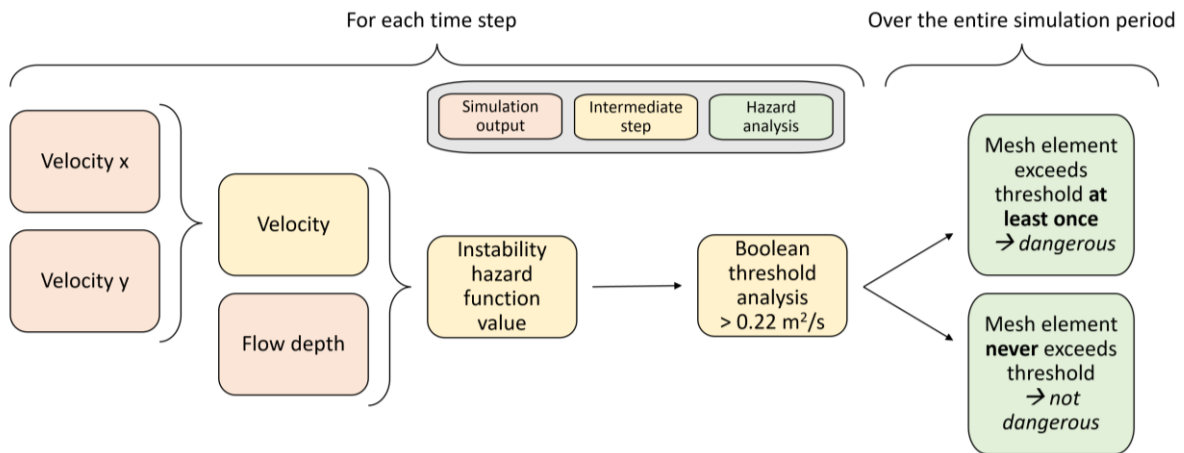


Figure 15: Workflow for instability function hazard analysis (own illustration)

### 2.3.3.3 Degree of loss and simulated damage in Swiss Francs (CHF)

The most complex hazard analysis is the calculation of the possible damage reduction. For this analysis, the *degree of loss* as well as the predicted resulting financial damage to the buildings in the simulation perimeter are calculated. The *degree of loss (dol)* is the combined result of the flow depth and a vulnerability function. It indicates the damage to the building, or more precisely, the percentage loss of the building (Bermudez and Zischg 2018). Multiplying the *dol* with the reconstruction value of the building returns the loss in monetary units, e.g. CHF, also known as damage (Bermudez and Zischg 2018). The *dol* and the damage value are calculated for each individual building. Once each building is assigned a value, they can be summed up at the study area level for the total damage. This hazard analysis consists of several steps and is illustrated in Figure 16.

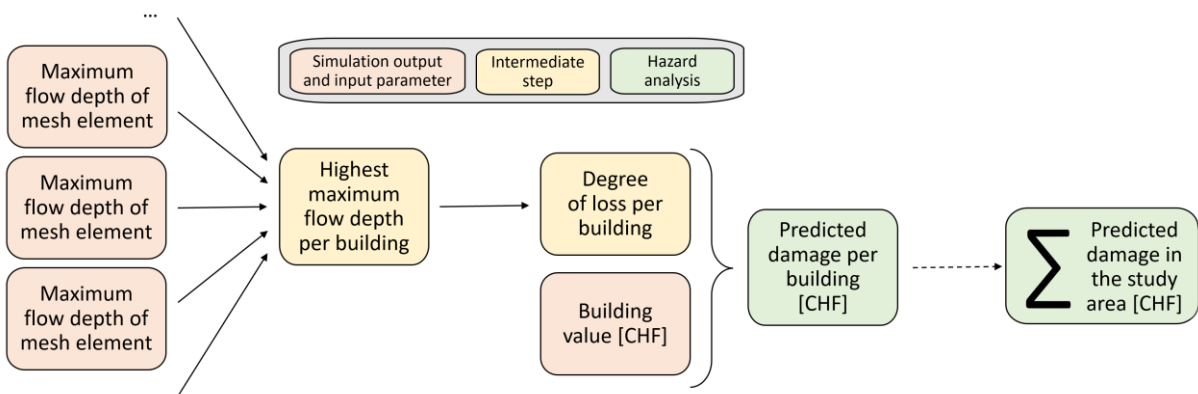


Figure 16: Degree of loss and predicted damage in CHF hazard analysis process

The first step is to locate the highest maximum flow depth touching a building. To accomplish this, a 1 m buffer is applied to each building. Then, all mesh elements overlapped by this buffer are analyzed for their maximum flow depth. The highest of these is then attributed to the building. This process can be automated in QGIS using the *Join attributes by location (summary)* function. All mesh elements that intersect with, are overlapped by, or are contained within the building buffer ring are considered. The function addition *summary* ensures that only the maximum of these values is attributed to the building. An example of this process is shown in Figure 17.

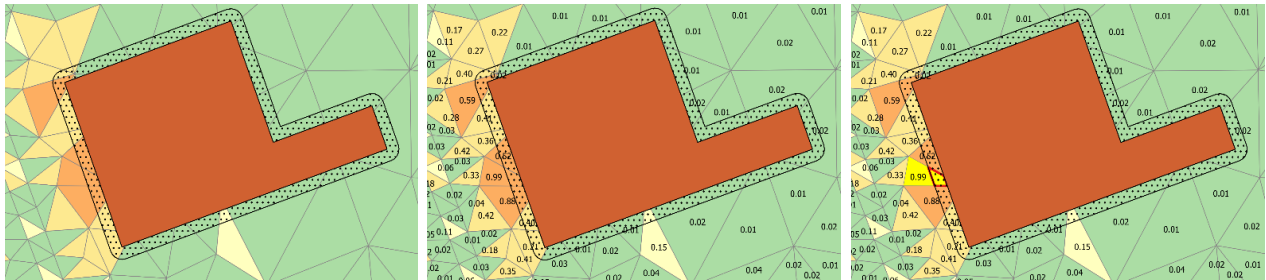


Figure 17: Process to extract the highest maximum flow depth for an individual building (*future\_noNBS scenario*)

As can be seen in the last image of Figure 17, the highest maximum flow depth for this building is 0.99 m. This value is attributed to the building and can later be used to calculate the *degree of loss*.

The other input data for this analysis is the building value in Swiss Francs. For the Bern simulation, the *swissTLM3D buildings* layer with the calculated building value in the attribute table is used. This data is generously provided by Röthlisberger, Zischg and Keiler (2018). In their paper they discuss five different value estimation methods for flood-exposed buildings in Switzerland. The M5 model, which calculates an individual value per building and is based on linear regression, performs better than the rest of the evaluated models (Röthlisberger, Zischg and Keiler 2018). Since the calculated building values of all models are obtained from the study authors, the complex calculation method of the M5 model can be left out of sight for the present work. The estimated building values from the M5 model are used without further processing for the Bern simulation hazard analysis. The only change to the dataset is made by deleting one building (the multi-level building connecting the train station with the Grosse Schanze) from the simulation perimeter since it is an underground building and therefore not part of the urban pluvial flood hazard zone. The building used for the example has an attributed value of 520'747 CHF.

To calculate the *dol* for the Bern simulations, the *dol* formula developed by Kaltenrieder (2017) is used. This formula includes a vulnerability function and expresses the *degree of loss* as a function of the maximum flow depth. It can be written like this:

$$\text{degree of loss} = \min \{ \max \{ (0.18846 + 0.17152 * \max \{ 0, \text{flowdepth} \})^2, 0 \}, 1 \}$$



For easier understanding, the formula can also be represented as a mathematical decision tree as is shown in Figure 18.

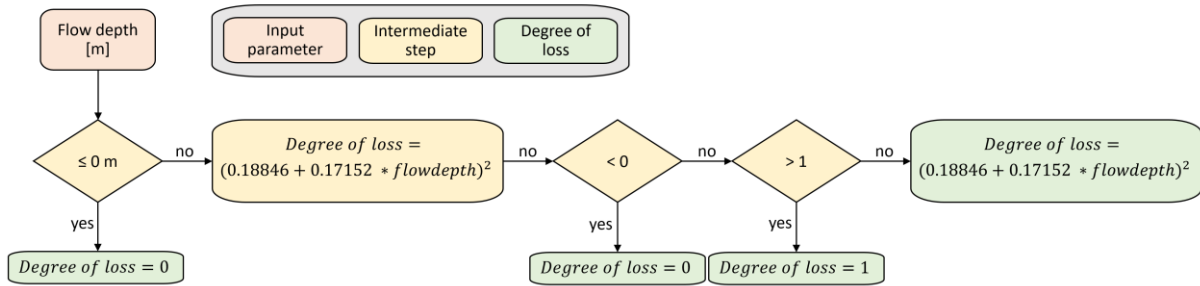


Figure 18: Calculation of degree of loss as a function of maximum flow depth

The formula can also be visualized in a x-y-plot. The orange line in Figure 19 shows the *degree of loss* as a function of the maximum flow depth. The black dashed lines serve as a reading example. The previously highlighted building has an attributed maximum flow depth of 0.99 m. The associated *degree of loss* amounts to 0.13.

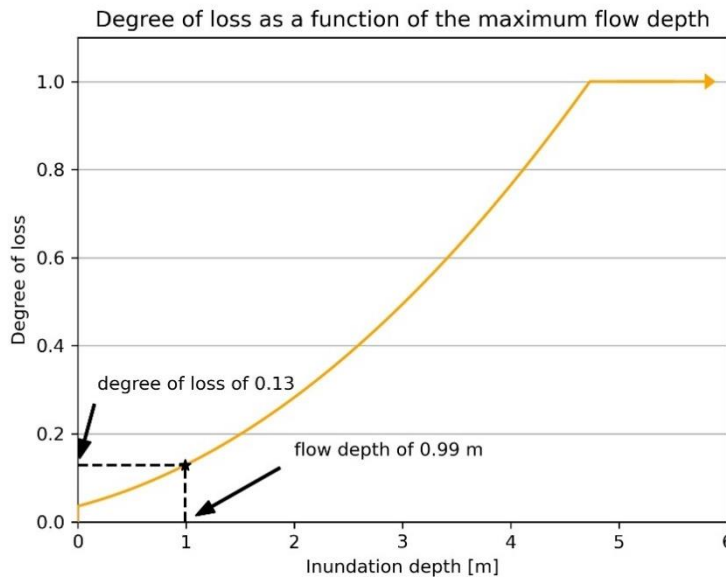


Figure 19: Degree of loss as a function of the maximum flow depth. In addition, the maximum flow depth in the future\_noNBS scenario and the resulting degree of loss of the building from the example above are plotted.

To obtain the damages in CHF, the *degree of loss* is multiplied with the building’s value.

$$damage [CHF] = degree\ of\ loss * building\ value [CHF]$$

For the building used in the example above, the *dol* is 0.13 and the building value amounts to 520'747 CHF. This results in the following damage calculation.

$$damage [CHF] = 0.13 * 520'747 CHF = 67'697 CHF$$

The calculations for the *degree of loss* and the predicted damage in CHF for each scenario are executed with a Python script called “DOLandDamageCalculation.py”. It can be found in the appendix.

As discussed in chapter 1.3 *The risk of urban pluvial flooding*, there are many different costs to be considered in a flooding event. However, in order not to go beyond the scope of this work, only direct

tangible costs incurred on the buildings are considered. At this point, it is important to note that the direct tangible costs comprise of more than just these costs. Damage to public infrastructure, for example, is also a direct tangible cost, but is not considered in this paper. Thus, the costs calculated here represent only a portion of all direct tangible costs. In addition, no indirect or intangible costs are considered, which, however, are certainly incurred in an UPF event.

#### 2.3.3.4 Hazard reduction and hazard increase

The simulation outputs have limited significance without a comparative context. Therefore, the hazard parameters are compared within and across the scenario time steps. To calculate the hazard reduction associated with the implementation of NBS on today's parking spots, the following calculations are made.

$$\begin{aligned} & \textit{Hazard parameter}_{\textit{Hazard reduction through NBS}} \\ & = \textit{Hazard parameter}_{\textit{scenario\_noNBS}} - \textit{Hazard parameter}_{\textit{scenario\_withNBS}} \end{aligned}$$

To calculate the hazard increase associated with the higher rainfall intensity, the following calculations are made.

$$\begin{aligned} & \textit{Hazard parameter}_{\textit{Hazard increase through climate change}} \\ & = \textit{Hazard parameter}_{\textit{future\_noNBS}} - \textit{Hazard parameter}_{\textit{current\_noNBS}} \end{aligned}$$

The hazard reduction calculation for the hazard parameters *flow depth* and *instability* are done in Python using the script "Hazard\_reduction.py" that can be found in the appendix. The reduction in *dol* and damages in CHF on building level is executed in QGIS using the field calculator.

### 3 Results

The main results are presented according to the research questions.

1. What is the current proportion of public parking spots relative to the urban area?
2. Can the simulation program BASEMENT (v2.8) be used to model urban pluvial flooding?
3. What is the associated hazard reduction by replacing today's parking spots with nature-based solutions? How do the results with today's rainfall values differ from those with the assumed end-of-century values?
4. What is the simulated hazard increase due to higher precipitation intensities assumed due to climate change? Are the magnitudes of hazard increase due to climate change and hazard reduction through the implementation of NBS measures on today's parking spots comparable?
5. What are the co-benefits of replacing today's parking spots with nature-based solutions?

#### 3.1 Proportion of parking area relative to the urban area

The whole area on which the simulation is executed consists of 1'385'206 m<sup>2</sup>. Of this, 26'873 m<sup>2</sup> is parking area. Therefore, the parking area makes up 1.94% of the urban area within the simulation perimeter.

#### 3.2 Modelling urban pluvial flooding with BASEMENT (v2.8)

The short answer is yes, it is possible to model urban pluvial flooding with the BASEMENT (v2.8) simulation environment. A more detailed answer will be given in chapter 4.2. As proof of concept, the results of the baseline scenario (*current\_noNBS*) are presented. Figure 20 on page 50 shows the maximum flow depth in meters per mesh element.

The fact that this map can be produced, and the output does not appear arbitrary proves that it is possible to model UPF with BASEMENT (v2.8). Higher flow depths occur along roads and local depressions. Concerning the different hazard categories, it can be said that in most areas there is no relevant hazard. However, some areas and spots exhibit a *moderate*, *high* and even *very high hazard*. The spatial distribution of the flow depth will be covered in a brief assessment of the results in chapter 4.2 *Modelling urban pluvial flooding with BASEMENT (v2.8)* on page 64.

To test the usefulness of modelling UPF with BASEMENT (v2.8), the hazard parameters discussed above are calculated for all scenarios. To save space, only the results from the baseline scenario are shown here. All other maps can be found in the appendix.

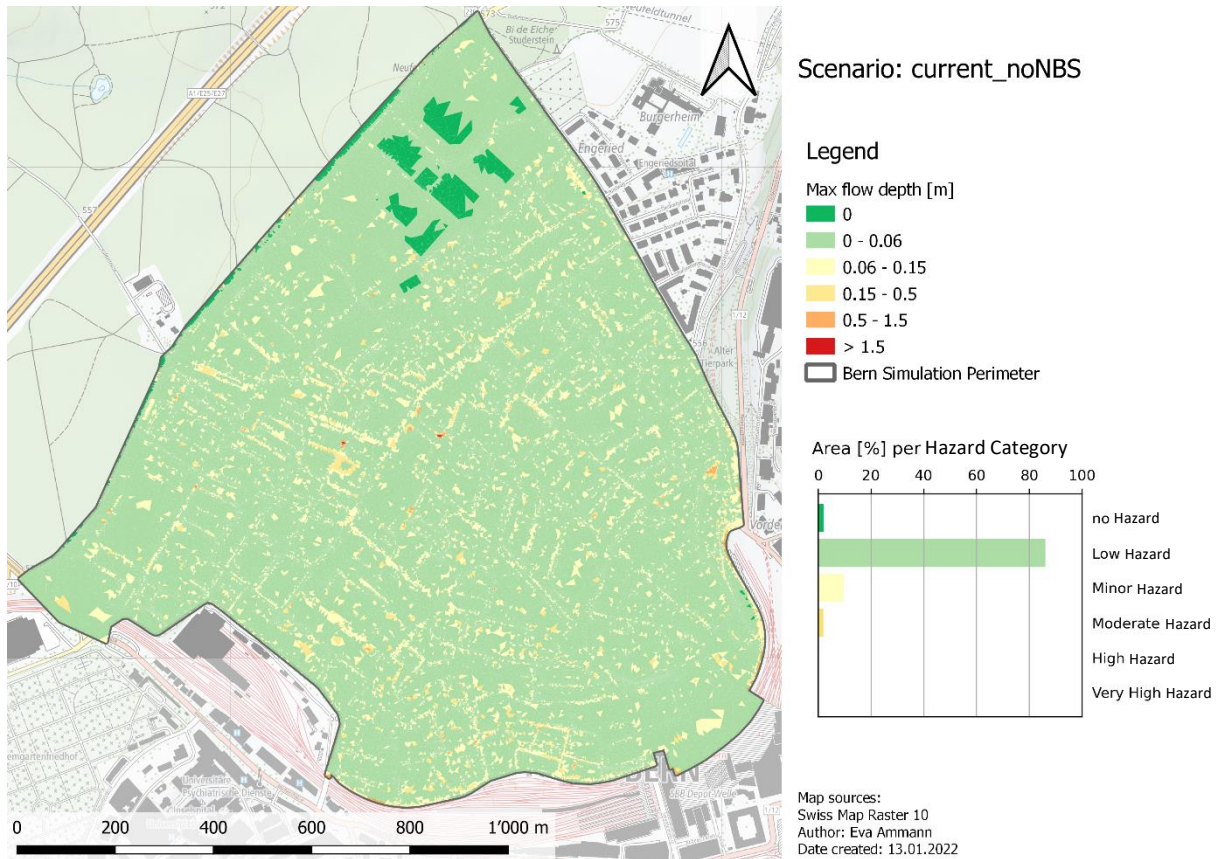


Figure 20: Map of Bern simulation perimeter displaying the maximum flow depth per mesh element in the baseline scenario

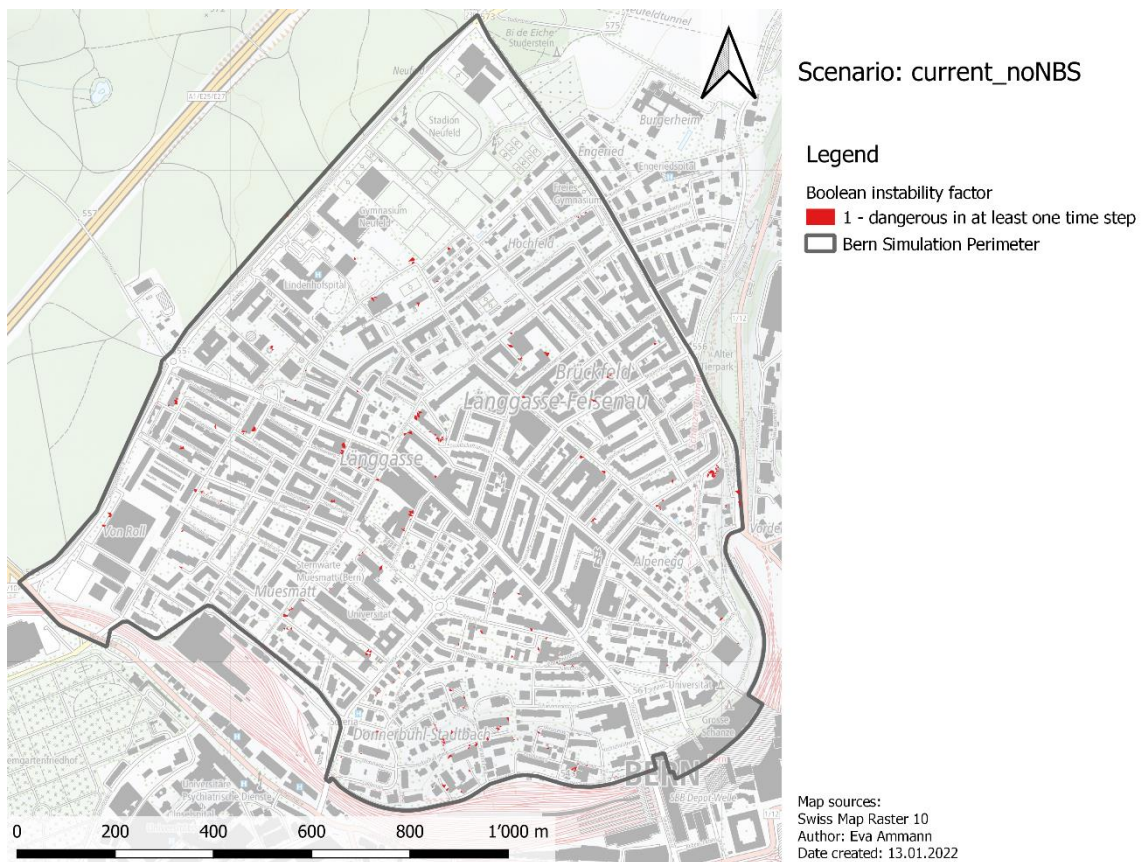


Figure 21: Map of Bern simulation perimeter displaying the boolean instability factor per mesh element in the baseline scenario

According to the BASEMENT (v2.8) simulation results and the instability function provided by Martínez-Gomariz, Gómez and Russo (2016), it can be said that 0.21% of the total area can potentially threaten human stability over the course of the two-hour simulation. The affected triangles are highlighted in Figure 21 on page 50.

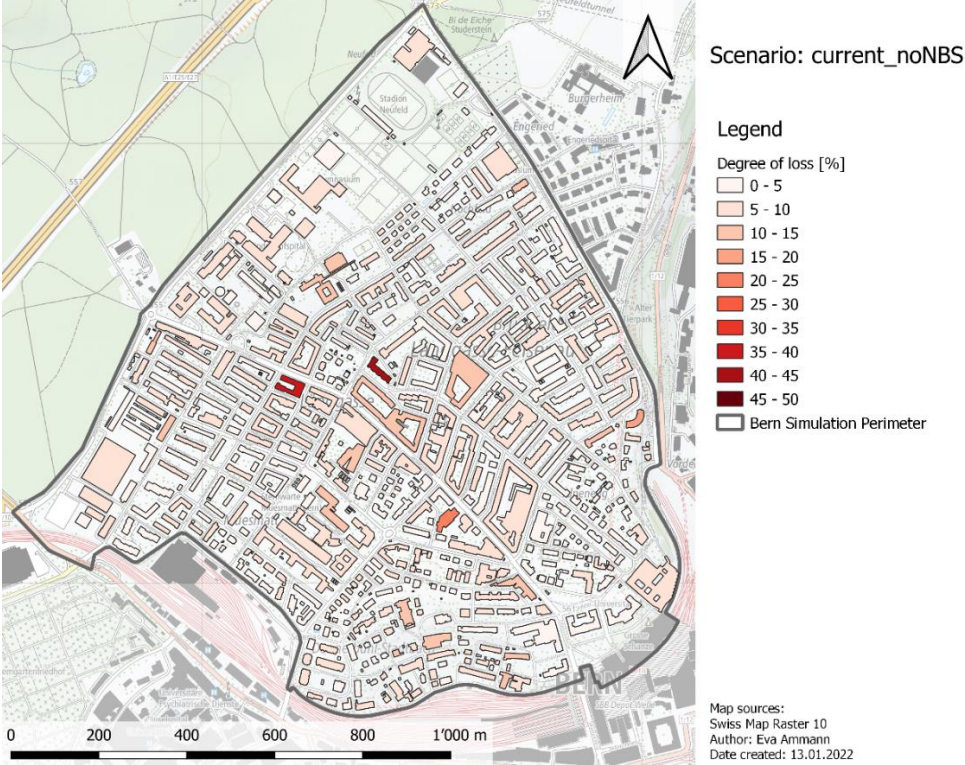


Figure 22: Map of Bern simulation perimeter displaying the degree of loss per building in the baseline scenario

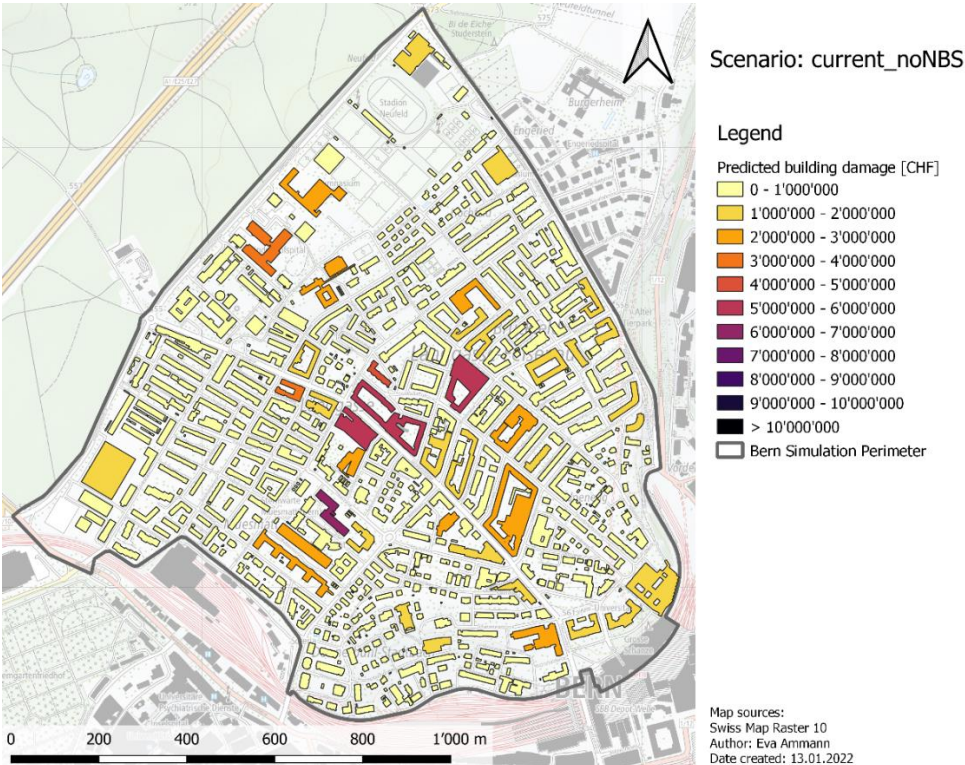


Figure 23: Map of Bern simulation perimeter displaying the predicted damage in CHF per building in the baseline scenario

Figure 22 on page 51 displays the *degree of loss* calculated per house with the help of Kaltenrieder's *dol* formula (2017). The average *dol* amounts to 5.25%. Figure 23 on page 51 combines this result with the building value calculated by Röthlisberger, Zischg and Keiler (2018) and returns the predicted damage per building in Swiss Francs in the baseline scenario. The predicted damage amounts to 201'144'314 CHF. This is 6.26% of the total building value.

### **3.3 Hazard reduction through the implementation of NBS on today's parking spots**

The potential simulated hazard mitigations through the implementation of NBS on today's parking spots are presented using the same hazard parameters as described above. To keep the analyses concise, the results from the *current* and the *future* scenario are handled in two separate subsections. The following maps and figures are supposed to help capturing the different extent of the simulated hazard reduction. Commentaries on the data is largely abstained from. A closer look and, more importantly, a comparison of the result can be found in chapter 4.3 *Hazard reduction through the implementation of NBS on today's parking spots*.

#### **3.3.1 Hazard reduction in the current scenario**

##### *3.3.1.1 Max flow depth*

Figure 24 on page 53 shows the reduction in the maximum flow depth per mesh element in meters. The green mesh elements exhibit lower maximum flow depths in the *withNBS* scenario than in the *noNBS* scenario. These elements follow the expected behavior. The red elements, however, show higher maximum flow depths in the scenario where today's parking spots are replaced with NBS implementation measures. These elements follow a counterintuitive behavior. This will be discussed in chapter 4.3.1.1 *Max flow depth* on page 69.

Figure 25 on page 53 displays a stacked bar chart that represents how the simulation perimeter area is distributed among the hazard categories in the *current\_noNBS* and *current\_withNBS* scenario. The different area distribution is barely noticeable visually. Therefore, a few numbers are presented along with the chart. From the *current\_noNBS* to the *current\_withNBS* scenario, the *no hazard* category increases from 2.01% to 2.39%. The *low hazard* category decreases from 86.23% to 86.08%, the *minor hazard* category decreases from 9.74% to 9.59% and the *moderate hazard* category decreases from 1.91% to 1.82% while the *high hazard* category remains constant at 0.11%.

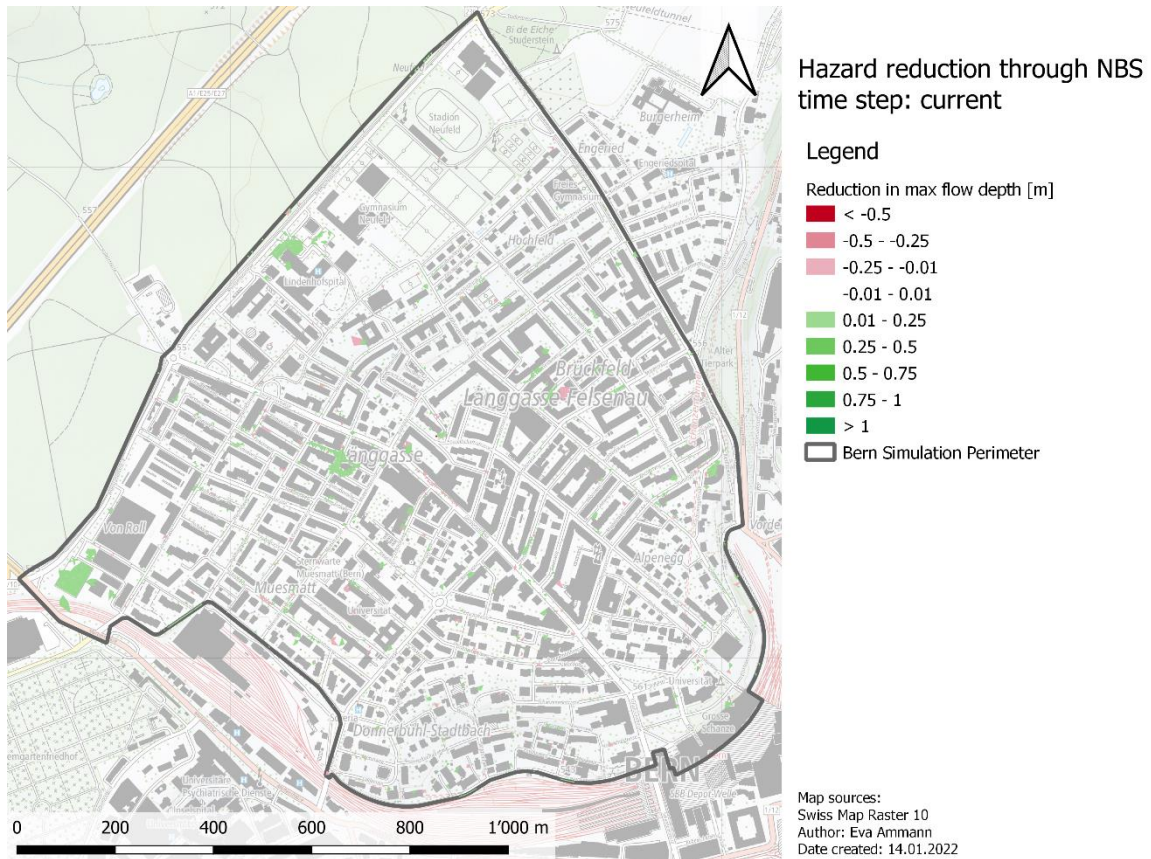


Figure 24: Map of Bern simulation perimeter displaying the reduction in maximum flow depth through the implementation of NBS measures in the current scenario

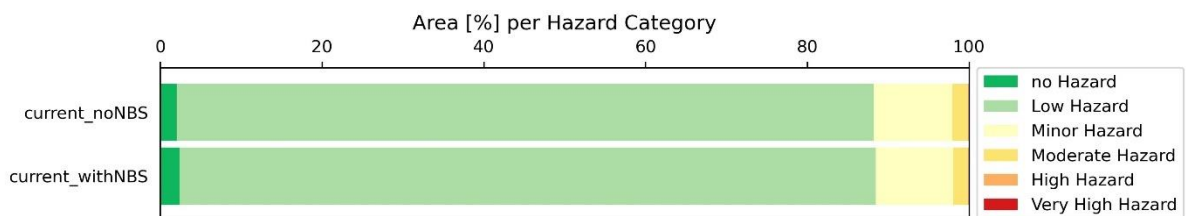


Figure 25: Stacked bar charts representing the area percentage of the simulation perimeter according to the different Hazard Categories

### 3.3.1.2 Instability factor

Figure 26 on page 54 displays the change in the stability indicator from the *current\_noNBS* to the *current\_withNBS* scenario. The green mesh elements exhibit the expected behavior. They are possibly dangerous in the *noNBS* scenario but no longer so in the *withNBS* scenario. The red mesh elements show the opposite and therefore unexpected behavior. Since it is difficult to spot the mesh elements that actually do change in behavior, black arrows point to selected mesh elements and numbers are presented alongside the map. The possibly dangerous area reduces from 0.21% to 0.20% of the simulation perimeter area. While 343m<sup>2</sup> become less dangerous, 138 m<sup>2</sup> become more dangerous with the simulated implementation of NBS measures. This analysis raises questions that are answered in chapter 4.3 in the discussion part.

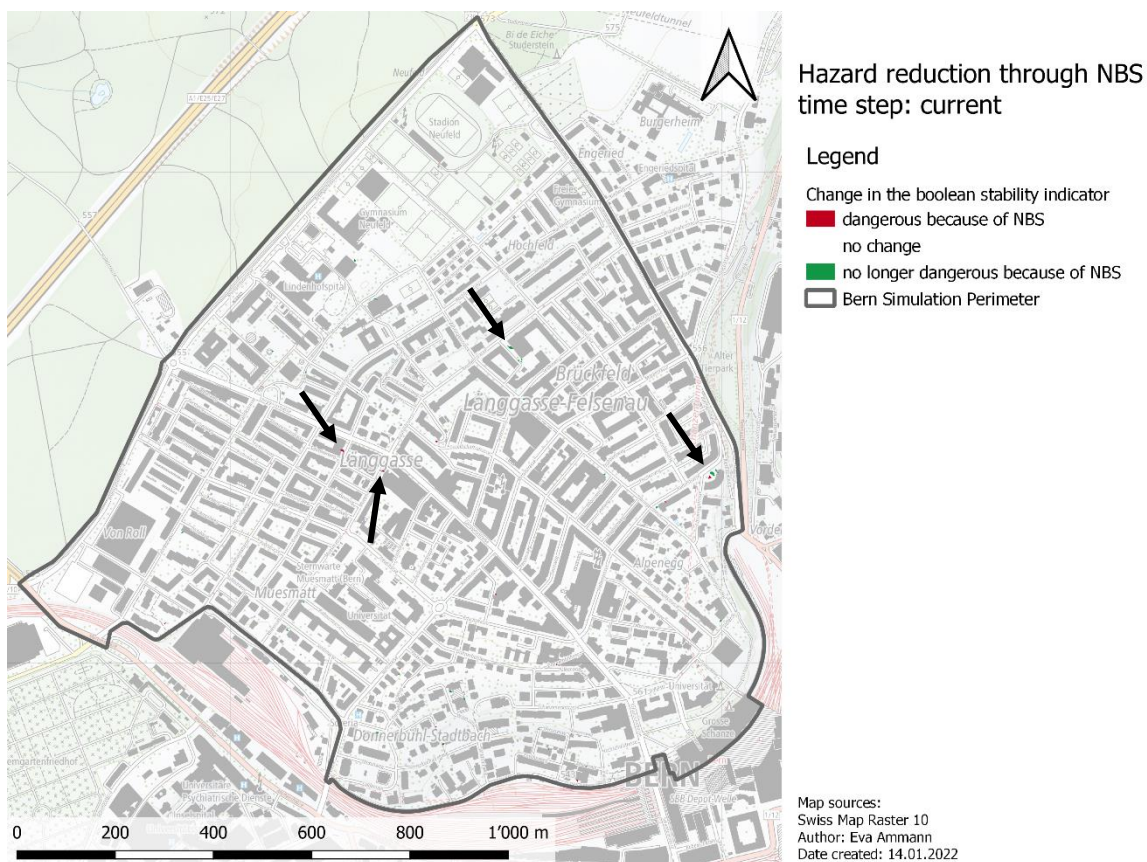


Figure 26: Map of Bern simulation perimeter displaying the change in the boolean stability indicator through the implementation of NBS measures in the current scenario

### 3.3.1.3 Degree of loss and damage in CHF

Figure 27 on page 55 displays the change of the *degree of loss* from the *current\_noNBS* to the *current\_withNBS* scenario. Since the *degree of loss* is expressed in percent, the change is expressed in percentage points. As with the preceding hazard reduction analyses, the green buildings show the expected behavior presenting a lower *dol* after the implementation of NBS measures.



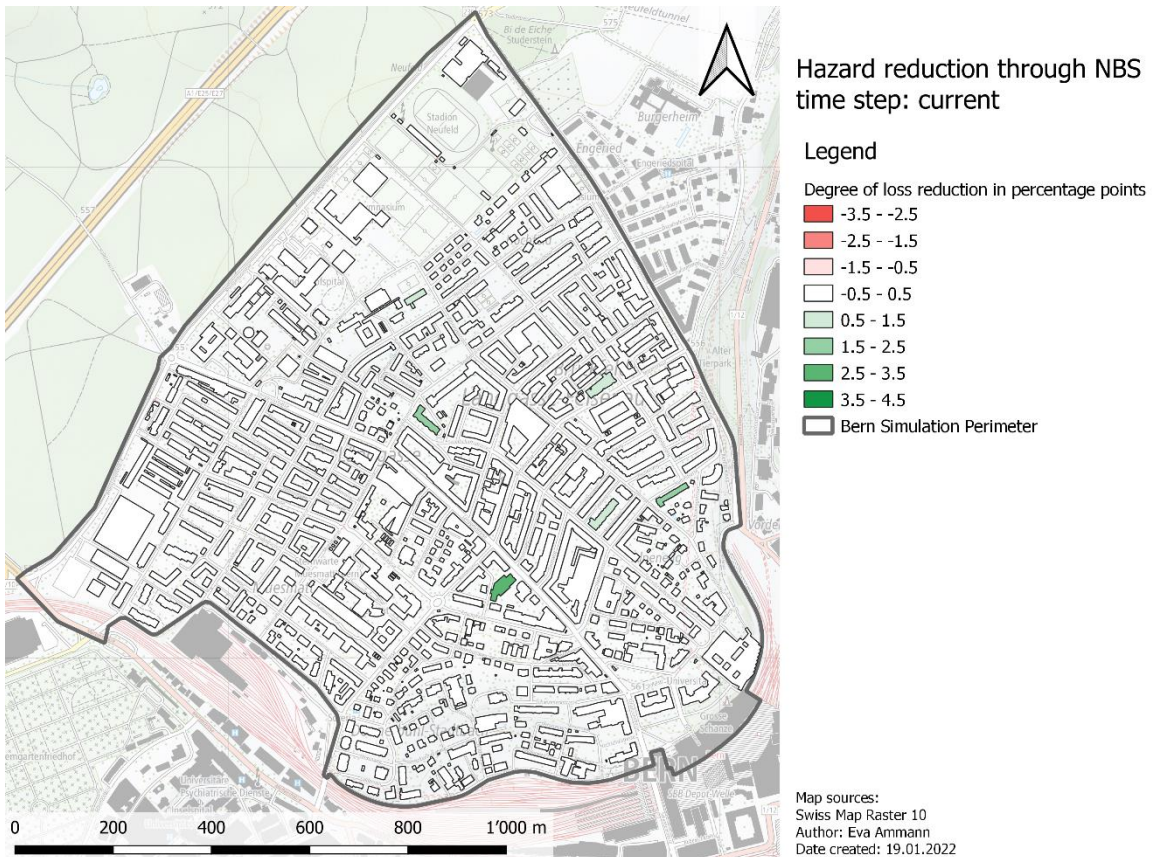


Figure 27: Map of Bern simulation perimeter displaying the change in degree of loss through the implementation of NBS measures in the current scenario

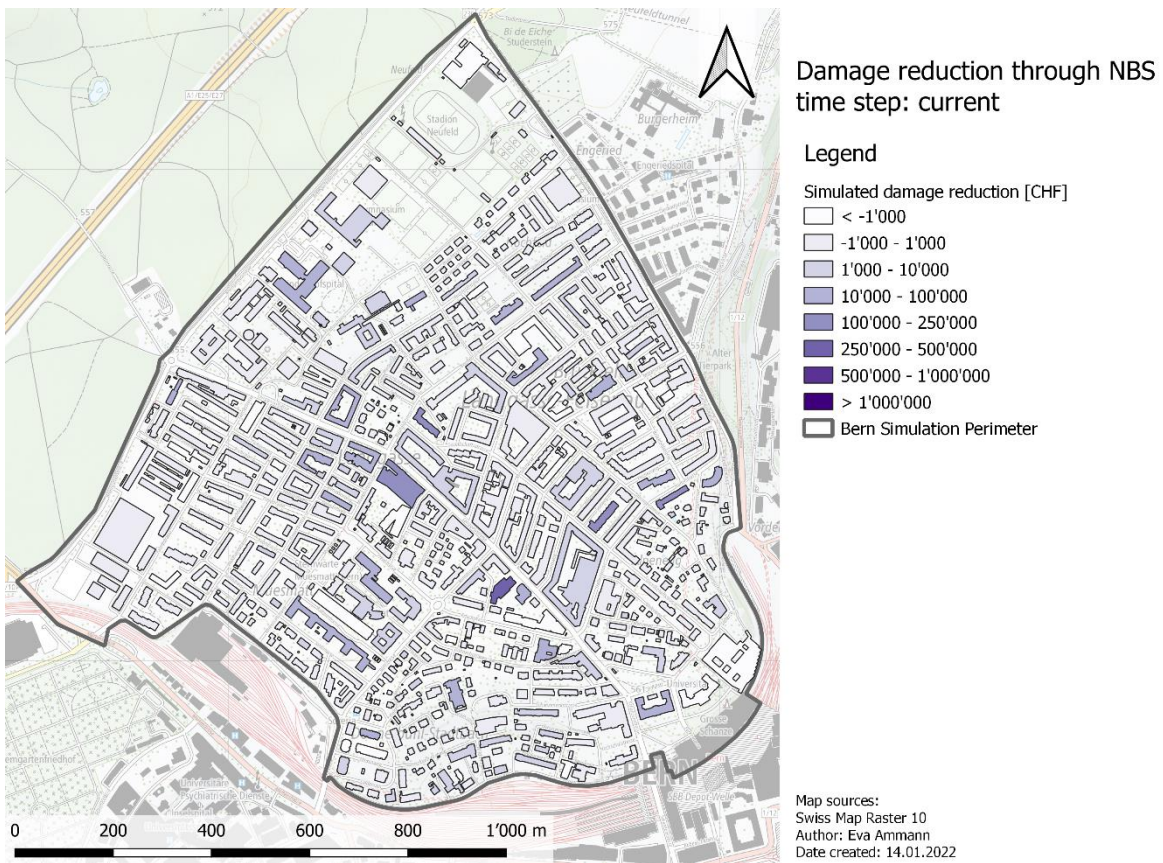


Figure 28: Map of Bern simulation perimeter displaying the simulated damage reduction in CHF through the implementation of NBS measures in the current scenario

Figure 28 on page 55 displays the simulated damage reduction in Swiss Francs. Since a possible counterintuitive *dol* development over the two scenarios could be identified in the respective *dol* map and because the building value has a major impact on the predicted damage reduction, the red-green color scheme was dispensed with. Instead, the darkness of the color represents the total simulated damage reduction. This allows identifying buildings with the highest damage mitigation potential.

Table 13 summarizes the most important metrics from these two analyses. The average *degree of loss* is reduced from 5.25% to 5.22% from the *noNBS* to the *withNBS* scenario. This is a reduction by 0.44%. The predicted damage to the buildings is reduced by 0.71% or 1'426'681 CHF.

Table 13: Summary of *dol* and damage reduction through the implementation of NBS measures in the current scenario

	Current_noNBS	Current_withNBS	Change
Average <i>dol</i> [%]	5.25%	5.22%	-0.44%
Total damage estimated [CHF and % of total building value]	201'144'314 CHF	199'717'633 CHF	-0.71%
	6.26%	6.21%	

### 3.3.2 Hazard reduction in the future scenario

Since the analyses are the same as in the chapter before, the maps and figures are presented with only the most necessary comments.

#### 3.3.2.1 Max flow depth

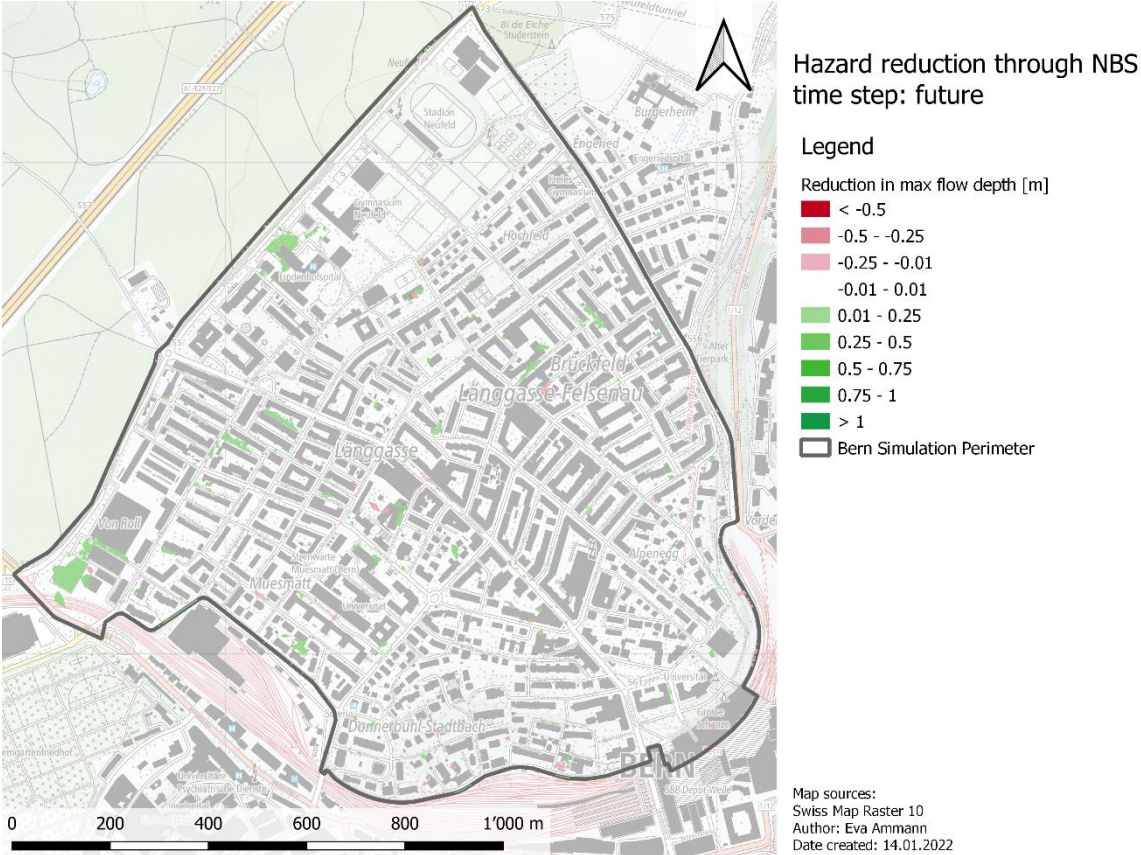


Figure 29: Map of Bern simulation perimeter displaying the reduction in maximum flow depth through the implementation of NBS measures in the future scenario

Since the differences between the *future\_noNBS* and the *future\_withNBS* scenario are again barely noticeable in Figure 30, the same numbers as before are presented. The *no hazard* category increases from 1.49% to 1.82% of the total area. The *low, minor and moderate hazard* category reduce from 81.79% to 81.71%, from 13.02% to 12.86% and from 3.42% to 3.35%, respectively. The *high and very high hazard* category remain nearly constant (0.26% to 0.25% and 0.01% for both scenarios).

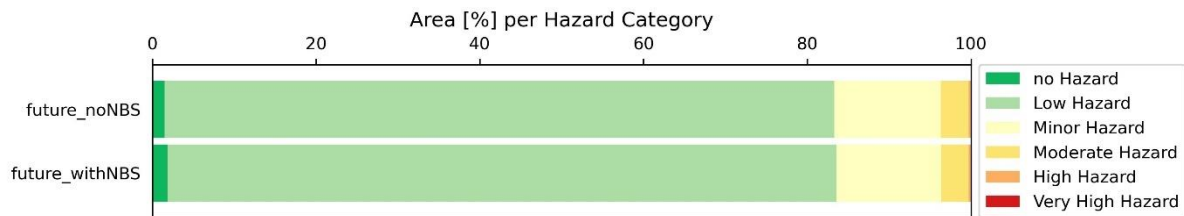


Figure 30: Stacked bar charts representing the area percentage of the simulation perimeter according to the different Hazard Categories

### 3.3.2.2 Instability factor

Because it is again difficult to spot the colored mesh elements in Figure 31, black circles are drawn around some affected areas. In this scenario, the possibly dangerous area actually increases from 0.43% to 0.44% with the introduction of NBS measures. Here, the counterintuitively behaving area (642 m<sup>2</sup>) outweighs the area that behaves as expected (410 m<sup>2</sup>).

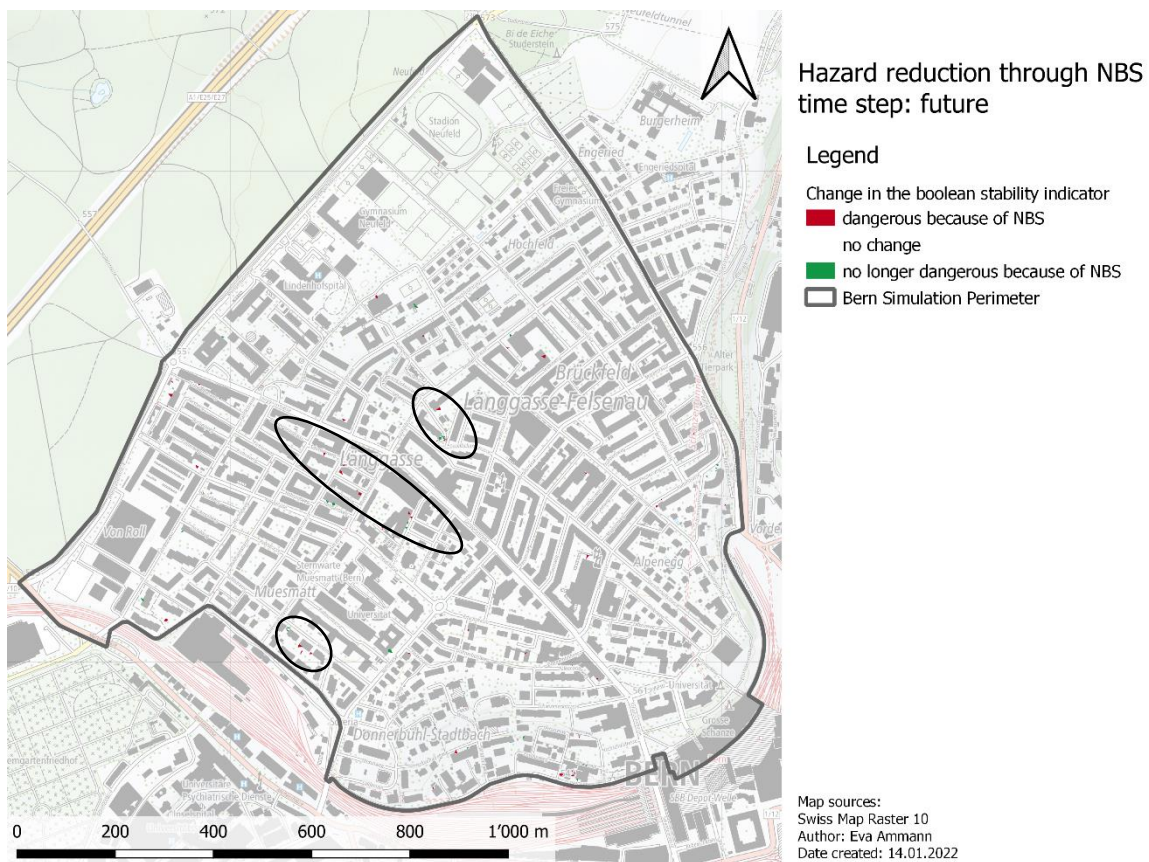


Figure 31: Map of Bern simulation perimeter displaying the change in the boolean stability indicator through the implementation of NBS measures in the future scenario

### 3.3.2.3 Degree of loss and predicted damage in CHF

Figure 32 displays the change in the *degree of loss* for the *future* scenario. These red buildings show the unexpected behavior of exhibiting a higher *dol* when NBS measures are implemented compared to when no NBS measures are implemented. Figure 33 displays the associated damage reduction.

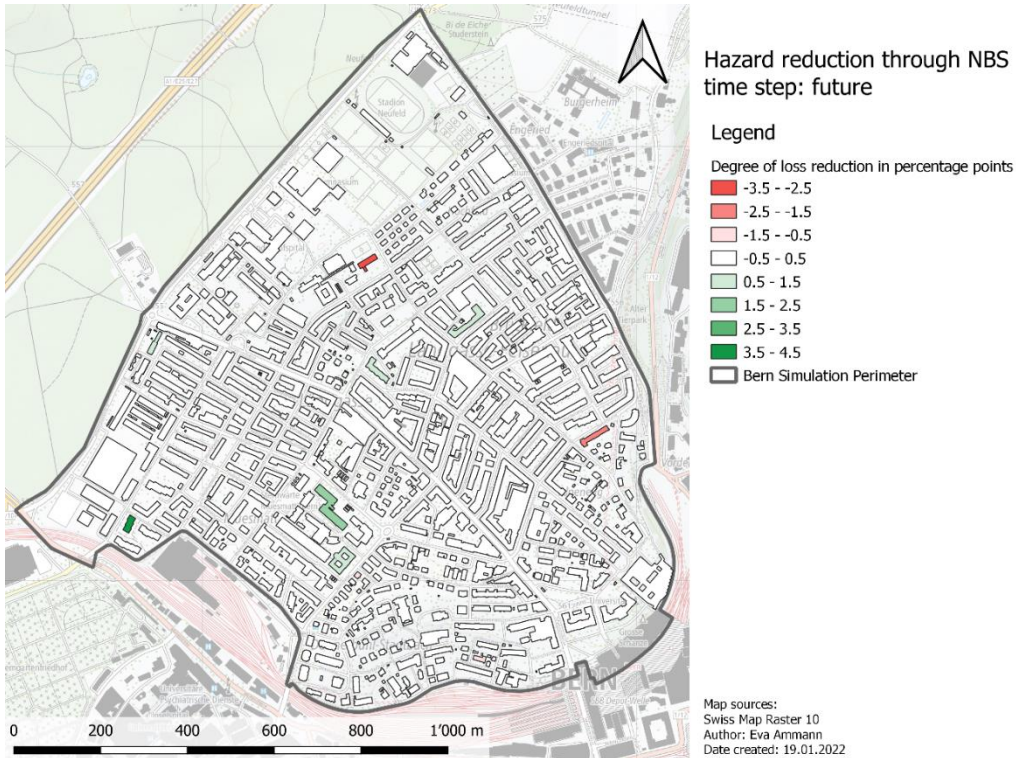


Figure 32: Map of Bern simulation perimeter displaying the change in degree of loss through the implementation of NBS measures in the future scenario

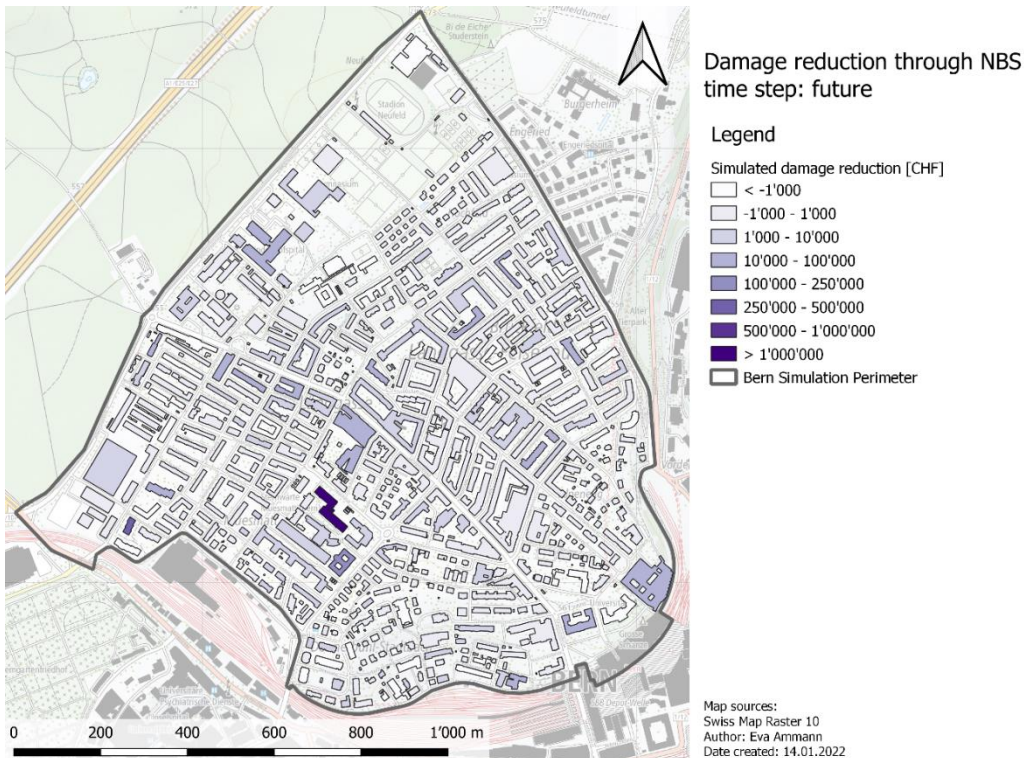


Figure 33: Map of Bern simulation perimeter displaying the simulated damage reduction in CHF through the implementation of NBS measures in the future scenario

The appearance of buildings exhibiting a higher *dol* after the implementation of NBS can also be seen in the smaller reduction of the average *dol*. As is shown in Table 14, the average *dol* is reduced from 5.70% to 5.69%. This is a reduction by only 0.24%. Meanwhile, the predicted damage reduces from 231'693'076 CHF to 229'720'593 CHF through the implementation of NBS on today's parking spots. This is a reduction of 1'972'483 CHF or 0.85%. Thus, the relative hazard reduction in the *future* scenario exceeds the same metric in the *current* scenario.

Table 14: Summary of *dol* and damage reduction through the implementation of NBS measures in the *future* scenario

	Future_noNBS	Future_withNBS	Change
<b>Average dol</b>	5.70%	5.69%	-0.24%
<b>Total damage estimated</b>	231'693'076 CHF	229'720'593 CHF	
<b>[CHF and % of total building value]</b>	7.21%	7.15%	-0.85%

**3.4 Hazard increase due to climate change**

To put the proportion of hazard reduction through the implementation of NBS measures in the *current* and in the *future* scenario into perspective, the following chapter will present the hazard increase from the *current* to the *future* scenario. To avoid complicating the analysis unnecessarily, the *noNBS* scenario is used in both time steps. Again, unnecessary or repeating comments are omitted since the same hazard parameters are analyzed. Additionally, in order to keep the sentences short, the term “because of/due to climate change” refers to the in subchapter 2.3.2.2 *Rainfall* on page 39 assumed increased rainfall intensity as a result of climate change.

*3.4.1.1 Max flow depth*

Figure 34 on page 60 displays the simulated increase in max flow depth from the *current* to the *future* scenario. While the reader's brain might already be accustomed to attributing counterintuitive behavior to the red colored mesh elements, this is no longer true in this set of analyses. Since a hazard increase is expected from the *current* to the *future* scenario and a higher flow depth is shown in red, the red color is now representing the expected behavior.

In Figure 35 on page 60, changes in the hazard category area percentages are noticeable. The area percentages associated to the *no hazard* (2.01% to 1.49%) and the *low hazard* category (86.23% to 81.79%) are reduced, the area percentages attributed to the *minor* (9.74% to 13.02%), *moderate* (1.91% to 3.42%) and *high hazard* category (1.91% to 3.42%) are increased.

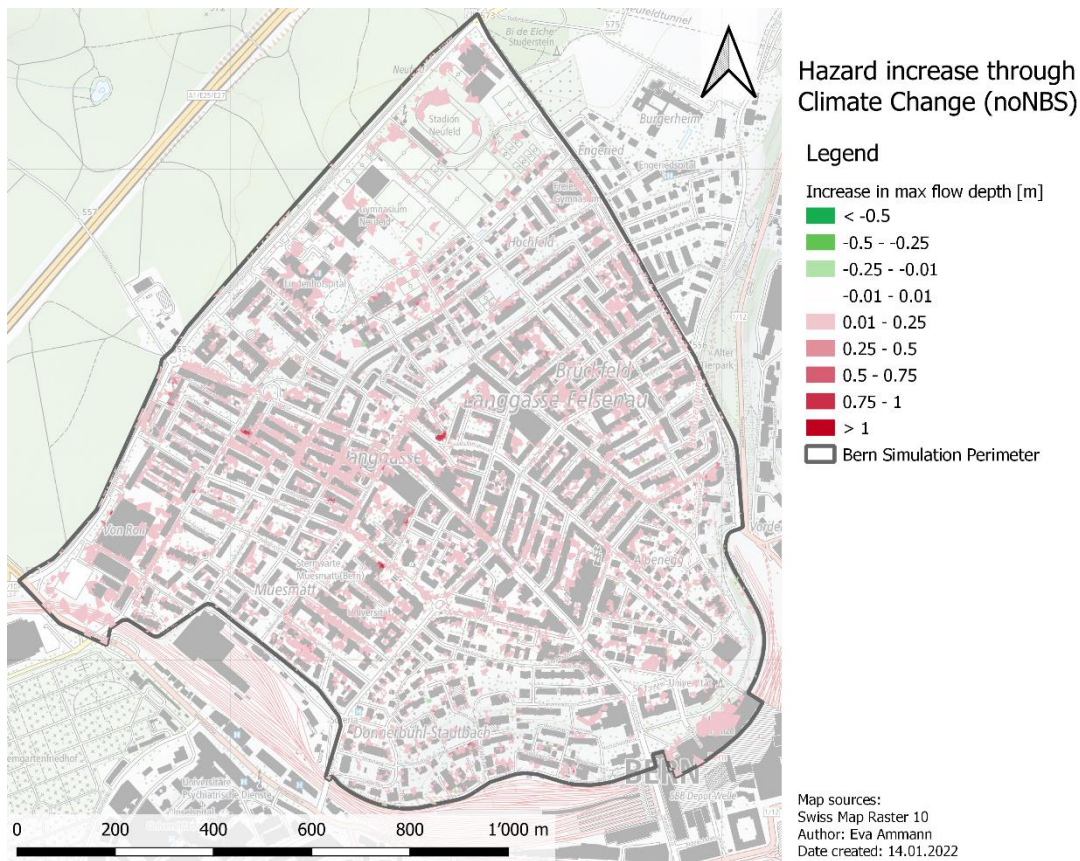


Figure 34: Map of Bern simulation perimeter displaying the increase in maximum flow depth through climate change

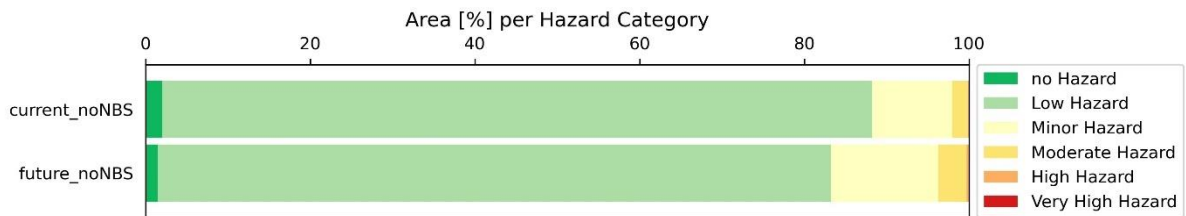


Figure 35: Stacked bar charts representing the area percentage of the simulation perimeter according to the different Hazard Categories

### 3.4.1.2 Instability factor

As can be seen from Figure 36, the area possibly dangerous to human stability is increases from 0.21% to 0.43%. While this might not sound like much, it is still a doubling of the affected area and a manifold of the change ratio within the same scenario time step. Contributing to this result are the 3'066 m<sup>2</sup> that become dangerous due to climate change opposed to 123 m<sup>2</sup> that lose their “possibly dangerous” label.

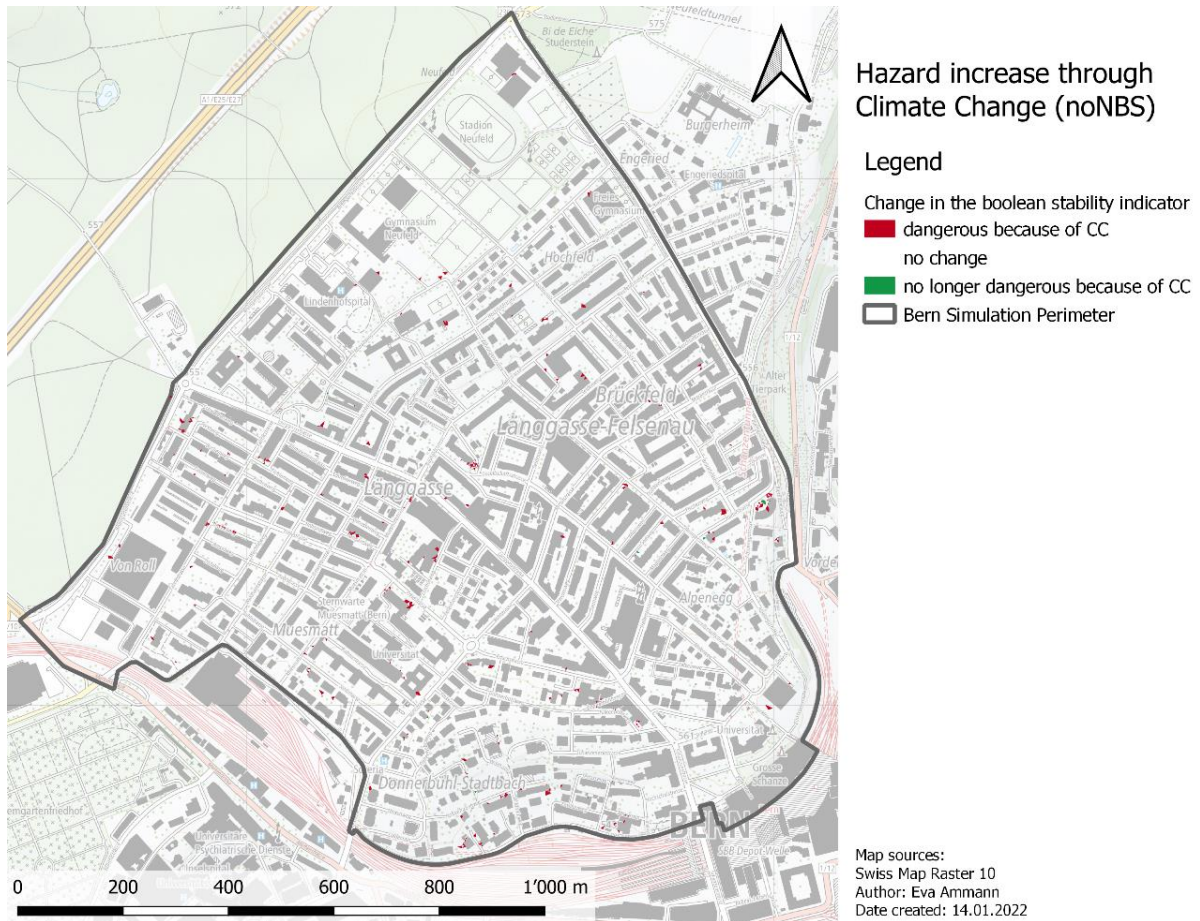


Figure 36: Map of Bern simulation perimeter displaying the change in the boolean stability indicator through climate change

### 3.4.1.3 Degree of loss and predicted damage in CHF

In Figure 37, the red color indicates a hazard increase. Since this analysis observes the development from the *current* to the *future* scenario, the red color represents the buildings with the expected behavior. To maintain the overview, the color scale is limited at the value of 10.5 even though the maximum value is close to 19. Figure 38 shows the associated increase in building damage.

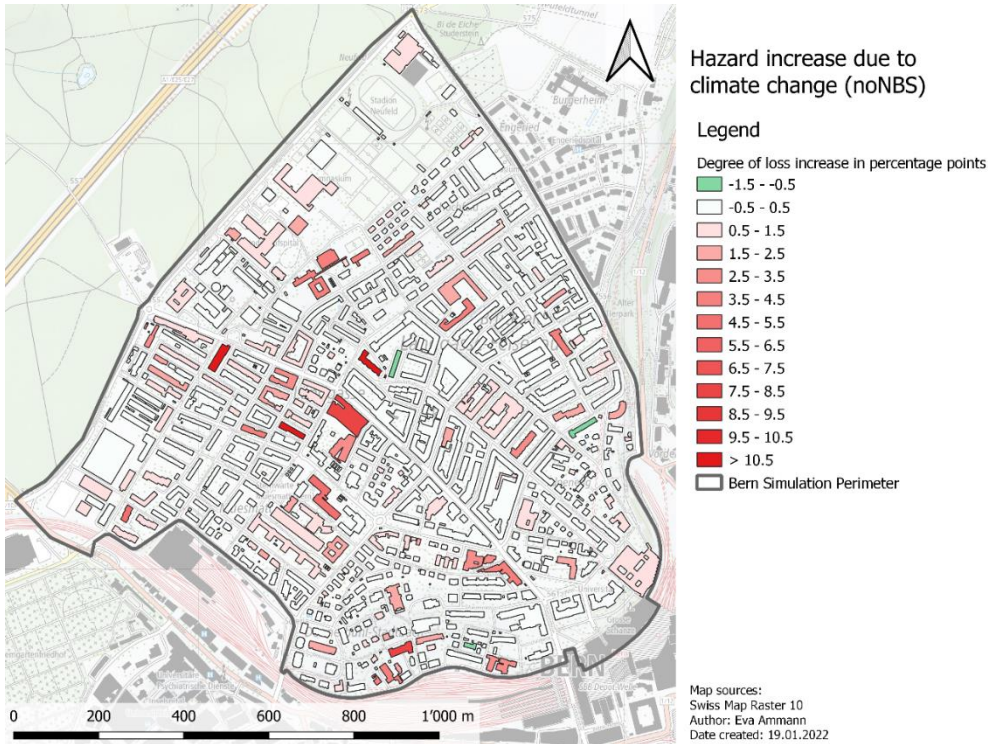


Figure 37: Map of Bern simulation perimeter displaying the change in degree of loss through climate change

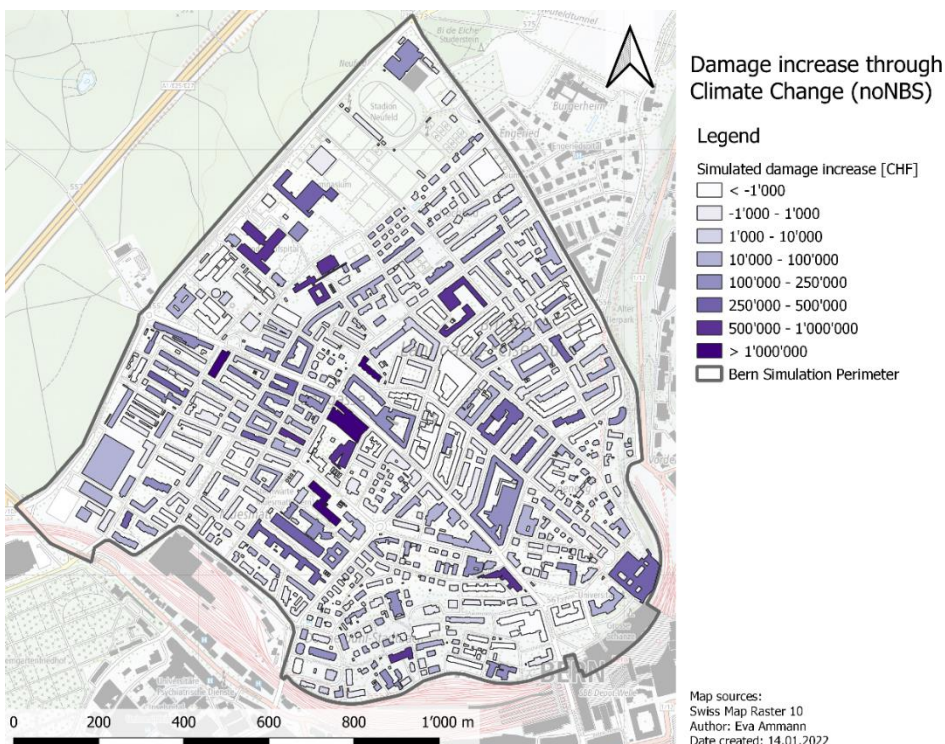


Figure 38: Map of Bern simulation perimeter displaying the simulated damage increase in CHF through climate change



As can be gathered from Table 15, the average *dol* increases from 5.25% to 5.70%. This is an increase of 8.71%. The estimated damage is increased by 15.19% or 30'548'762 CHF.

Table 15: Summary of *dol* and damage increase through climate change

	Current_noNBS	Future_noNBS	Change
<b>Average <i>dol</i></b>	5.25%	5.70%	+8.71%
<b>Total damage estimated</b>	201'144'314 CHF	231'693'076 CHF	
<b>[CHF and % of total building value]</b>	6.26%	7.21%	+15.19%

**3.5 Co-benefits of replacing today’s parking spots with nature-based solutions**

Since no data is collected to quantify the co-benefits of implementing NBS, no results can be shown. However, the research question is addressed in chapter 4.6 *Co-benefits of replacing today’s parking spots with nature-based solutions* on page 75.

## 4 Discussion

In the following subchapters, the previously presented results are discussed and set into context. Each research question is answered in the corresponding subchapter. This chapter concludes with the implications of the results and the limitations of this paper.

### 4.1 Proportion of parking area relative to the urban area

The parking area in the Bern simulation perimeter makes up 1.94% of the total area. In the study published by Zellner et al. (2016), it is stated that NBS must make up at least 10% (20% - 30% for larger storms) of the total area to have a significant flood-reduction effect. Since this threshold is missed by a wide margin, it should not be surprising that the simulated hazard reduction finds itself at a very low level.

### 4.2 Modelling urban pluvial flooding with BASEMENT (v2.8)

This discussion part consists of two parts. First, a brief assessment will provide information about the plausibility of the simulation results. Second, the usability of BASEMENT (v2.8) as a simulation tool for UPF is discussed. These two parts are intended to answer the question of whether it is possible and, if so, useful to use BASEMENT (v2.8) as a modelling tool for UPF.

#### 4.2.1.1 Assessment of the simulation results

In 2018, the FOEN (2018) published a surface runoff risk map. It was created because surface runoff resulting from heavy precipitation increased in occurrence and accounts for up to 50% of flood damage in Switzerland. The map is of practical use to urban planners and emergency responders, but it has no legal status. It is done for all of Switzerland, thus, it also includes the Bern simulation perimeter used in this work. It was developed through modelling, ignores underpasses as well as protection measures and it was not validated at the location (FOEN 2018). Therefore, the comparison outcome must be treated with caution. The surface runoff risk map is modelled for a design event with an estimated return period of more than 100 years (FOEN 2018). From the BASEMENT (v2.8) simulation output collection, the *future\_noNBS* scenario is used to compare the maximum flow depth with the surface runoff risk map. This is because the *future* scenario's return period currently also exceeds 100 years and thus, the two compared map scenarios share a similar return period. Figure 39 on page 65 shows the surface runoff risk map published by the FOEN (2018) and Figure 40 on page 65 shows the *future\_noNBS* maximum flow depth map. To facilitate comparison, the same style is applied.

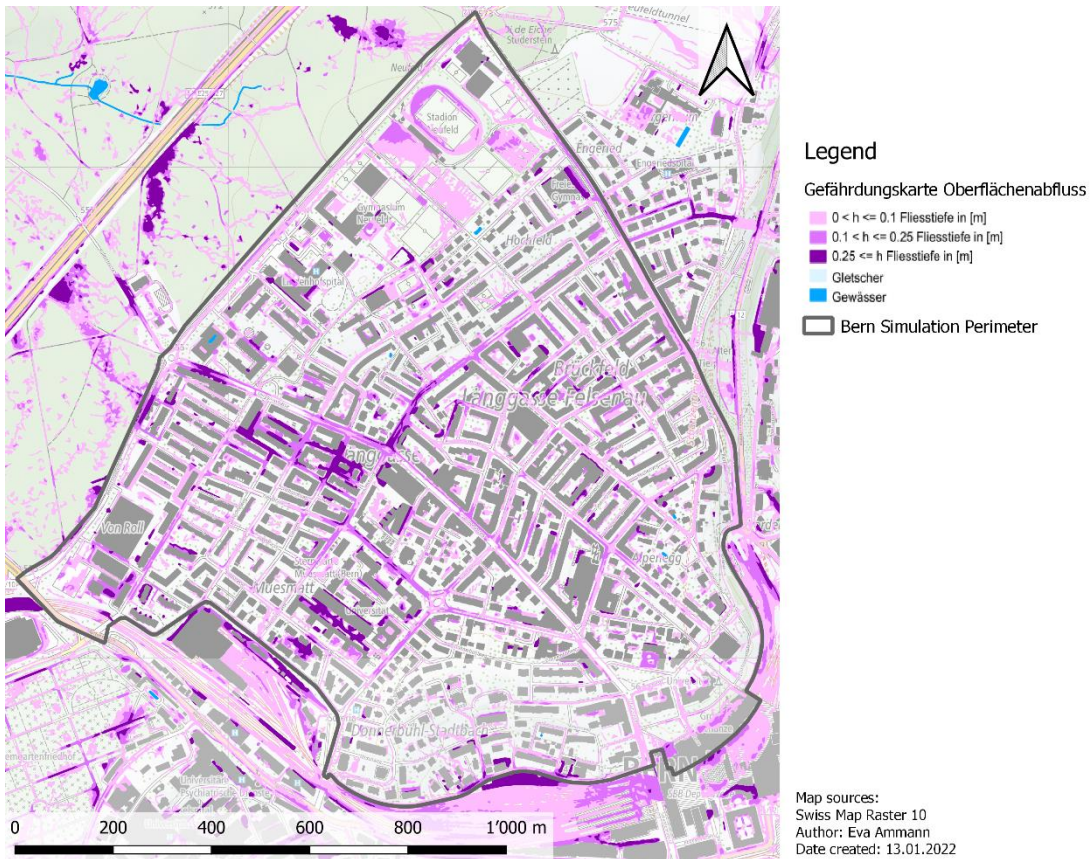


Figure 39: Map of Bern simulation perimeter displaying the surface runoff risk map published by the FOEN (2018)

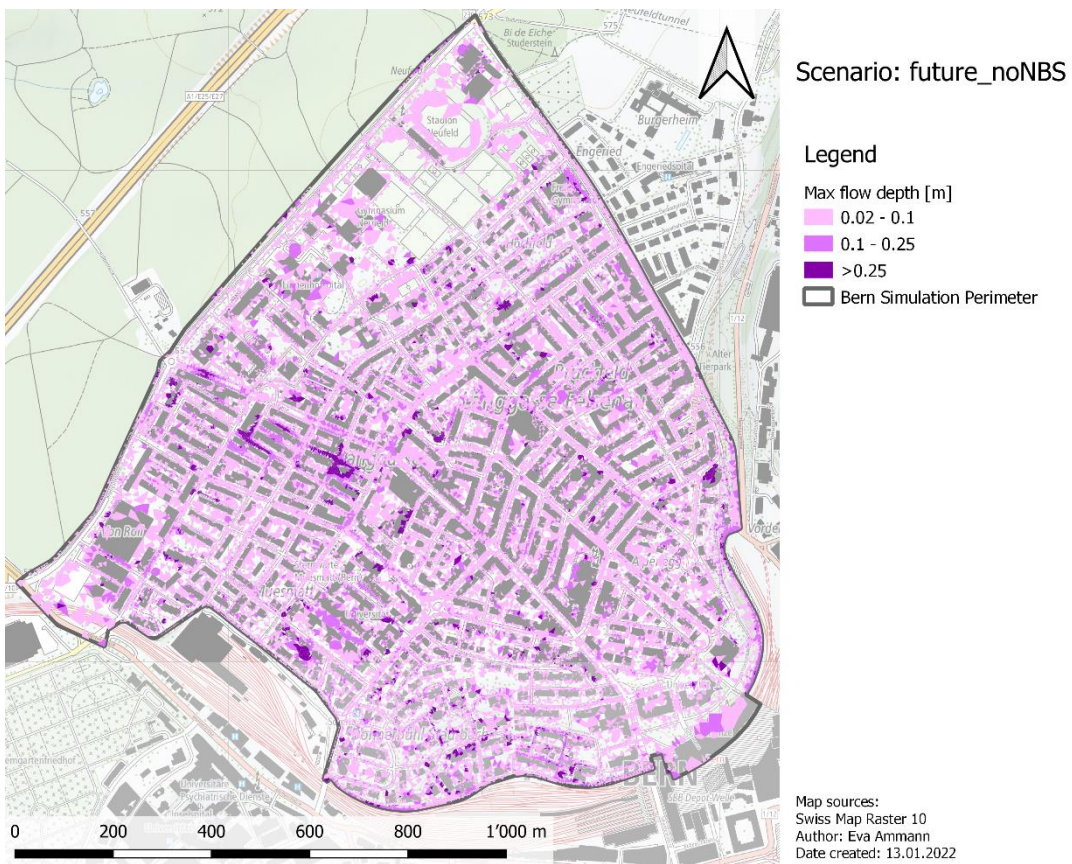


Figure 40: Map of Bern simulation perimeter displaying the maximum flow depth for the future\_noNBS scenario using the same legend as the surface runoff risk map published by the FOEN

An in-depth numerical analysis of the two maps is beyond the scope of this work and would only offer limited benefits due to all the limitations applying to the surface runoff risk map (FOEN 2018). However, a short visual inspection reveals that the two maps show a very similar pattern. The surface runoff hotspots (dark purple) within the simulation perimeter are congruently determined and the light purple area representing minor inundation is located along the roads in both maps. The fact that this comparison does not provide any counterevidence lends credibility to the simulation results. To further validate the results, the two areas indicating the biggest hazard are analyzed in situ. The hazard locations are shown in Figure 41.

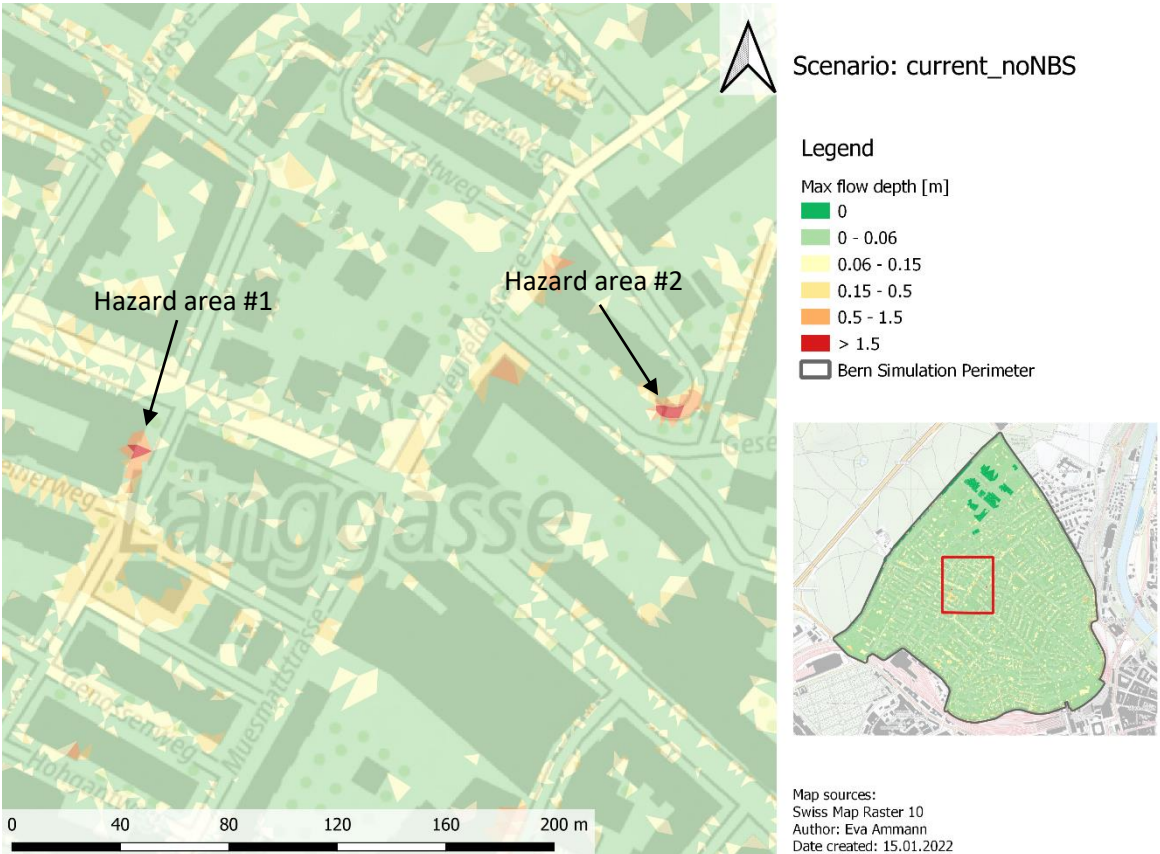


Figure 41: Closeup of Bern simulation perimeter locating the two areas with the highest predicted hazard in the current\_noNBS scenario

A short inspection shows that both areas are underground parking entrances. Figure 42 shows pictures from hazard area #1 and Figure 43 on page 67 shows pictures from hazard area #2.



Figure 42: two pictures showing hazard area #1 (own images taken on 13.01.2022)



Figure 43: Three pictures showing hazard area #2 (own images taken on 13.01.2022)

The pictures prove that topographical weak spots in the urban environment are identified in the BASEMENT (v2.8) simulation. These two assessment methods must suffice for this work. It is demonstrated that BASEMENT (v2.8) is capable of modelling urban pluvial flooding, provided that good quality data has been carefully prepared.

#### 4.2.1.2 BASEMENT (v2.8) as simulation environment for urban pluvial flooding

As is demonstrated before, it is possible to model urban pluvial flooding with BASEMENT (v2.8). However, the author does not recommend it. As the extensive “Data and Methods” chapter of this work shows, the workflow is tedious and not very user-friendly. Without going into too much detail, the shortcomings and obstacles to model UPF with BASEMENT (v2.8) are listed in Table 16. For a better overview, they are summarized according to the process steps.

It is important to emphasize that this is in no way a criticism of the simulation program itself. BASEMENT (v2.8) was developed for simulating fluvial floods rather than pluvial floods. Therefore, the criticisms in Table 16 on page 68 are aimed exclusively at the use of BASEMENT (v2.8) as a modeling tool for UPF. In addition, the issues concerning the pre-processing must be put into perspective. This is because pre-processing must be performed for every simulation program. Moreover, it cannot be taken for granted, that there exists a specifically developed plugin to help with this process step.

Conclusively it can be said that it is possible to model urban pluvial flooding with BASEMENT (v2.8), however, it is not recommended. The simulation software is very powerful and can calculate different simulation setups in a reasonable time frame. That said, it must be admitted that modelling UPF is not the intended use of this software. Any user who tries it anyway is quickly and somewhat tediously made aware of it.

A separate discussion of the calculated hazard parameter results for the *current\_noNBS* scenario is omitted. A short visual inspection of the figures does not bring to light any unrealistic values. Since no counter-indicator for the results’ plausibility is found, the following subchapters discuss the simulated reduction or increase of the various hazard parameters and the simulated scenario sensitivity.

Table 16: List of shortcomings and obstacles to model UPF with BASEMENT (v2.8)

Process step	Issues
<b>Pre-Processing</b>	<ul style="list-style-type: none"> <li>▪ The creation of the computational mesh is a lengthy process.</li> <li>▪ The generation of the quality mesh is not designed for a simulation area with features from many different layers.</li> <li>▪ The urban area consists of many closely spaced features that need to be incorporated. This can lead to the creation of very small mesh elements. These cannot be handled by BaseMESH and hinder the further calculation process.</li> <li>▪ The centroids required for the generation of the computational mesh are tedious to implement with thousands of feature polygons.</li> <li>▪ Even though the StringDefs are nicely defined, they are not always written correctly in the .2dm file when several nodes are close together (radius of 10 m – 20 m) or arranged around a corner.</li> <li>▪ Many errors only appear a few steps later in the simulation process. This leads to very lengthy correction processes.</li> <li>▪ Several times, only the first error of a type is shown. This leads to lengthy and iterative correction processes. Exemplary of this are the over 60 quality mesh and the 20 computational mesh versions that exist for this simulation alone.</li> </ul>
<b>Simulation process</b>	<ul style="list-style-type: none"> <li>▪ While the user interface works well, it is tedious to implement changes. For example, the same changes in the StringDefs must be carried out at different points in the program.</li> <li>▪ The rainfall must be implemented in m<sup>3</sup>/s per area. This requires a complex and error-prone calculation process. Attention: In the meanwhile, BASEMENT (v3.1) has been released. In this version, it is possible to implement rainfall in the more useful units of mm/h. However, the new version reacts more sensibly to “mass balance errors”. This is a type of error that occurs at several triangles using v2.8. A stricter handling of these errors would make it impossible to simulate UPF with the used computational mesh.</li> <li>▪ The simulation program is not able to handle very steep areas. However, abrupt height changes are a key feature of urban areas. Using a manipulated DTM is helpful, but does not entirely solve the problem.</li> <li>▪ Even with properly defined StringDefs, the zero_gradient boundary condition leads to flow velocities exceeding 200 m/s and negative outflows. Both are impossible in this specific simulation setup.</li> </ul>
<b>Post-processing</b>	<ul style="list-style-type: none"> <li>▪ The flow velocity is exported separately in x-velocity and y-velocity. This requires some additional steps to display the flow velocity.</li> </ul>

### 4.3 Hazard reduction through the implementation of NBS on today's parking spots

The goal is to capture the different extents to which the same measure (implementing NBS on today's parking lots) can mitigate a heavy rainfall event in the *current* and *future* scenario. Therefore, the hazard parameter reduction in the *current* and *future* scenario are discussed in parallel.

#### 4.3.1.1 Max flow depth

The changes in the area percentage per hazard category are minimal in both scenario time steps. It is striking that the differences are barely visible in the stacked bar charts. The reduction of the higher hazard classification (sum of *moderate*, *high* and *very high hazard* category) is reduced from 2.02% to 1.94% in the *current* and from 3.69% to 3.61% in the *future* scenario. This is a reduction by 4.32% and 2.19%, respectively. The reduction is therefore very limited. However, it is worth noting that the area with a reduced hazard is larger than the area on which the NBS are implemented. Therefore, some amplifying hazard reduction effects can be expected. Furthermore, the percentual hazard reduction is larger in the *current* than in the *future* scenario. This pattern is supported by Huang et al. (2020) who show that the reduction potential of NBS measures decreases with an increasing rainfall intensity.

The question arises why some mesh elements exhibit higher max flow depth in the *withNBS* than in the *noNBS* scenario. To answer it conclusively, the calculation process of the simulation software would need to be investigated. However, this is beyond the scope of this paper. Therefore, three hypotheses are given. First, it is possible that the focus on the maximum flow depth is deceiving because statistical outliers are overrepresented. A focus on the median flow depth (or similar) could be more accurate. Second, this behavior could be introduced by the many "mass balance errors" that occur during the simulation but are ignored. Third, the calculation process might differ between dry and wet mesh elements. Since the calculation method is based on the *excessive rainfall*, the parking areas are treated as dry in the *withNBS* scenario. Once water flows into these mesh elements, the minimum water depth of 0.01 m must be reached before the water can flow into the next mesh element. This can lead to different flow path calculations between the scenarios. This hypothesis is supported by Figure 44, which overlays the change in maximum flow depth in the *future* scenario with the MatID. It is shown that the change in maximum flow depth layer shows an uneven pattern along the border of the parking area.

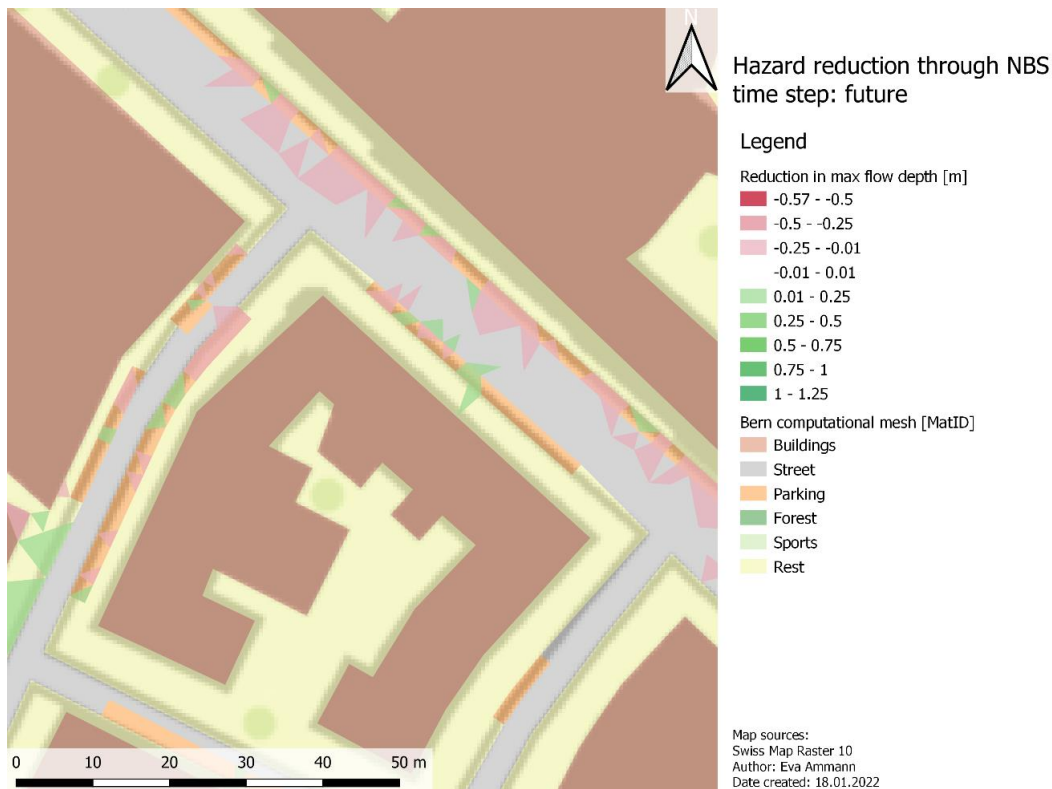


Figure 44: Closeup of Bern simulation perimeter displaying the reduction in max flow depth in the future scenario and the computational mesh MatID

#### 4.3.1.2 Instability factor

First, it must be said that the calculated area possibly dangerous to human stability is very small in both scenarios. In the current scenario, the area in question is reduced from 0.21% to 0.20%. In the future scenario, however, the area increases from 0.43% to 0.44% with the implementation of NBS measures. This sets warning bells ringing and calls for a thorough examination. To understand the predicted increase, it makes sense to look at the boolean stability function map for both scenarios. On page 71, Figure 45 shows the boolean stability function for the *future\_noNBS* scenario, Figure 46 the same hazard parameter for the *future\_withNBS* scenario. It is noticeable that almost all red triangles are adjacent to building polygons. It is expected that the areas possibly dangerous to human stability are along steep roads. These can act as a channel and thus cause increased flow velocities. However, as can be seen by the blue arrows in Figure 45, none of the selected steep roads seem to be affected.

An explanation for this illogical hazard parameter outcome might lie in the generation of the computational mesh. Each mesh element is assigned a height to its center that is derived from the heights of the three nodes forming the triangle. Now, if one or two points are on a building polygon border, they have a height of  $DTM_{at\ this\ location} + 2m$ . The remaining one or two points are on street level and have a height of  $DTM_{at\ this\ location}$ . Thus, the triangle must bridge the two-meter height gap. This leads to very steep triangles, which in turn can lead to high flow velocities, which might classify a triangle as possibly dangerous.



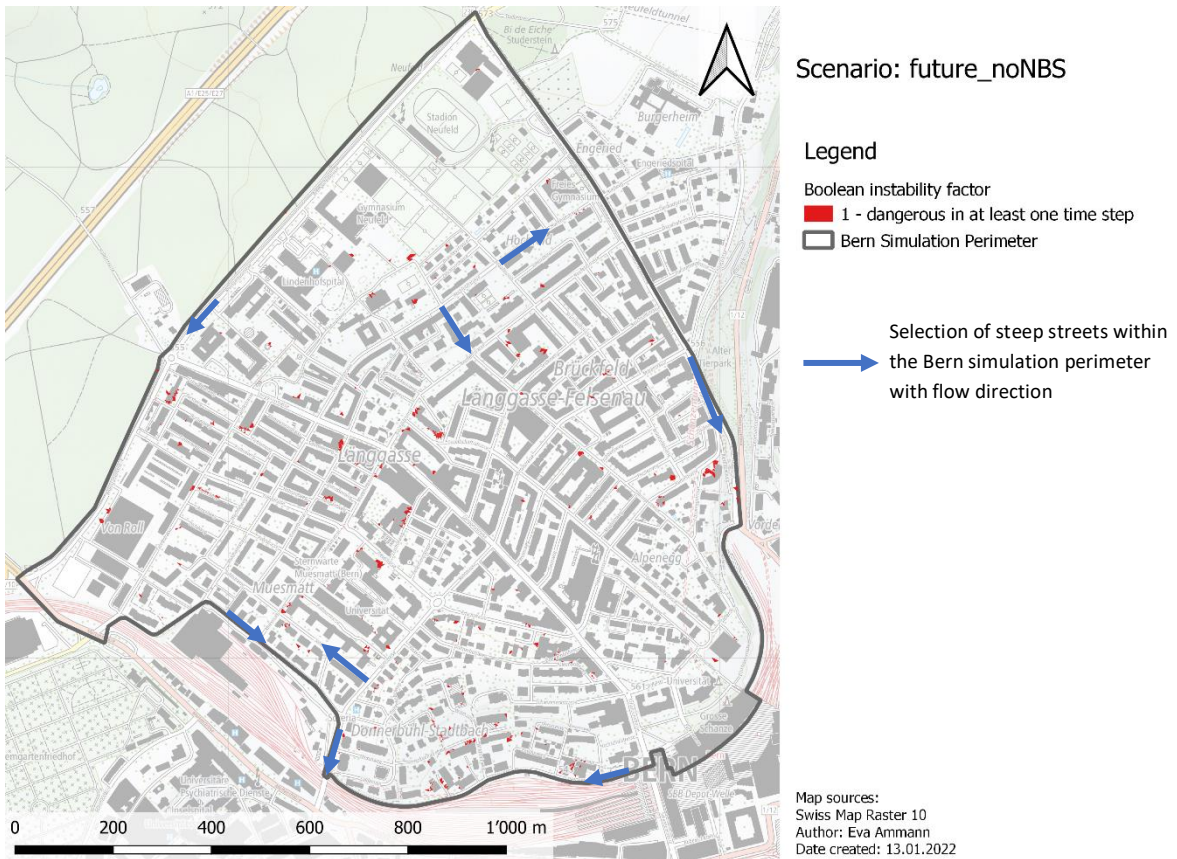


Figure 45: Map of Bern simulation perimeter displaying the boolean instability factor per mesh element in the future\_noNBS scenario with a selection of steep streets shown as blue arrows

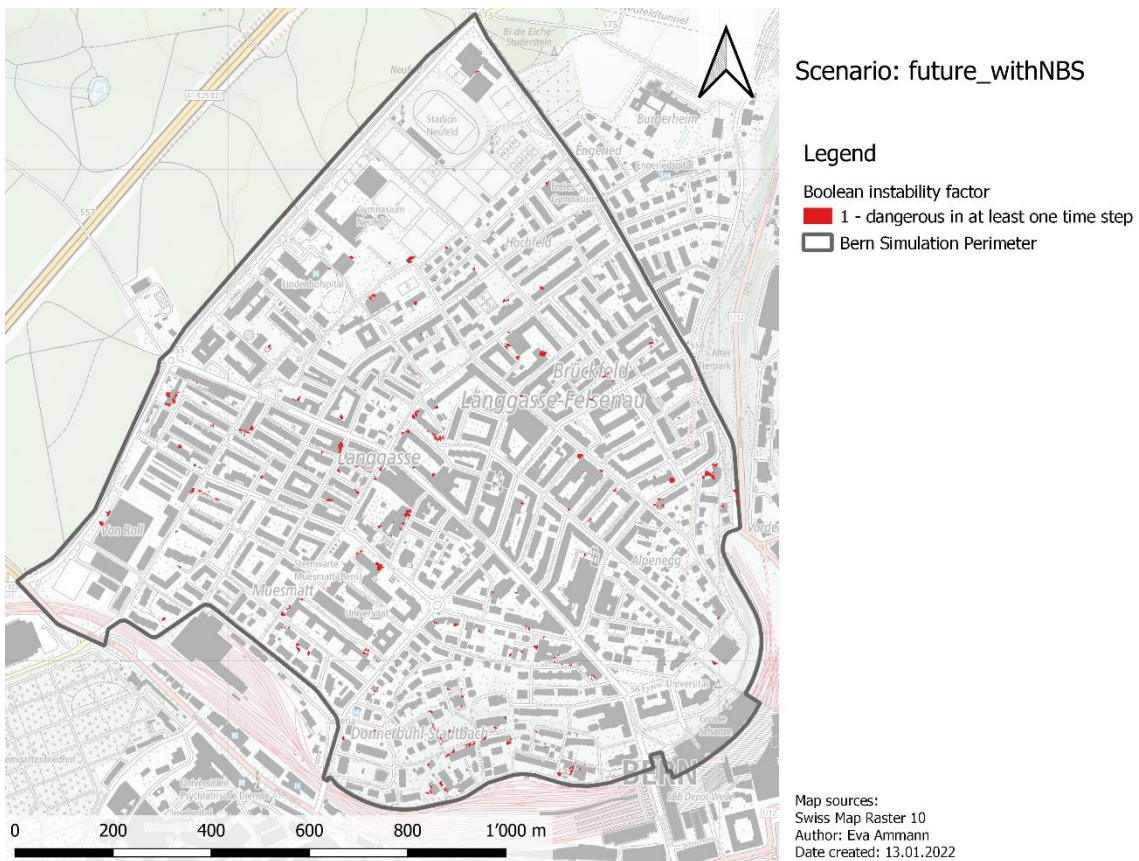


Figure 46: Map of Bern simulation perimeter displaying the boolean instability factor per mesh element in the future\_withNBS scenario

This instability function is calculated based on the flow depth and the flow velocity of a mesh element. However, no disproportionate change in max flow depth can be attributed specifically to mesh elements adjacent to building polygons. Therefore, the cause for the discussed pattern in the instability function must lie in the flow velocity. Consequently, no further analyses are executed based on flow velocities. This leads to rendering void the presented instability function results. Thus, no further analyses for this hazard parameter are considered and discussed.

4.3.1.3 Degree of loss and predicted damage in CHF

In the subchapter 4.3.1.1 Max flow depth on page 69, it is shown that the implementation of NBS on today’s parking spots has a greater flood-reducing impact in the *current* than in the more intense *future* scenario. This effect can also be observed in the comparison of the respective *dol* reduction. In the *current* scenario, the average *dol* is reduced by 0.44%. In the *future* scenario, the average *dol* is only reduced by 0.24%. However, the total predicted damage in CHF is reduced by 0.71% in the *current* and 0.85% in the *future* scenario. This leads to damage-reduction-to-dol-reduction-ratios of 1.60 and 3.57, respectively.

The higher damage reduction potential in the *future* scenario, however, can be explained to a large extent through a single building. The building at Freistrasse 3 is the chemistry, biochemistry and pharmtech building of the university of Bern (University of Bern 2022). It has an attributed estimated value of 57’036’775 CHF (Röthlisberger, Zischg and Keiler 2018). In the *current* scenario, the attributed *dol* is reduced from 11.60% to 11.44%, resulting in a damage reduction of 86’191 CHF. However, in the *future* scenario the implementation of NBS leads to a *dol* reduction for this building from 16.72% to 14.83%. This results in a damage reduction of 1’078’671 CHF. For a better understanding, the simulated damage in CHF reduction maps are shown in Figure 47 for both scenario time steps. The building in question is highlighted.

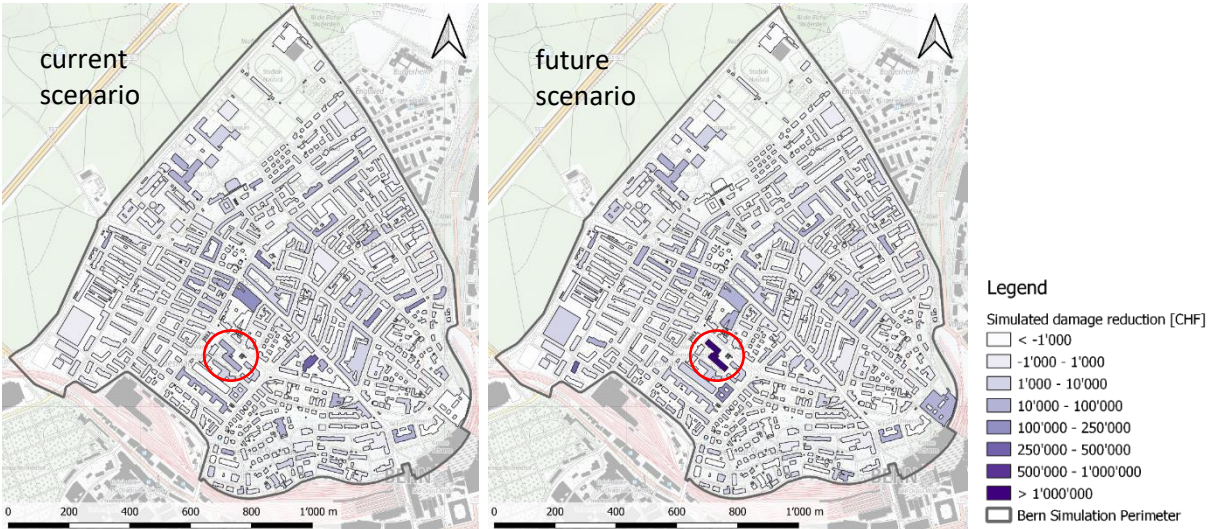


Figure 47: Simulated damage reduction in CHF per building for the current and the future scenario. The chemistry building of the university of Bern is highlighted in a red circle.

To conclude, the *dol* reduction through the implementation of NBS on today's parking spots works to a higher degree in the *current* than in the *future* scenario. Thus, two out of three hazard parameter reduction analyses support the hypothesis presented by Huang et al. (2020) that the NBS reduction potential decreases with an increasing rainfall intensity.

However, this conclusion cannot be applied to the damage reduction. The absolute monetary value of the individual building can outweigh the relative impact of the *dol* reduction. This is because not all buildings are affected equally by the implementation of NBS on today's parking spots. This has been demonstrated exemplarily by the university's chemistry building in the Bern simulation.

At this point, it should be pointed out once again that the parameter *damage in CHF* refers only to the predicted direct tangible costs incurred on buildings. Direct tangible costs incurred, for example, on public infrastructure or cars, are not included. Indirect and intangible costs are also not accounted for.

#### **4.4 Hazard increase due to climate change**

This chapter examines the extent to which the hazard is projected to increase due to climate change. Then, the different magnitudes of hazard reduction through NBS and hazard increase through climate change are compared. For better comparability, the absolute values are considered since the change values often display opposite signs (+/-).

##### *4.4.1.1 Max flow depth*

As can be seen in Figure 34, the maximum flow depth increases across the entire simulation perimeter. Since much more mesh elements are colored in this than in the preceding *change in max flow depth* maps, it is obvious that the extent of hazard increase due to climate change exceeds the extent of hazard reduction through the implementation of NBS measures. This finding is also supported by the numbers. The higher hazard classification (sum of *moderate*, *high* and *very high hazard* category) increases from 2.02% to 3.69%. This is an increase of 82.43% and a manifold of the previously discussed reductions by 4.32% and 2.19% through the implementation of NBS measures.

It is also obvious that the predicted increase in maximum flow depth from the *current* to the *future* scenario can in no way be mitigated through the introduction of NBS measures in the *future* scenario. The extent to which the higher hazard classification area increases from the *current\_noNBS* to the *future\_withNBS* scenario still amounts to 78.42%.

Since the hazard parameter *instability factor* has been declared not fit for purpose in the last chapter, the corresponding subchapter will be omitted here.

#### 4.4.1.2 Degree of loss and predicted damage in CHF

The average *dol* increases from 5.25% to 5.70%. This is an increase by 8.71%, again a manifold of the previously discussed reductions of 0.24% and 0.71%. However, as can be seen in Figure 37, a handful of buildings are displayed in green, meaning that the *dol* decreases from the *current* to the *future* scenario. This behavior is not consistent with the development of the maximum flow depth which shows a very steady increase across the entire simulation perimeter. However, it can be explained through the calculation procedure attributing a *dol* to each building.

As is explained in Figure 16, the highest flow depth within the building buffer is attributed to the building and then used for the *dol* calculation. If the mesh element with the highest max flow depth in the *current* scenario within this buffer is one of the few mesh elements that have a reduced max flow depth in the *future* scenario, a different mesh element will be used to attribute the max flow depth to the building. If this new chosen mesh element's max flow depth in the *future* scenario is lower than the max flow depth of the original mesh element in the *current* scenario, it will result in a lower *dol* for the building in the *future* scenario. This is a very rare case since only 2.98% of the simulation area is exhibiting a lower max flow depth in the *future* scenario. Meanwhile, 40.27% of the simulation area exhibits a higher and 56.75% the same max flow depth in the *future* scenario.

The behavior described above could theoretically be eliminated by attributing the average of all max flow depth values from the mesh elements in the building buffer to the building as max flow depth. Verifying this hypothesis is beyond the scope of this paper.

Disregarding the few exceptions, most of the buildings show a considerable increase in *dol* percentage points. Moreover, the average *dol* increases from 5.25% to 5.69% from the *current\_noNBS* to the *future\_withNBS* scenario. Thus, this hazard parameter also supports the hypothesis that the implementation of NBS on today's parking spots is not be able to mitigate the expected hazard intensity increase due to climate change.

As can be expected from the results obtained before, the predicted damage increase through climate change is many times larger than the possible damage reduction through the implementation of NBS on today's parking spots. To be specific, the predicted damage increase is 30'548'762 CHF. This is an increase of 15.19% compared to the reduction magnitudes of 0.71% and 0.85%, respectively. From the *current\_noNBS* to the *future\_withNBS* scenario, the predicted damage increases from 201'144'314 CHF to 229'720'593 CHF. This is an increase of 14.21%. In other words, the implementation of NBS on today's parking spot areas could mitigate 6.46% of the predicted damage increase due to climate change.

#### 4.5 Putting simulated damage reduction into perspective

In the *current* scenario, the implementation of NBS on today's parking spots is able to save 0.04% of the total buildings value. Figure 48 displays the possible predicted damage reduction. The entire rectangle represents the total buildings value in the simulation perimeter (3'215'121'780 CHF). The left column, meaning red and blue combined, represents the predicted damage in the *current\_noNBS* scenario (201'144'314 CHF). The blue column represents the predicted damage in the *current\_withNBS* scenario (199'717'633 CHF). Thus, the red bar in the upper left corner represents the possible damage reduction through the implementation of NBS on today's parking spots.

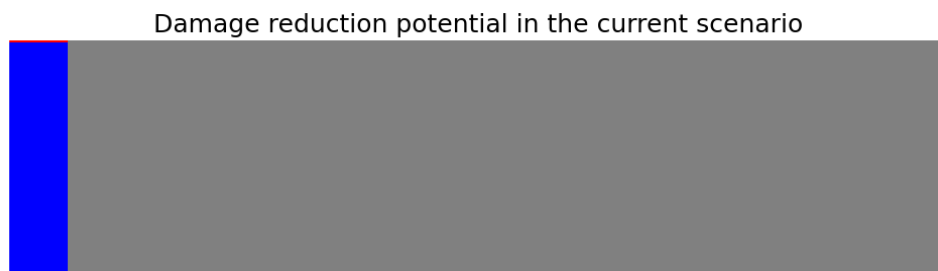


Figure 48: Visual representation of possible predicted damage reduction through the implementation of NBS on today's parking spots in the current scenario

Before this possible damage reduction is sent to insignificance, the following calculation should be considered. It is based on a rule of thumb and is intended to be a brain teaser rather than meet the requirements of a scientific calculation.

Implementing NBS on today's parking spots could possibly save 1'426'681 CHF if a 1-in-100 years rainfall event occurred. Thus, the theoretical yearly damage reduction amounts to  $\frac{1'426'681\text{CHF}}{100\text{ years}} = 14'267 \frac{\text{CHF}}{\text{year}}$ . Within the simulation perimeter, there are about 1'700 car parking spaces (Stadt Bern 2021c, swissTLM3D). Thus, each car parking space exhibits yearly costs of  $\frac{14'267 \frac{\text{CHF}}{\text{year}}}{1'700} = 8.39 \frac{\text{CHF}}{\text{year}}$  that are potentially externalized to insurance companies.

#### 4.6 Co-benefits of replacing today's parking spots with nature-based solutions

Based on the presented simulation results, the introduction of NBS on today's parking spots is not recommended as urban pluvial flooding hazard mitigation strategy. The potential savings are simply not sufficient. However, if NBS are implemented to mitigate another side effect of climate change, for example the urban heat island effect, the simulated savings potential of 1'426'681 CHF in the *current* or 1'972'483 CHF in the *future* scenario must be included in a potential cost-benefit-analysis.

#### 4.7 Limitations of this work

In this work, the BASEMENT (v2.8) simulation program is used for a purpose other than that intended by the developers. Since there is no published record of this having been attempted before, a lot of experimentation is required. As the various learning processes cannot be repeated infinitely, this

inevitably leads to some limitations. Some of them are introduced by the simulation program and are described in the chapter *4.2 Modelling urban pluvial flooding with BASEMENT (v2.8)* on page 64. Other limitations are introduced by the author and are listed below.

First, the entire parking area provided by the city of Bern (2021c) is used. Only at a late stage in the results analysis, it was realized that some of this area is designated bike parking. However, one of this paper's motivation is the idea of car-free cities. This approach would probably lead to a higher bike usage and therefore bike parking areas must not be replaced with NBS implementation measures.

Second, the simulation perimeter is divided into six different MatIDs, only based on the above described data. A lot of urban features such as gardens are never introduced. The data assumptions for the modelling are generally very rudimentary. Examples are the calculated sewer capacity and the increase in rainfall intensity due to climate change.

Third, many urban features must be changed or adapted because the simulation program cannot handle very small triangles. This adaptation of urban features is error-prone because features possibly important to the UPF process might be overridden.

Fourth, as discussed in subchapter *4.3.1.2 Instability factor* on page 70, not even the manipulated DTM is able to solve the problem of too steep surfaces. Future attempts could be made with a differently manipulated DTM in which the buildings are shortened to less than a meter or by defining the building polygons as holes in the computational mesh. Holes do not interact with the actual simulation system. Then, however, excessive water from buildings would not be incorporated in the model.

Fifth, there is an entrance near the train station, which leads to an underground road. This entrance is not on the system boundary but would need to be defined as a possible outflow boundary, too.

Sixth, the outdoor sports field of the Neufeld school is classified as asphalt based on freely available satellite imagery. However, on a walk through the simulation perimeter it can be noticed that this area has been renovated and is now (January 2022) a grass area. Therefore, a different MatID should be assigned. This is just one example that the urban area is constantly changing, and the validity of simulation results have therefore very limited duration.

Sixth, all hazard parameters are calculated on the maximum flow depth of a mesh element. This favors extreme values and statistical outliers. Although it is not clear which flow depth value is most appropriate for UPF analysis, the statistical characteristics on the max flow depth used in this paper must be considered in the interpretation of the results.

Lastly, all hazard parameter analyses are performed on the entire simulation perimeter. This can lead to misleading results, for example, when analyzing the maximum flow depth. This is because the maximum flow depth on roofs is of less interest than the values at street level.

## 5 Conclusion

The present work examines whether it is possible, and if so, useful to simulate urban pluvial flooding with BASEMENT (v2.8), a tool originally developed for fluvial modelling. The results are presented with the help of a case study in the city of Bern in which a potential hazard reduction through the implementation of NBS on today's parking spots as well as a potential hazard increase due to climate change are simulated.

Since the research questions are answered in the *Discussion* chapter, all that remains is to accept or reject the hypotheses, wrap up the results, and provide a research outlook both on using BASEMENT (v2.8) as a modelling tool for urban pluvial flooding as well as the implementation of NBS as a mitigation measure for UPF.

### 5.1 Hypotheses

1. The simulation program BASEMENT (v2.8) can be used to model possible urban pluvial flooding.
2. Replacing today's parking spots with nature-based solutions in the defined research area will reduce the present and future urban pluvial flood hazard modeled by the BASEMENT (v2.8) program.

Both hypotheses can be accepted in principle but are subject to numerous limitations.

### 5.2 Wrap-up

It is shown that it is possible to model urban pluvial flooding with BASEMENT (v2.8). The simulated flow depths pass two simple assessment methods. Although it is possible to model urban pluvial flooding with BASEMENT (v2.8), it is not recommended. There are several reasons for this. First, the workflow is too intricate, too user-unfriendly, and error-prone due to the many manual corrections needed. Second, the underlying computational methods cannot handle areas that are too steep or features that are very small (<0.1m). The former leads to unrealistic flow velocities and the latter hinders the calculation process. However, the two mentioned features are characteristic for urban environments and may have a decisive influence on the course of UPF.

The second half of the research objective leads to a couple of conclusions. First, it is shown that the implementation of NBS measures on dispersed 1.94% of the total area is not able to drastically reduce the urban pluvial flood hazard parameters. The available area is limited to that amount since the idea is to replace nothing more than today's parking area with NBS measures. Second, although the implementation of NBS on today's parking area results in a small reduction in maximum flow depth, mean dol, and predicted total building damage in the current as well as the future scenario, the results are not too promising. On the one hand because the hazard parameter reductions in the future scenario are smaller than in the current scenario. This supports the hypothesis that the potential hazard reduction from NBS decreases inversely proportional to the rainfall intensity magnitude. In

other words, the more intense the precipitation event, the smaller the potential hazard reduction. On the other hand, because the hazard parameter reductions through the implementation of NBS in the current as well as the future scenario represent only a fraction of the hazard parameter increase from the current to the future scenario. In other words, the simulated hazard parameter increase due to climate change can only be mitigated to a very small part through the implementation of NBS on today's parking spots.

These conclusions lead to the fact that an implementation of NBS on today's parking area as a mitigation strategy for urban pluvial flooding must be advised against. However, the small projected mitigation effect can be considered a co-benefit if NBS measures are implemented to mitigate another climate change-induced hazard. In addition, the projected annual damage reduction of slightly more than 14'000 CHF should be considered in future cost-benefit analyses.

### **5.3 Outlook**

Considering the usability of BASEMENT (v2.8) to model urban pluvial flooding, it can be said that not much further research needs to be conducted. Unless there are major changes in a new version, researchers are advised to look for a different simulation tool.

Considering the implementation of NBS as a mitigation measure for UPF, the calculated results dampen the excitement for NBS. The simulation outputs show that the dispersed small-scale implementation of NBS is not able to achieve significant UPF mitigation results. Nevertheless, research must be continued on both UPF and NBS for several reasons.

Further research on UPF is needed because this hazard can cause considerable damage to buildings and public infrastructure and is likely to occur more often in the future due to climate change. The concept of NBS needs to be further explored, as its resilience-building approach could prove very valuable when societies face more complex and interconnected challenges due to climate change. The unique advantage of NBS lies in the co-benefits provided. If a NBS implementation measure is found to address a particular hazard in the urban area, many co-benefits, such as for example a small reduction in the UPF hazard, are provided at no additional cost. In order to produce meaningful results in future research, the definition, implementation methods, and monitoring techniques of NBS must be consistently defined and aligned.

In addition, the hypothesis that the effectiveness of NBS is inversely proportional to the magnitude of the hazard should be further investigated and, if proven correct, considered in future applications of NBS.



## **Acknowledgements**

A thank you is extended to Prof. Dr. Andreas Zischg and Markus Mosimann for their help with the simulation workflow, to Markus Flückiger (Stadt Bern) for his fast and precise answers about the urban water management system of Bern as well as to all the people whose data I was allowed to use such as Rahel Kaltenrieder, Veronika Röthlisberger, Margreth Keiler and Simon Bratschi (Stadt Bern). Additionally, a thank you goes to the developers of BASEMENT (v2.8), the users in the BASEMENT (v2.8) user forum and the providers of QGIS. And finally, a thank you is extended to all the members of my family who proofread this very long thesis.

## Literature

- Angel, S.; Parent, J.; Civco, D.; Blei, A. and Potere, D. (2011a): The dimensions of global urban expansion: Estimates and projections for all countries, 2000-2050. *Progress in Planning*, Vol. 75: 53-107.
- Armson, D.; Stringer, P. and Ennos, A.R. (2013): The effect of street trees and amenity grass on urban surface water runoff in Manchester, UK. *Urban Forestry & Urban Greening*, Vol. 12: 282-286.
- Axelsson, C.; Giove, S.; Soriani, S. and Culligan P.J. (2021): Urban Pluvial Flood Management Part 2: Global Perceptions and Priorities in Urban Stormwater Adaptation Management and Policy Alternatives. *Water*, Vol. 13: 2433-2450.
- Bermudez, M. and Zischg, A.P. (2017): Sensitivity of flood loss estimates to building representation and flow depth attribution methods in micro-scale flood modelling. *Natural Hazards*, Vol. 92(3): 1633-1648.
- Bowler, D.E.; Buyung-Ali, L.; Knight, T.M. and Pullin, A.S. (2010): Urban greening to cool towns and cities: A systematic review of the empirical evidence. *Landscape and Urban Planning*, Vol. 97: 147-155.
- Bultj, D.T. and Abebe, B.G. (2020): A review of flood modeling methods for urban pluvial flood application. Review Article. *Modeling Earth Systems and Environment*, Vol. 6: 1293-1302.
- Cheng, J.D., Lin, L.L. and Lu H.S. (2002): Influences of forests on water flows from headwater watersheds in Taiwan. *Forest Ecology and Management*, Vol. 165: 11-28.
- Cohen-Shacham, E.; Walters, G.; Janzen, C. and Maginnis, S. (2016): Nature-based Solutions to address global societal challenges. IUCN.
- Coutts, A.M.; Tapper, N.J.; Beringer, J.; Loughnan, M. and Demuzere, M. (2012): Watering our cities: The capacity for Water Sensitive Urban Design to support urban cooling and improve human thermal comfort in the Australian context. *Progress in Physical Geography*, Vol. 37(1): 2-28.
- Crichton, D. (1999): The risk triangle. *Natural disaster Management*, Vol. 102(3).
- Dietz, M.E. (2007): Low Impact Development Practices: A Review of Current Research and Recommendations for Future Directions. *Water Air Soil Pollution*, Vol. 186: 351-363.
- ETHZ Eidgenössische Technische Hochschule Zürich (2021): BASEMENT – Basic Simulation Environment. Publications. <https://basement.ethz.ch/publications-and-awards.html> (access 26.11.2021)

- European Commission (2015): Towards an EU Research and Innovation policy agenda for Nature-Based Solutions & Re-Naturing Cities. Final Report of the Horizon 2020 Expert Group on 'Nature-Based Solutions and Re-Naturing Cities'. Directorate-General for Research and Innovation, Directorate I - Climate Action and Resource Efficiency, Unit I.3 - Sustainable Management of Natural Resources.
- Falconer, R.H.; Cobby, D.; Smyth, P.; Astle, G.; Dent, J. and Golding, B. (2009): Pluvial flooding: new approaches in flood warning, mapping and risk management. *Journal of Flood Risk Management*, Vol. 2: 198-208.
- FOEN Federal Office for the Environment (2018): Surface runoff risk map. Map and Factsheet. <https://www.bafu.admin.ch/bafu/en/home/topics/natural-hazards/info-specialists/hazard-situation-and-land-use/hazard-basics/surface-runoff-risk-map.html> (access 11.01.2022)
- FOEN Federal Office for the Environment (2021): Hochwasser Juli 2021: Intensive Niederschläge führten verbreitet zu Überschwemmungen. <https://www.bafu.admin.ch/bafu/de/home/themen/wasser/dossiers/hochwasser-juli-2021-intensive-niederschlaege-fuehrten-verbreitet-zu-ueberschwemmungen.html> (access 16.11.2021)
- Flückiger, M. (2021): Phone interview and mail exchange on 06<sup>th</sup> of December 2021. See appendix.
- Giupponi, C.; Mojtahed, V.; Gain, A.K.; Biscaro, C. and Balbi, S. (2015): Integrated Risk Assessment of Water-Related Disasters. In: Paron, P.; di Baldassarre, G. and Shroder, J.F. (Eds.): *Hydro-Meteorological hazards, risks, and disasters*. Hazards and disasters series. Elsevier: 163-200.
- Green, D.; O'Donnell, E.; Johnson, M.; Slater, L.; Thorne, C.; Zheng, S.; Stirling, R.; Chan, F.K.S.; Li, L. and Boothroyd, R.J. (2021): Green infrastructure: The future of urban flood risk management?. *Wiley Interdisciplinary Reviews: Water*, Vol. 8(6): e1560.
- Hammond, M.; Chen, A., Djordjevic, S. et al. (2013): Urban flood impact assessment: A state-of-the-art review. *Urban Water Journal*, Vol. 12(1): 14-29.
- Hobbie, S.E. and Grimm, N.B. (2019): Nature-based approaches to managing climate change impacts in cities. *Philosophical Transactions B. The Royal Society Publishing*, Vol. 375: 1-14.
- Houston, D.; Werritty, A.; Bassett, D.; Geddes, A.; Hoolachan, A. and McMillan, M. (2011): Pluvial (rain-related) flooding in urban areas: the invisible hazard. Joseph Rowntree Foundation.
- Huang, Y.; Tian, Z.; Ke, Q.; Liu, J.; Irannezhad, M.; Fan, D.; Hou, M. and Sun, L. (2020): Nature-based solutions for urban pluvial flood risk management. *Wiley Interdisciplinary Reviews: Water*, Vol. 7(3): 1-17.

- Illgen, M. (2000): Überprüfung von Standard-Abflussbeiwerten durch Niederschlag-Abfluss-Simulation. Diplomarbeit. Fachgebiet Siedlungswasserwirtschaft. Universität Kaiserslautern, Kaiserslautern.
- IPCC Intergovernmental Panel on Climate Change (2013): Summary for Policymakers. In: Stocker, T.F.; Qin, D.; Plattner, G.-K.; Tignor, M.; Allen, S.K.; Boschung, J.; Nauels, A.; Xia, Y.; Bex, V. and Midgley, P.M. (Eds.): Climate Change 2013: The Physical Science Basis. Contribution of Working Group I to the Fifth Assessment Report of the Intergovernmental Panel on Climate Change. Cambridge University Press.
- IUCN Water International Union for Conservation of Nature (2021): Natural Infrastructure for Water Management - Investing in nature for multiple objectives. Infographics. <https://www.iucn.org/theme/water/resources/infographics> (access 27.10.2021)
- Jamali, B.; Löwe, R.; Bach, P.M.; Urich, C.; Arnbjerg-Nielsen, K. and Deletic A. (2018): A rapid urban flood inundation and damage assessment model. *Journal of Hydrology*, Vol. 564: 1085-1098.
- Jayasooriya, V.M. and Ng, A.W.M. (2014): Tools for Modeling of Stormwater Mangement and Economics of Green Infrastructure Practices: a Review. *Water Air Soil Pollution*, Vol. 225(8): 1-20.
- Jiang, Y.; Zevenbergen, C. and Ma, Y. (2018): Urban pluvial flooding and stormwater management: A contemporary review of China's challenges and "sponge cities" strategy. *Environmental Science and Policy*, Vol. 80: 132-143.
- Jongman, B. (2018): Effective adaptation to rising flood risk. *Nature communications*, Vol. 9(1): 1-3.
- Kaltenrieder, R. (2017): Physische Vulnerabilität von Gebäuden gegenüber Hochwasserereignissen: Statistische Analyse der Einflussfaktoren von Hochwasserereignissen auf Gebäudeschäden, basierend auf Versicherungsdaten und Ereignisdokumentationen. Master's thesis. Department of Geography. University of Bern, Bern.
- KAWA Amt für Wald des Kantons Bern (2014): Erläuterungen zu den LiDAR Besandesinformationen Wald BE. Technischer Bericht.
- KAWA Amt für Wald des Kantons Bern (2015): LiDAR Bern – Airborne Laserscanning. Gesamtbericht Befliegung – Befliegung Kanton Bern 2011 – 2014.
- Kluck, J. (2011): Water in en om de stad. Meer energie voor water. Inauguration, Amsterdam University of Applied Sciences, School of Technology, Lectureship Urban Water Management.

- Krauze, K. and Wagner, I. (2019): From classical water-ecosystem theories to nature-based solutions – Contextualizing nature-based solutions for sustainable city. *Science of the Total Environment*, Vol. 655: 697-706.
- Kron, W. (2002): Keynote lecture: Flood risk = hazard x exposure x vulnerability. In: Wu et al. (Eds.): *Flood Defence '2002*. Science Press, New York Ltd.
- Lashford, C.; Rubinato, M.; Yanpeng, C.; Hou, J.; Abolfathi, S.; Coupe, S., Charlesworth, S. and Tait, S. (2019): SuDS & Sponge Cities: A Comparative Analysis of the Implementation of Pluvial Flood Management in the UK and China. *Review. Sustainability*, Vol. 11(1): 213-227.
- Loucks, D.P. and van Beek, E. (2017): *Water Resource Systems Planning and Management. An Introduction to Methods, Models, and Applications*. Deltares and UNESCO-IHE.
- Ma, Q.; Ngoc Vo, D. and Gourbesville, P. (2018): Application of Deterministic Distributed Hydrological Model in Mediterranean Region, Case Study in Var Catchment, France. *EPiC Series in Engineering*, Vol. 3: 1270 – 1280.
- Mark, O.; Weesakul, S.; Apirumaneklu, C.; Boonya Aroonnet, S. and Djordjevic, S. (2004): Potential and limitations of 1D modelling of urban flooding. *Journal of Hydrology*, Vol. 299: 284-299.
- Martínez-Gomariz, E.; Gómez, M. and Russo, B. (2016): Experimental study of the stability of pedestrians exposed to urban pluvial flooding. *Natural Hazards*, Vol. 82: 1259-1278.
- MeteoSwiss 2021: Bern / Zollikofen. Extreme Value Analysis: 1-hour precipitation. Available at: <https://www.meteoswiss.admin.ch/home/climate/swiss-climate-in-detail/extreme-value-analyses/standard-period.html?station=ber>. (access 23.11.2021)
- Moon, S.-H.; Kim, Y.-H.; Lee Y.H. and Moon, B.-R. (2019): Application of machine learning to an early warning system for very short-term heavy rainfall. *Journal of Hydrology*, Vol. 568: 1042-1054.
- NCCS National Centre for Climate Services (2021): Heavy precipitation. <https://www.nccs.admin.ch/nccs/en/home/climate-change-and-impacts/swiss-climate-change-scenarios/key-messages/heavy-precipitation.html> (access 30.12.2021)
- Nieuwenhuijsen, M. and Khreis, H. (2019): *Integrating Human Health into Urban and Transport Planning. A Framework*. Springer.
- Priest, S.J.; Suykens, C.; Van Rijswick, H.F.M.W.; Schellenberger, T.; Goytia, S., Kundzewicz, Z.W.; van Doorn-Hoekveld, W.J.; Beyers, J.-C. and Homewood, S. (2016): The European Union approach to flood risk management and improving societal resilience: lessons from the implementation of the Floods Directive in six European countries. *Ecology and Society*, Vol. 21(4): 50

- Raymond, C.M.; Frantzeskaki, N.; Kabisch, N.; Berry, P.; Breil, M.; Razvan Nita, M.; Geneletti, D. and Calfapietra, C. (2017): A framework for assessing and implementing the co-benefits of nature-based solutions in urban areas. *Environmental Science and Policy*, Vol. 77: 15-24.
- Rentschler, J. and Salhab, M. (2020): People in Harm's Way. Flood Exposure and Poverty in 189 Countries. World Bank Group, Policy Research Working Paper no. 9447.
- Rosenzweig, B.; Ruddell, B.L.; McPhillips, L.; Hobbins, R.; McPhearson, T.; Cheng, Z.; Chang, H. and Kim, Y. (2019): Developing knowledge systems for urban resilience to cloudburst rain events. *Environmental Science and Policy*, Vol. 99: 150-159.
- Röthlisberger, V.; Zischg, A.P. and Keiler, M. (2018): A comparison of building value models for flood risk analysis. *Natural Hazards and Earth System Science*, Vol. 18, pp. 2431-2453.
- Schneiderbauer, S. and Ehrlich, D. (2004): Risk, hazard and people's vulnerability to natural hazards. A review of definitions, concepts and data. European Commission Joint Research Centre, EUR 21410 EN.
- Sportplatzwelt (2021): Hintergrundwissen: Laufbahn- und Spielfeldbeläge für Außensportanlagen. <https://www.sportplatzwelt.de/fachwissen/20941/hintergrundwissen-laufbahn-und-spielfeldbelaege-fuer-aussensportanlagen> (access 09.12.2021)
- Stadt Bern (2015): Abflüsse Aare Bern grösser als 400 m<sup>3</sup>/s in der Zeitperiode 1917 - 2015. Direktion für Sicherheit. Umwelt und Energie.
- Stadt Bern (2018): Gestaltungsprinzipien (Standards). Handbuch – Planen und Bauen im öffentlichen Raum.
- Stadt Bern (2021a): Fläche Ende 2020 - Stadtteile und Statistische Bezirke. Abteilung Aussenbeziehungen und Statistik (Austa). Statistik Stadt Bern. (Access: <https://www.bern.ch/themen/stadt-recht-und-politik/bern-in-zahlen/katost/02raumw>)
- Stadt Bern (2021b): Bevölkerungsstruktur Ende 2020. Abteilung Aussenbeziehungen und Statistik (Austa). Statistik Stadt Bern. (Access: <https://www.bern.ch/themen/stadt-recht-und-politik/bern-in-zahlen/katost/01bev>)
- Stadt Bern (2021c): Gis Daten öffentliche Parkplätze. Mail exchange between Simon Bratschi and Prof. Dr. Andreas Paul Zischg, 26<sup>th</sup> of April 2021.
- Swisstopo Federal Office of Topography (2021a): Free Geodata. [https://shop.swisstopo.admin.ch/en/products/free\\_geodata](https://shop.swisstopo.admin.ch/en/products/free_geodata) (access 08.12.2021)

- Swisstopo Federal Office of Topography (2021b): swissTLM3D. <https://www.swisstopo.admin.ch/en/geodata/landscape/tlm3d.html> (access 08.12.2021)
- Tages-Anzeiger (2021): Schweizweiter Regen-Rekord in Lausanne. <https://www.tagesanzeiger.ch/panorama/vermishtes/bahnhof-lausanne-unter-wasser-strecken-unterbrochen/story/27499062> (access 16.11.2021)
- Tennis Uni (2020): Tennisplatz – Maße, Bodenbeläge & Platzbau. <https://tennis-uni.com/tennisplatz-tennisfeld/> (access 09.12.2021)
- United Nations (2019): World Urbanization Prospects. The 2018 Revision (ST/ESA/SER.A/420). United Nations, Department of Economic and Social Affairs.
- University of Bern (2022): University Muesmatt. Campus maps and lecture halls and classrooms. [https://www.unibe.ch/university/campus\\_and\\_infrastructure/campus\\_maps\\_and\\_lecture\\_halls\\_and\\_classrooms/maps/9\\_university\\_muesmatt/index\\_eng.html](https://www.unibe.ch/university/campus_and_infrastructure/campus_maps_and_lecture_halls_and_classrooms/maps/9_university_muesmatt/index_eng.html) (access 15.01.2022)
- Van Dijk, E.; van der Meulen, J.; Kluck, J. and Straatman, J. H. M. (2014): Comparing modelling techniques for analysing urban pluvial flooding. *Water science and technology*, Vol. 69(2): 305-311.
- Vetsch D.; Siviglia A.; Bürgler M.; Caponi F.; Ehrbar D.; Facchini M.; Faeh R.; Farshi D.; Gerber M.; Gerke E.; Kammerer S.; Koch A.; Mueller R.; Peter S.; Rousselot P.; Vanzo D.; Veprek R.; Volz C.; Vonwiller L. and Weberndorfer M. (2020): System Manuals of BASEMENT - Version 2.8.1. Laboratory of Hydraulics; Glaciology and Hydrology (VAW). ETH Zurich. Available from <http://www.basement.ethz.ch>. (access 20.08.2021)
- Zellner, M.; Massey, D.; Minor, E. and Gonzalez-Meler, M. (2016): Exploring the effects of green infrastructure placement on neighborhood-level flooding via spatially explicit simulations. *Computers, Environment and Urban Systems*, Vol. 59: 116-128.
- Zhao, L.; Lee, X.; Smith, R.B. and Oleson, K. (2014): Strong contributions of local background climate to urban heat islands. *Nature*. Vol. 511 (7508): 216-219.
- 20 Minuten (2021): Unwetter in der Schweiz. Zuger Bahnhof steht unter Wasser. <https://www.20min.ch/video/zuger-bahnhof-steht-unter-wasser-404509714828> (access 16.11.2021)

## Map resources

### Building values

- Röthlisberger, V.; Zischg, A.P. and Keiler, M. (2018): A comparison of building value models for flood risk analysis. *Natural Hazards and Earth System Science*, Vol. 18, pp. 2431-2453.

### Canton of Bern

- KAWA Amt für Wald des Kantons Bern: Erläuterungen zu den LiDAR Bestandesinformationen Wald BE. Technischer Bericht, 2014.
- KAWA Amt für Wald des Kantons Bern: LiDAR Bern – Airborne Laserscanning. Gesamtbericht Befliegung – Befliegung Kanton Bern 2011 – 2014., 2015.

### City of Bern

- Gis Daten öffentliche Parkplätze. Mail exchange between Simon Bratschi and Prof. Dr. Andreas Paul Zischg, 26<sup>th</sup> of April 2021.

### Federal Office of Topography swisstopo:

- swissBOUNDARIES3D:  
<https://www.swisstopo.admin.ch/de/geodata/landscape/boundaries3d.html>. (access 14.12.2021)
- Swiss Map Raster 10: <https://www.swisstopo.admin.ch/en/geodata/maps/smr/smr10.html>. Tiles 1166-2 and 1166-4. (access 01.12.2021)
- swissTLM3D: <https://www.swisstopo.admin.ch/en/geodata/landscape/tlm3d.html>. (access 23.11.2021)
- WMS-BGDI Tiles: <https://wms.geo.admin.ch/>. Accessed in January 2022.

### Overview map

- OpenStreetMap's Standard tile layer: <https://tile.openstreetmap.org/{z}/{x}/{y}.png>. Accessed from September 2021 to January 2022.

### Satellite imagery

- Google Maps Satellite Only layer:  
<http://mt0.google.com/vt/lyrs=s&hl=en&x={x}&y={y}&z={z}>. Accessed from September to December 2021.



## **Image sources**

BASEMENT: <https://basement.ethz.ch/> (access 17.12.2021)

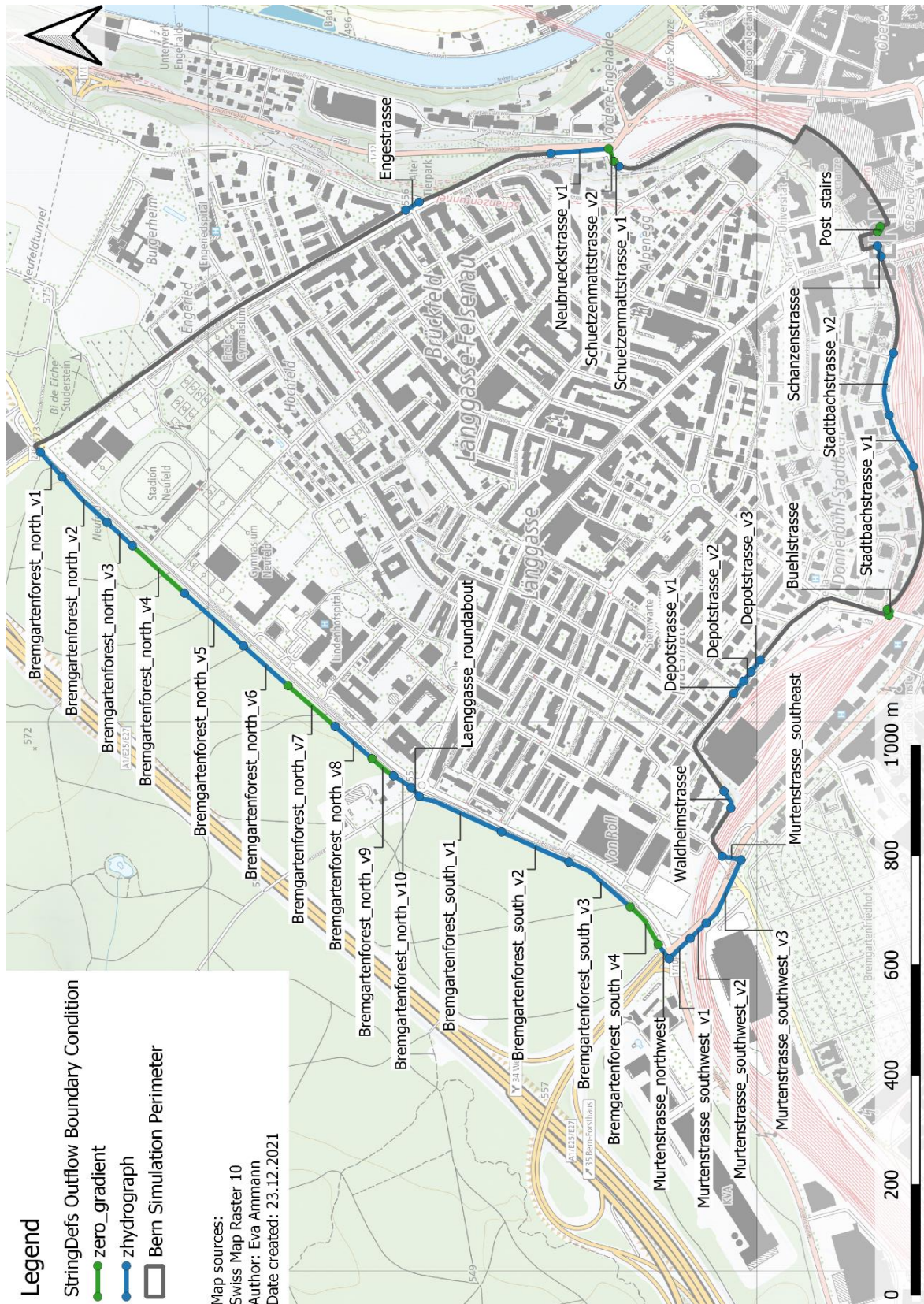
BASEmesh: <https://basement.ethz.ch/download/tools/basemesh.html> (access 09.12.2021)

Excel: <https://developer.microsoft.com/de-de/microsoft-365> (access 17.12.2021)

Python: <https://de.m.wikipedia.org/wiki/Datei:Python-logo-notext.svg> (access 09.12.2021)

QGis: <https://www.qgis.org/lt/site/getinvolved/styleguide.html> (access 09.12.2021)

# Appendix



## Python Codes

```
#####                               TITLE: DoubleNodes.py                               #####  
  
## ----- ##  
  
import csv  
import pandas as pd  
#Setting Panda options  
pd.set_option('display.max_rows',None)  
pd.set_option('display.float_format', '{:,}'.format)  
  
#Loading the SMS 2D File  
all_nodes = pd.read_csv("Bern_quality-mesh_v16.2dm", delimiter=";", header=  
None)  
print ("I have finished reading")  
  
#Processing the file  
print("removing first two rows")  
all_nodes = all_nodes.iloc[2:]  
print("removing E3T")  
NDandNS = all_nodes[~all_nodes[0].str.contains("E3T")]  
print("removing NodeStrings")  
NOnly = NDandNS[~NDandNS[0].str.contains("NS")]  
print("reducing unnecessary spaces")  
NOnly_v1 = NOnly[0].str.replace(" ", ";")  
NOnly_v2 = NOnly_v1.str.replace(";;", ";")  
NOnly_v3 = NOnly_v2.str.replace(";;", ";")  
NOnly_v4 = NOnly_v3.str.replace(";;", ";")  
print("splitting the table and adding column names")  
nodes = NOnly_v4.str.split(";", expand =True)  
nodes.columns = ["Category", "Nr", "XCoord", "YCoord", "ZCoord"]  
  
print("Convert XCoord to float")  
nodes["XCoord"] = pd.to_numeric(nodes["XCoord"], downcast="float")  
print("XCoord is now float")  
  
print("Convert YCoord to float")  
nodes["YCoord"] = pd.to_numeric(nodes["YCoord"], downcast="float")  
print("YCoord is now float")  
  
nodes["XandY"] = nodes["XCoord"].astype(str) + "," + nodes["YCoord"].astype(str)  
  
#To have even bigger mesh elements (1m apart)  
#nodes["XandY"] = nodes["XCoord"].astype(str).str[:7] + "," +  
nodes["YCoord"].astype(str).str[:7]  
  
##Reading the double values  
print("here come the double values")  
double_nodes = nodes[nodes.duplicated("XandY", keep=False)].sort_values("XandY")  
  
if len(double_nodes)==0:  
    print("There are no duplicate nodes!")  
else:  
    double_nodes_no_duplicates = double_nodes.drop_duplicates(subset="XandY",  
keep= "first", inplace=False)  
    print(double_nodes_no_duplicates)  
    print("There are "+str(len(double_nodes_no_duplicates))+" double nodes in  
this SMS 2DM File")
```

```

###                               TITLE: VelocityandStability.py                               ###

##-----##

import pandas as pd
import math
import os

#define scenario
#scenario = "current_noNBS"
#scenario = "current_withNBS"
#scenario = "future_noNBS"
scenario = "future_withNBS"

#read path
path = os.getcwd()
print('Get current working directory : ', path)

#read csv files
velocity_x = pd.read_csv(scenario+'_velocity_x_csv.csv', index_col=0)
velocity_y = pd.read_csv(scenario+'_velocity_y_csv.csv', index_col=0)
depth = pd.read_csv(scenario+'_depth_csv.csv', index_col=0)

#Retrieve header and index list
header_list = list(velocity_x)
print(header_list)
index_list = velocity_x.index.to_list()

#define progress bar
count = len(index_list)

progress_bar = [10,20,30,40,50,60,70,80,90,100]
progress_bar_values = []
for progress in progress_bar:
    progress_bar_values.append(round(len(index_list)*(progress/100)))

#create new dataframes
velocity = pd.DataFrame(index=index_list,columns=header_list)
instability_values = pd.DataFrame(index=index_list,columns=header_list)
instability_boolean = pd.DataFrame(index=index_list,columns=["Instability"])

progress_value = 0

for row in index_list:
    for column in header_list:
        velocity.at[row,column] =
math.sqrt(pow(velocity_x.at[row,column],2)+pow(velocity_y.at[row, column],2))
        instability_value_cell = velocity.at[row,column]*depth.at[row,column]
        instability_values.at[row,column] = instability_value_cell
        if instability_boolean.at[row, "Instability"] == 1:
            continue
        elif instability_value_cell > 0.22:
            instability_boolean.at[row, "Instability"] = 1
            #print("I have found an instability!")
        else:
            instability_boolean.at[row,"Instability"] = 0
    if row in progress_bar_values:
        print(progress_bar[progress_value],"% done!")
        progress_value += 1

#export dataframes to csv

velocity.to_csv(path+"/"+scenario+"_velocity.csv")
instability_values.to_csv(path+"/"+scenario+"_instability_values.csv")
instability_boolean.to_csv(path+"/"+scenario+"_instability_boolean.csv")

```

```

###                                     Title: DOLandDamageCalculation.py                                     ###
##-----##

import pandas as pd
import math
import os

# read path
path = os.getcwd()
print('Get current working directory : ', path)

# read csv file
all_data = pd.read_csv('Bern_tlm_footprints_values_bufferonly_allmaxflowdepth_csv.csv',
header=0, index_col=0)

# Retrieve header and index list, show index name
header_list = list(all_data)
print(header_list)

index_list = all_data.index.to_list()
print(index_list[:10])

print(all_data.index.name)

# crate a flowdepth, dol, dol_percent and damageCHF scenario list and corresponding
dictionaries
flowdepth_scenario_list = ['current_noNBS_max_depth', 'current_withNBS_max_depth',
'future_noNBS_max_depth', 'future_withNBS_max_depth']
dol_scenario_list = ["current_noNBS_dol", "current_withNBS_dol", "future_noNBS_dol",
"future_withNBS_dol"]
dol_percent_scenario_list = ["current_noNBS_dol_percent", "current_withNBS_dol_percent",
"future_noNBS_dol_percent", "future_withNBS_dol_percent"]
damageCHF_scenario_list = ["current_noNBS_damageCHF", "current_withNBS_damageCHF",
"future_noNBS_damageCHF", "future_withNBS_damageCHF"]

flowdepth_to_dol_dictionary = dict(zip(flowdepth_scenario_list, dol_scenario_list))
flowdepth_to_dol_percent_dictionary = dict(zip(flowdepth_scenario_list,
dol_percent_scenario_list))
flowdepth_to_damageCHF_dictionary = dict(zip(flowdepth_scenario_list, damageCHF_scenario_list))

#create new columns for dol, dol_percent and damageCHF scenarios
new_columns = dol_scenario_list + dol_percent_scenario_list + damageCHF_scenario_list

for column in new_columns:
    all_data[column]=0.00

# calculate dol, dol_percent and damageCHF
for column_flowdepth in flowdepth_scenario_list:
    column_dol = flowdepth_to_dol_dictionary.get(column_flowdepth)
    column_dol_percent = flowdepth_to_dol_percent_dictionary.get(column_flowdepth)
    column_damageCHF = flowdepth_to_damageCHF_dictionary.get(column_flowdepth)
    print(column_flowdepth, " ", column_dol, " ", column_dol_percent, " ", column_damageCHF)
    for row in index_list:
        dol = 0.0
        flowdepth = all_data.at[row, column_flowdepth]
        if flowdepth <= 0:
            dol = 0.0
        else:
            dol = math.pow((0.18846 + 0.17152 * flowdepth), 2)
        if dol > 1:
            dol = 1.0
        elif dol < 0:
            dol = 0.0
        dol_percent = dol*100
        damageCHF = all_data.at[row, 'vm5']*dol
        all_data.at[row, column_dol] = dol
        all_data.at[row, column_dol_percent] = dol_percent
        all_data.at[row, column_damageCHF] = damageCHF

#export dataframes to csv
all_data.to_csv(path+"/all_damage_data_csv.csv")

```

```

##                                     Hazard_reduction.py                                     ##
###-----

import pandas as pd
import os

#read path
path = os.getcwd()
print('Get current working directory: ', path)

###import dataframes
##read csv files
#simulation without NBS implementation
max_depth_noNBS = pd.read_csv('future_noNBS_max_depth_csv.csv',
index_col=0)
instability_boolean_noNBS =
pd.read_csv('future_noNBS_instability_boolean.csv', index_col=0)

#simulation with NBS implementation
max_depth_withNBS = pd.read_csv('future_withNBS_max_depth_csv.csv',
index_col=0)
instability_boolean_NBS =
pd.read_csv('future_withNBS_instability_boolean.csv', index_col=0)

#create index list to use in new dataframes
index_list = max_depth_noNBS.index.to_list()

#create new dataframes
hazard_reduction_max_depth =
pd.DataFrame(index=index_list, columns=["hazard_reduction"])
hazard_reduction_instability_boolean =
pd.DataFrame(index=index_list, columns=["hazard_free_bcoNBS"])

#fill new dataframe with data
for row in index_list:
    hazard_reduction_max_depth.at[row, "hazard_reduction"] = \
        max_depth_noNBS.at[row, "max_depth"] - max_depth_withNBS.at[row,
"max_depth"]
    hazard_reduction_instability_boolean.at[row, "hazard_free_bcoNBS"] =\
        instability_boolean_noNBS.at[row, "Instability"] -
instability_boolean_NBS.at[row, "Instability"]

#export dataframes to csv
hazard_reduction_max_depth.to_csv(path+"/future_hazard_reduction_max_depth.
csv")
hazard_reduction_instability_boolean.to_csv(path+"/future_hazard_reduction_
instability_boolean.csv")
print("Both files have been exported")

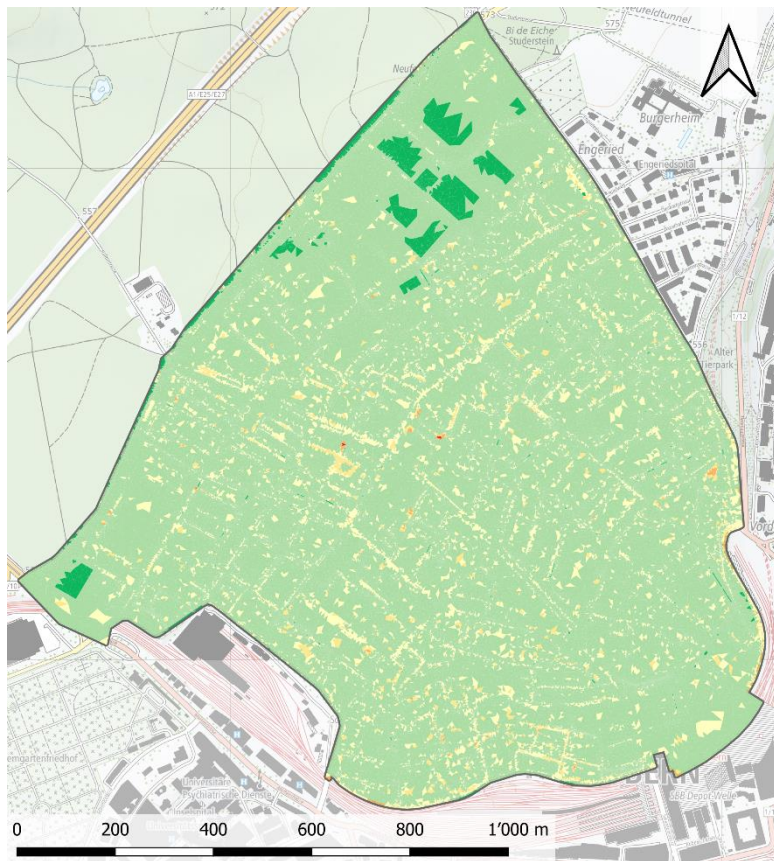
```

### **Statements from Markus Flückiger (city of Bern)**

The expert interview with Markus Flückiger was conducted by phone. This was followed by an exchange of mails. Written consent to the following statements was obtained on the 06<sup>th</sup> of December 2021 (in German).

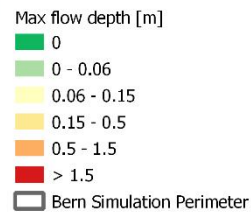
1. Das Abwassersystem in der Länggasse ist auf ein 5-jährliches Regen-Ereignis ausgelegt. Wird diese Niederschlagsmenge überschritten, kann es zu Rückstau im Kanalnetz kommen. Bei sehr grossen Ereignissen ist ein Austritt aus den Schächten und somit ein Oberflächenabfluss möglich.
2. Von den Gebäuden sollte möglichst kein Regenabwasser ins Abwassersystem kommen. Alles Wasser, welches auf den Dächern und Vorplätzen anfällt, muss versickern wenn es der Untergrund und die gesetzlichen Vorgaben erlauben. Versickerungen sollten mindestens auf ein  $z=5$  dimensioniert werden
3. In der Länggasse ist das Abwassersystem ein Mischsystem. Im Extremfall kann durch Fäkalien verunreinigtes Wasser aus den Schächten austreten. In der Länggasse ist dieses Risiko vergleichsweise klein, weil die Kanäle sehr tief verlegt sind. In der Dimensionierungsrichtlinie der Stadt Bern ist festgelegt, dass bei einem Regen mit  $z=5$  kein Abwasser aus den Schächten austreten darf, sonst sind Massnahmen umzusetzen.

## Hazard parameter maps

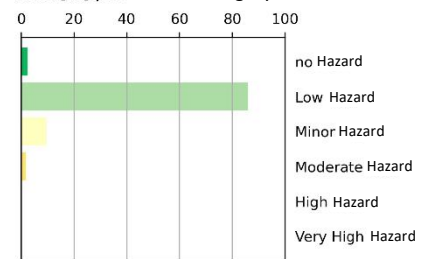


Scenario: current\_withNBS

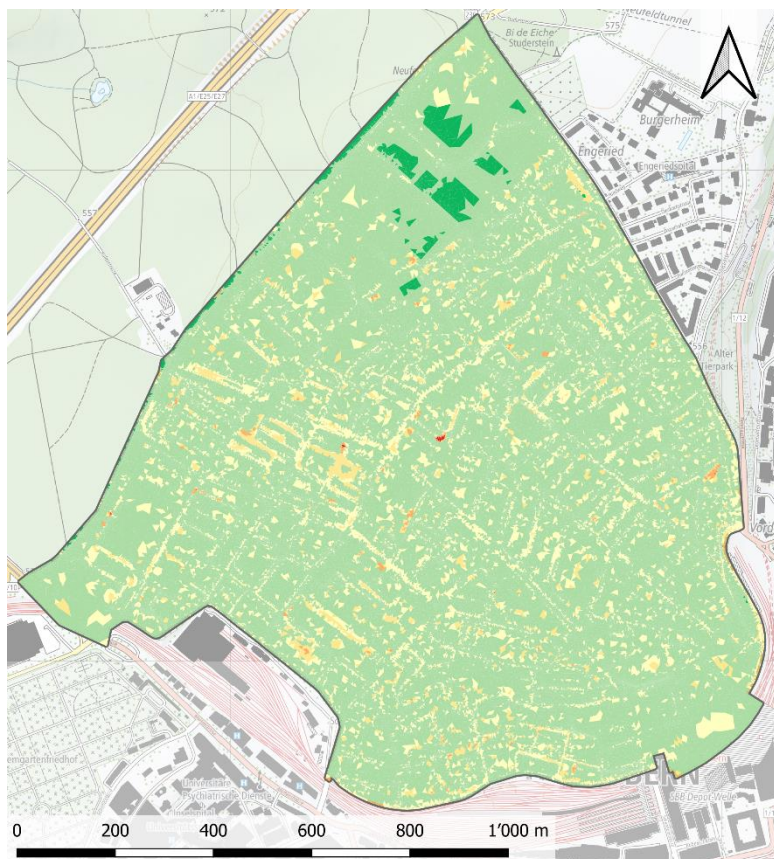
### Legend



### Area [%] per Hazard Category

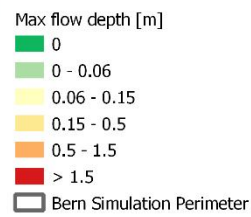


Map sources:  
Swiss Map Raster 10  
Author: Eva Ammann  
Date created: 13.01.2022

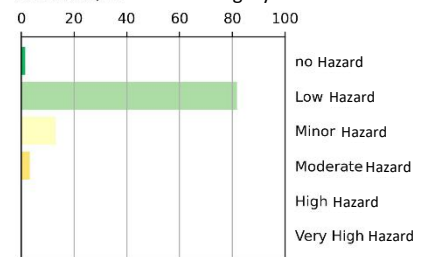


Scenario: future\_noNBS

### Legend

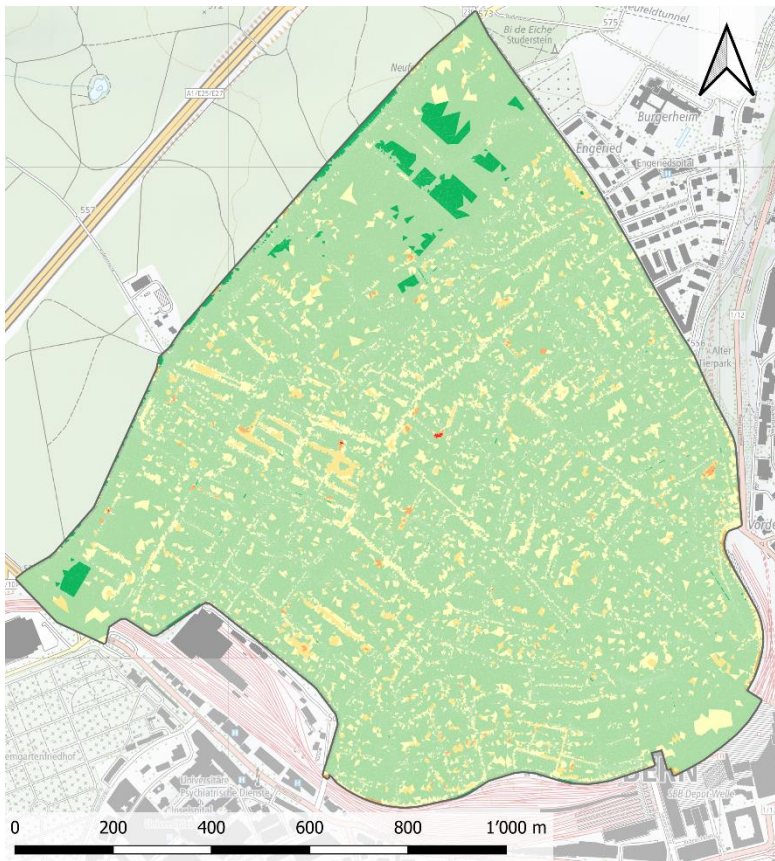


### Area [%] per Hazard Category

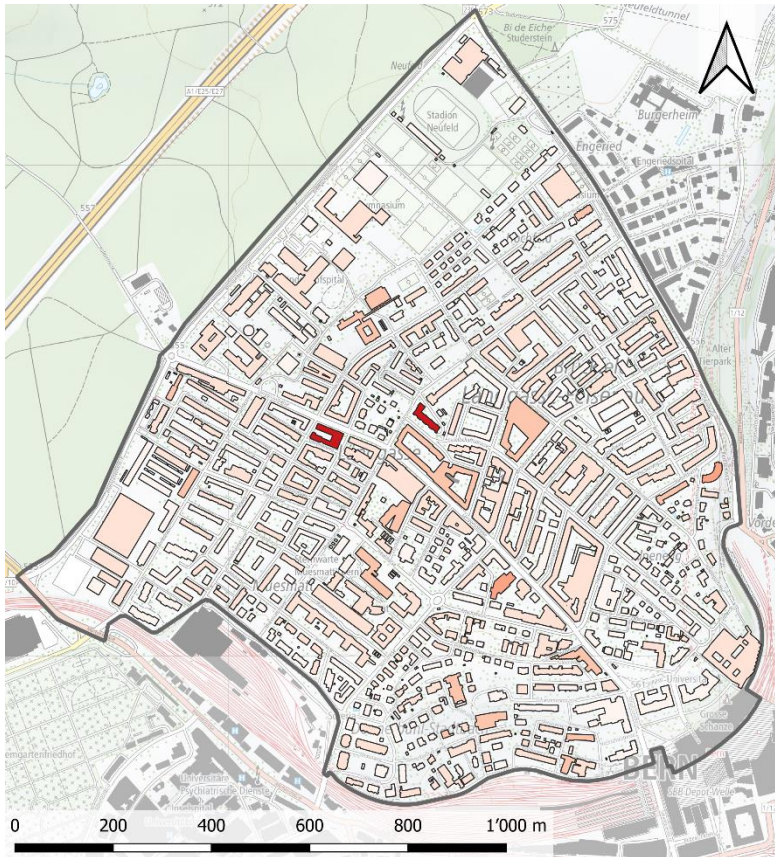


Map sources:  
Swiss Map Raster 10  
Author: Eva Ammann  
Date created: 13.01.2022





The corresponding maps for the *future\_noNBS* and the *future\_withNBS* scenario can be found in the discussion part.

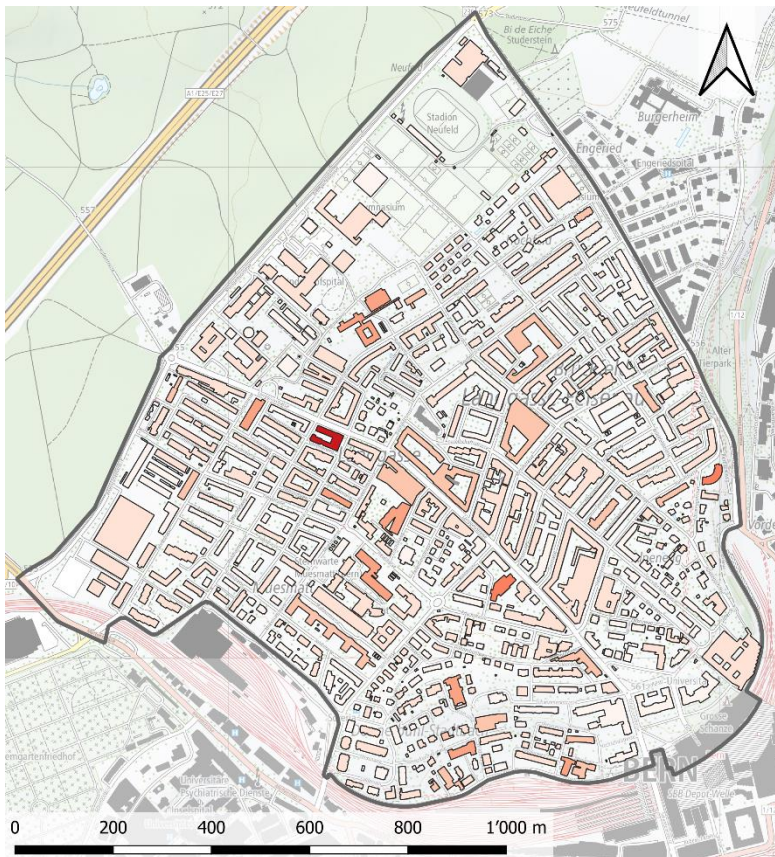


Scenario: current\_withNBS

Legend

- Degree of loss [%]
- 0 - 5
  - 5 - 10
  - 10 - 15
  - 15 - 20
  - 20 - 25
  - 25 - 30
  - 30 - 35
  - 35 - 40
  - 40 - 45
  - 45 - 50
  - Bern Simulation Perimeter

Map sources:  
Swiss Map Raster 10  
Author: Eva Ammann  
Date created: 13.01.2022

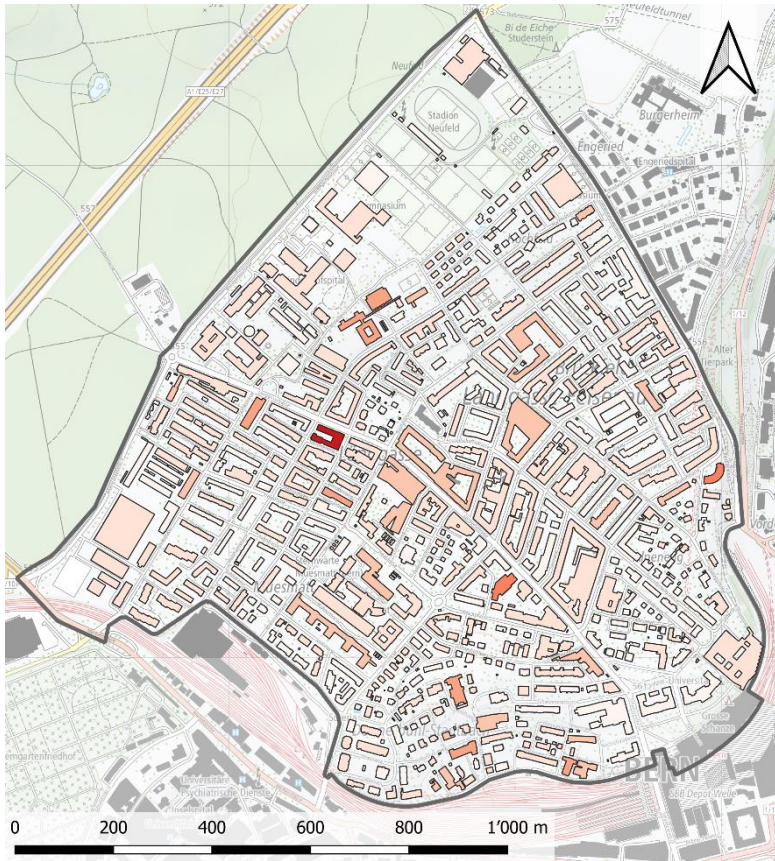


Scenario: future\_noNBS

Legend

- Degree of loss [%]
- 0 - 5
  - 5 - 10
  - 10 - 15
  - 15 - 20
  - 20 - 25
  - 25 - 30
  - 30 - 35
  - 35 - 40
  - 40 - 45
  - 45 - 50
  - Bern Simulation Perimeter

Map sources:  
Swiss Map Raster 10  
Author: Eva Ammann  
Date created: 13.01.2022

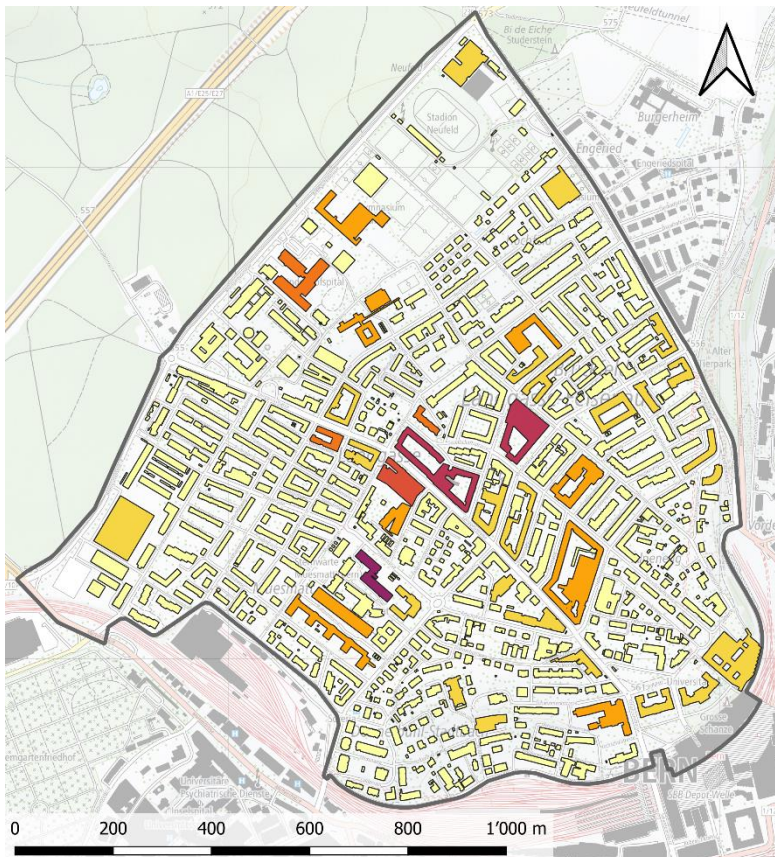


Scenario: future\_withNBS

Legend

- Degree of loss [%]
- 0 - 5
  - 5 - 10
  - 10 - 15
  - 15 - 20
  - 20 - 25
  - 25 - 30
  - 30 - 35
  - 35 - 40
  - 40 - 45
  - 45 - 50
  - Bern Simulation Perimeter

Map sources:  
 Swiss Map Raster 10  
 Author: Eva Ammann  
 Date created: 13.01.2022

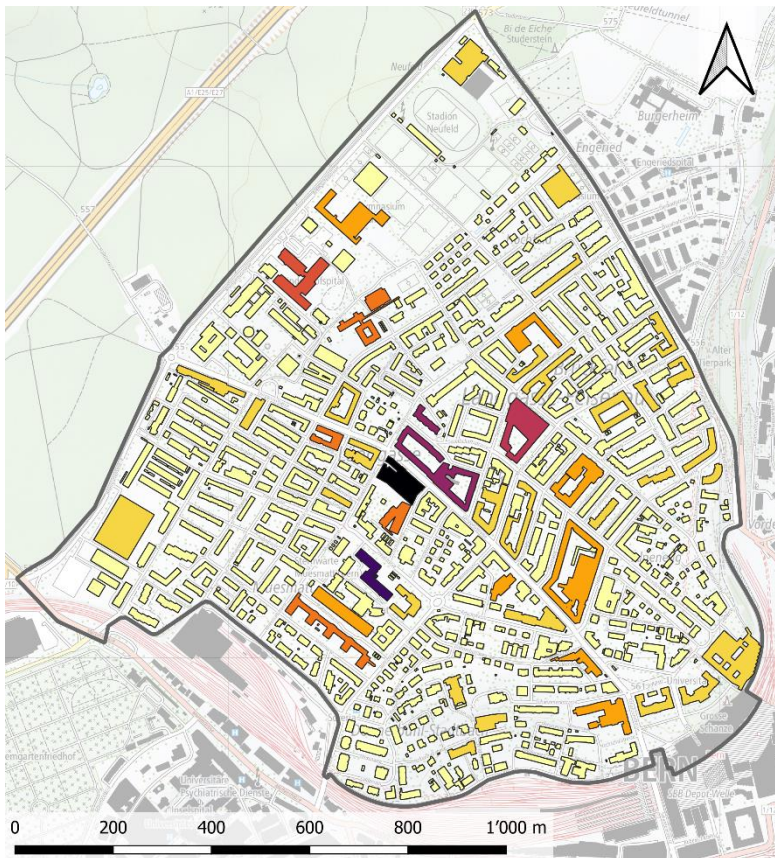
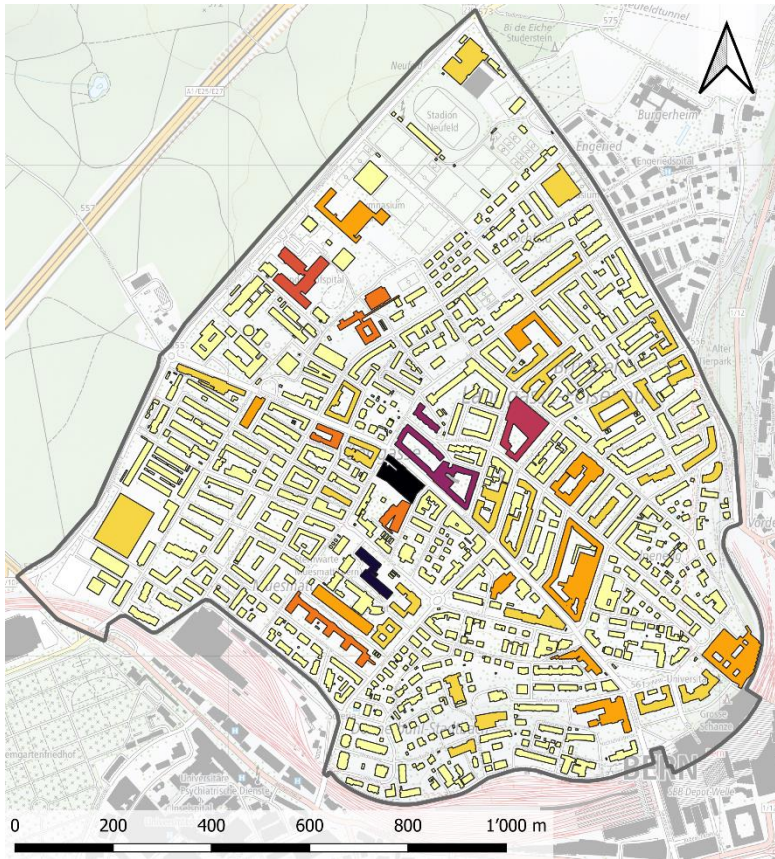


Scenario: current\_withNBS

Legend

- Predicted building damage [CHF]
- 0 - 1'000'000
  - 1'000'000 - 2'000'000
  - 2'000'000 - 3'000'000
  - 3'000'000 - 4'000'000
  - 4'000'000 - 5'000'000
  - 5'000'000 - 6'000'000
  - 6'000'000 - 7'000'000
  - 7'000'000 - 8'000'000
  - 8'000'000 - 9'000'000
  - 9'000'000 - 10'000'000
  - > 10'000'000
  - Bern Simulation Perimeter

Map sources:  
 Swiss Map Raster 10  
 Author: Eva Ammann  
 Date created: 13.01.2022



```

// -----
// BASEMENT log file:
// Version: v2.8.1// bmc file:
C:\SIMULATIONS\Bern_MA_Ammann\Bern_current_no
NBS/current_noNBS.bmc
// started: Thu Dec 23 16:19:23 2021
// -----
/*
-> InputParser: reading input from bmc file

'C:\SIMULATIONS\Bern_MA_Ammann\Bern_current_no
NBS/current_noNBS.bmc'
*/
PROJECT {
  title = Bern_current_noNBS
  author = anonymous_author
}
DOMAIN {
  multiregion = unnamed_multiregion
  PARALLEL {
    number_threads = 6
  }
  PHYSICAL_PROPERTIES {
    rho_fluid = 1000
    gravity = 9.81
    viscosity = 1e-06
  }
  BASEPLANE_2D {
    region_name = bern
  }
  TIMESTEP {
    total_run_time = 7200
    CFL = 1.0
    minimum_time_step = 0.001
    maximum_time_step = 100.0
    initial_time_step = 1.0
    start_time = -1.0
    ignore_wave_celerity = off
    morph_cycle = off
  }
  GEOMETRY {
    type = 2dm
    file = Bern_computational-mesh_v9.2dm
    STRINGDEF {
      name = Murtenstrasse_northwest
      node_ids = (8731 12292 2746 62607 61495 65688
5360)
      upstream_direction = left
    }
    STRINGDEF {
      name = Murtenstrasse_southwest_v1
      node_ids = (5360 10166 65893 19369 65961)
      upstream_direction = left
    }
    STRINGDEF {
      name = Murtenstrasse_southwest_v2
      node_ids = (65961 14350 65947 19371)
      upstream_direction = left
    }
    STRINGDEF {
      name = Murtenstrasse_southwest_v3
      node_ids = (19371 133 130 65637 13808 65980
6832)
      upstream_direction = left
    }
    STRINGDEF {

```

```

      name = Murtenstrasse_southeast
      node_ids = (6832 65933 9539)
      upstream_direction = left
    }
    STRINGDEF {
      name = Waldheimstrasse
      node_ids = (11461 11458 6857 6158 32139 35755
8713 32140 9312 29735 29873 3147)
      upstream_direction = left
    }
    STRINGDEF {
      name = Depotstrasse_v1
      node_ids = (10786 25178 21739 25179 17994
25175 21743 27645 397 32149)
      upstream_direction = left
    }
    STRINGDEF {
      name = Depotstrasse_v2
      node_ids = (32149 11191 28702 27646 28503
1849 34308 25462 43650 14850)
      upstream_direction = left
    }
    STRINGDEF {
      name = Depotstrasse_v3
      node_ids = (14850 43649 19668 11893 22941
19155 22944 34219 1844)
      upstream_direction = left
    }
    STRINGDEF {
      name = Buehlstrasse
      node_ids = (7444 6608 6605)
      upstream_direction = left
    }
    STRINGDEF {
      name = Stadtbachstrasse_v1
      node_ids = (4700 28854 28781 12282 25422
22009 4698 36158 32881 36156 5158 32883 5159 37130
34623 37129 25535 36701 33820 36704 13057 36880
34110 36879 20619 36164 32885 36162 11155 36617
33701 13955 59868 9269 56890 37855 57646 18756
37856 12828 40458)
      upstream_direction = left
    }
    STRINGDEF {
      name = Stadtbachstrasse_v2
      node_ids = (40458 20032 47954 15379 20039
57242 9267 57243 14430 3619 15305 42003 12714
54367 18439 44791 7377 32913 19879 46500 15145
49689 20685 12440 52320 36905 15144 54244 32916
36183 7375)
      upstream_direction = left
    }
    STRINGDEF {
      name = Schanzenstrasse
      node_ids = (49818 24360 53656 20584 64605
8175)
      upstream_direction = left
    }
    STRINGDEF {
      name = Post_stairs
      node_ids = (62067 3269 3268)
      upstream_direction = left
    }
    STRINGDEF {
      name = Schuetzenmattstrasse_v1

```

```

node_ids = (3331 11017 11014 3005)
upstream_direction = left
}
STRINGDEF {
name = Schuetzenmattstrasse_v2
node_ids = (3005 7376 1099 1096)
upstream_direction = left
}
STRINGDEF {
name = Neubrueckstrasse_v1
node_ids = (1096 35746 19401 61806 57114
14405 55882 64682 19405 23232 2630 63485 14966)
upstream_direction = left
}
STRINGDEF {
name = Engestrasse
node_ids = (2213 48982 12057 2210)
upstream_direction = left
}
STRINGDEF {
name = Bremgartenforest_north_v1
node_ids = (5365 29115 29477 7896 27112 20633
24389 9112 24388 17667 21570 16806 21567 17666
21568 14883 28294 23940 46585 20157 23961)
upstream_direction = left
}
STRINGDEF {
name = Bremgartenforest_north_v2
node_ids = (23961 11951 28227 22390 46479
18625 46520 22391 46480 3860 46519 21109 53718
16990 56380 21114 56165 15415 59623 55974)
upstream_direction = left
}
STRINGDEF {
name = Bremgartenforest_north_v3
node_ids = (59454 21115 59455 57890 59227
16989 58125 51739 57891 21116 58126 51758 57935
12900 57936 57887 59226 21141 58127 51760)
upstream_direction = left
}
STRINGDEF {
name = Bremgartenforest_north_v4
node_ids = (51760 16988 52359 22278 52280
15414 52708 21120 43697 16987 52711 26519 48535
1566 40084 17697 56964 40301 17013 61668)
upstream_direction = left
}
STRINGDEF {
name = Bremgartenforest_north_v5
node_ids = (56094 23144 56042 59427 15462
59428 56016 17696 40122 17012 51495 17695 52279
12980 52325 17694 47817 17011 49963 17693)
upstream_direction = left
}
STRINGDEF {
name = Bremgartenforest_north_v6
node_ids = (17693 60608 40092 60609 15461
61661 56402 17692 57070 39351 17010 57111 45182
17691 43180 56967 956 56565 48644 17843 43176)
upstream_direction = left
}
STRINGDEF {
name = Bremgartenforest_north_v7

```

```

node_ids = (43176 56916 17428 43580 56909
17842 43157 59452 16380 59453 56122 17841 59411
58498 59625 17427 56074 17840 56373 14371 52350)
upstream_direction = left
}
STRINGDEF {
name = Bremgartenforest_north_v8
node_ids = (52350 17838 55533 52339 55312
17425 40095 17837 51850 24963 50612 16379 46734
24958 50611 21404 46618 24959 46619 17424)
upstream_direction = left
}
STRINGDEF {
name = Bremgartenforest_north_v9
node_ids = (17424 50648 21686 46541 17860
46085 21687 46501 1143 950 53071 21688 47095 16354
43135)
upstream_direction = left
}
STRINGDEF {
name = Bremgartenforest_north_v10
node_ids = (43135 20703 14322 26335 16353
26334 20702 24447 32705 5751 9133)
upstream_direction = left
}
STRINGDEF {
name = Laenggasse_roundabout
node_ids = (9133 33873 14742 32699 10258
19598 14741 40834 8535 10667)
upstream_direction = left
}
STRINGDEF {
name = Bremgartenforest_south_v1
node_ids = (10667 10665 44436 13233 56000
58491 5026 56013 17850 56129 17452 56014 17849
56021 16430 49131 24478 49132 40865 20756 43575
24479 43689 14438 44977 43111 24477 27179 20757
43887 27191 43613 24500 35154 27192 29848 16429
30285 27173 24475)
upstream_direction = left
}
STRINGDEF {
name = Bremgartenforest_south_v2
node_ids = ( 24475 27178 20758 40429 27497
40143 24476 34898 27501 31019 11413 31155 24909
33780 15240 34959 27934 32508 12619 40627 28576
15239 39213 5025 27984 25890 27819 22614 47819
25897 18850 47676 25901 47794 22615 25900 13481
52331 25858 52263 22598)
upstream_direction = left
}
STRINGDEF {
name = Bremgartenforest_south_v3
node_ids = (22598 51774 25861 47659 18852
47855 25892 22612 27820 25896 27822 28552 5749
25151 21710 34271 17891 21927 17527 21709 17890
25011 16554 43029 17889 43881 17526 43882 17888
47841 14571 47658 21707 50051 17883 46635 21706
45987 16553 46543 17887)
upstream_direction = left
}
STRINGDEF {
name = Bremgartenforest_south_v4
node_ids = (17887 52257 17525 51776 17886
51970 3028 40012 23225 32246 35819 2749 27969

```

```

22990 26182 16725 47861 17622 14743 47824 20955
16724 20956 29905 8731)
    upstream_direction = left
  }
}
OUTPUT {
  console_time_step = 60
  restart_time_step = 7200
  SPECIAL_OUTPUT {
    type = element_centered
    output_time_step = 60
    format = shape
    values = (depth velocity)
    threshold_wse = -1000000
  }
  SPECIAL_OUTPUT {
    type = element_centered
    format = shape
    values = (max[depth] max[velocity])
    output_time_step = 7200
    threshold_wse = -1000000
  }
  SPECIAL_OUTPUT {
    type = stringdef_history
    output_time_step = 60
    stringdefs = (Murtenstrasse_northwest
Murtenstrasse_southwest_v1
Murtenstrasse_southwest_v2
Murtenstrasse_southwest_v3 Murtenstrasse_southeast
Waldheimstrasse Depotstrasse_v1 Depotstrasse_v2
Depotstrasse_v3 Buehlstrasse Stadtbachstrasse_v1
Stadtbachstrasse_v2 Schanzenstrasse Post_stairs
Schuetzenmattstrasse_v1 Schuetzenmattstrasse_v2
Neubrueckstrasse_v1 Engestrasse
Bremgartenforest_north_v1 Bremgartenforest_north_v2
Bremgartenforest_north_v3 Bremgartenforest_north_v4
Bremgartenforest_north_v5 Bremgartenforest_north_v6
Bremgartenforest_north_v7 Bremgartenforest_north_v8
Bremgartenforest_north_v9
Bremgartenforest_north_v10 Laenggasse_roundabout
Bremgartenforest_south_v1
Bremgartenforest_south_v2
Bremgartenforest_south_v3
Bremgartenforest_south_v4)
    stringdef_values = (Q wse)
    history_one_file = yes
    flush_all_num_steps = 0
    threshold_wse = -1000000
  }
}
}
HYDRAULICS {
  PARAMETER {
    minimum_water_depth = 0.01
    riemann_solver = exact
    riemann_tolerance = 1.0e-6
    simulation_scheme = exp
    velocity_update_partial = volume_area
    dynamic_depth_solver = on
    dynamic_depth_solver_precision = 0.005
    geo_min_area_ratio = 0.05
    geo_max_angle_quadrilateral = 45
    geo_min_aspect_ratio = 0.06
  }
}
FRICITION {
  type = strickler

```

```

input_type = index_table
default_friction = 30
wall_friction = off
index = (0 1 2 3 4 5)
friction = (50 50 50 50 2 2.5)
grain_size_friction = no
}
INITIAL {
  type = dry
}
SOURCE {
  EXTERNAL_SOURCE {
    name = rainoverbuilding
    type = source_discharge
    index = (1)
    file = rainoverbuilding.txt
  }
  EXTERNAL_SOURCE {
    name = rainoverstreet
    type = source_discharge
    index = (2)
    file = rainoverstreet.txt
  }
  EXTERNAL_SOURCE {
    name = rainoverparking
    type = source_discharge
    file = rainoverparking.txt
    index = (3)
  }
  EXTERNAL_SOURCE {
    name = rainoverrest
    type = source_discharge
    file = rainoverrest.txt
    index = (0)
  }
}
BOUNDARY {
  name = Murtenstrasse_northwest
  string_name = Murtenstrasse_northwest
  type = zhydrograph
  file = zhydrograph_file_553.txt
  inflow_possible = yes
  zero_velocity = no
}
BOUNDARY {
  name = Murtenstrasse_southwest_v1
  string_name = Murtenstrasse_southwest_v1
  type = zhydrograph
  file = zhydrograph_file_553.txt
  inflow_possible = yes
  zero_velocity = no
}
BOUNDARY {
  name = Murtenstrasse_southwest_v2
  string_name = Murtenstrasse_southwest_v2
  type = zhydrograph
  file = zhydrograph_file_549.txt
  inflow_possible = yes
  zero_velocity = no
}
BOUNDARY {
  name = Murtenstrasse_southwest_v3
  string_name = Murtenstrasse_southwest_v3
  type = zhydrograph
  file = zhydrograph_file_553.txt

```

```

inflow_possible = yes
zero_velocity = no
}
BOUNDARY {
name = Murtenstrasse_southeast
string_name = Murtenstrasse_southeast
type = zhydrograph
file = zhydrograph_file_553.txt
inflow_possible = yes
zero_velocity = no
}
BOUNDARY {
name = Waldheimstrasse
string_name = Waldheimstrasse
type = zhydrograph
file = zhydrograph_file_552.txt
inflow_possible = yes
zero_velocity = no
}
BOUNDARY {
name = Depotstrasse_v1
string_name = Depotstrasse_v1
type = zhydrograph
file = zhydrograph_file_545.txt
inflow_possible = yes
zero_velocity = no
}
BOUNDARY {
name = Depotstrasse_v2
string_name = Depotstrasse_v2
type = zhydrograph
file = zhydrograph_file_545.txt
inflow_possible = yes
zero_velocity = no
}
BOUNDARY {
name = Depotstrasse_v3
string_name = Depotstrasse_v3
type = zhydrograph
file = zhydrograph_file_545.txt
inflow_possible = yes
zero_velocity = no
}
BOUNDARY {
name = Buehlstrasse
string_name = Buehlstrasse
type = zero_gradient
}
BOUNDARY {
name = Stadtbachstrasse_v1
string_name = Stadtbachstrasse_v1
type = zhydrograph
file = zhydrograph_file_541.txt
inflow_possible = yes
zero_velocity = no
}
BOUNDARY {
name = Stadtbachstrasse_v2
string_name = Stadtbachstrasse_v2
type = zhydrograph
file = zhydrograph_file_541.txt
inflow_possible = yes
zero_velocity = no
}
BOUNDARY {
name = Schanzenstrasse
string_name = Schanzenstrasse
type = zhydrograph
file = zhydrograph_file_551.txt
inflow_possible = yes
zero_velocity = no
}
BOUNDARY {
name = Post_stairs
string_name = Post_stairs
type = zero_gradient
}
BOUNDARY {
name = Schuetzenmattstrasse_v1
string_name = Schuetzenmattstrasse_v1
type = zhydrograph
file = zhydrograph_file_538.txt
inflow_possible = yes
zero_velocity = no
}
BOUNDARY {
name = Schuetzenmattstrasse_v2
string_name = Schuetzenmattstrasse_v2
type = zero_gradient
}
BOUNDARY {
name = Neubrueckstrasse_v1
string_name = Neubrueckstrasse_v1
type = zhydrograph
file = zhydrograph_file_538.txt
inflow_possible = yes
zero_velocity = no
}
BOUNDARY {
name = Engestrasse
string_name = Engestrasse
type = zhydrograph
file = zhydrograph_file_554.txt
inflow_possible = yes
zero_velocity = no
}
BOUNDARY {
name = Bremgartenforest_north_v1
string_name = Bremgartenforest_north_v1
type = zhydrograph
file = zhydrograph_file_569.txt
inflow_possible = yes
zero_velocity = no
}
BOUNDARY {
name = Bremgartenforest_north_v2
string_name = Bremgartenforest_north_v2
type = zhydrograph
file = zhydrograph_file_567.txt
inflow_possible = yes
zero_velocity = no
}
BOUNDARY {
name = Bremgartenforest_north_v3
string_name = Bremgartenforest_north_v3
type = zhydrograph
file = zhydrograph_file_569.txt
inflow_possible = yes
zero_velocity = no
}

```





# Erklärung

gemäss Art. 30 RSL Phil.-nat. 18

Name/Vorname:

Matrikelnummer:

Studiengang:

Bachelor

Master

Dissertation

Titel der Arbeit:

LeiterIn der Arbeit:

Ich erkläre hiermit, dass ich diese Arbeit selbständig verfasst und keine anderen als die angegebenen Quellen benutzt habe. Alle Stellen, die wörtlich oder sinngemäss aus Quellen entnommen wurden, habe ich als solche gekennzeichnet. Mir ist bekannt, dass andernfalls der Senat gemäss Artikel 36 Absatz 1 Buchstabe r des Gesetzes vom 5. September 1996 über die Universität zum Entzug des auf Grund dieser Arbeit verliehenen Titels berechtigt ist.

Für die Zwecke der Begutachtung und der Überprüfung der Einhaltung der Selbständigkeitserklärung bzw. der Reglemente betreffend Plagiate erteile ich der Universität Bern das Recht, die dazu erforderlichen Personendaten zu bearbeiten und Nutzungshandlungen vorzunehmen, insbesondere die schriftliche Arbeit zu vervielfältigen und dauerhaft in einer Datenbank zu speichern sowie diese zur Überprüfung von Arbeiten Dritter zu verwenden oder hierzu zur Verfügung zu stellen.

Ort/Datum

Unterschrift

